

INVESTIGATION ON TRANSIENT BEHAVIOR OF GROUNDING SYSTEMS IN MULTILAYER EARTH STRUCTURE

Thesis

Submitted in partial fulfillment of the requirements for the degree of

DOCTOR OF PHILOSOPHY

by

R. T. SENTHILKUMAR



DEPARTMENT OF ELECTRICAL AND ELECTRONICS ENGINEERING

NATIONAL INSTITUTE OF TECHNOLOGY KARNATAKA

SURATHKAL, MANGALORE - 575025

FEBRUARY 2022

DECLARATION

by the Ph.D. Research Scholar

I hereby *declare* that the Research Thesis entitled **Investigation on Transient Behavior of Grounding Systems in Multilayer Earth Structure** which is being submitted to the **National Institute of Technology Karnataka, Surathkal** in partial fulfillment of the requirement for the award of the Degree of **Doctor of Philosophy** in **Department of Electrical and Electronics Engineering** is a *bonafide report of the research work carried out by me*. The material contained in this Research Thesis has not been submitted to any University or Institution for the award of any degree.



.....
R. T. Senthilkumar, 138011EE13F07

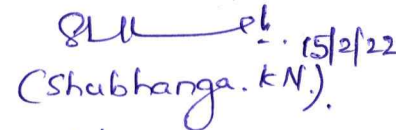
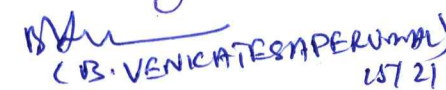
Department of Electrical and Electronics Engineering

Place: NITK Surathkal

Date: 11-02-2022

CERTIFICATE

This is to *certify* that the Research Thesis entitled **Investigation on Transient Behavior of Grounding Systems in Multilayer Earth Structure** submitted by **R. T. Senthilkumar** (Register Number: 138011EE13F07) as the record of the research work carried out by him, is *accepted as the Research Thesis submission* in partial fulfillment of the requirements for the award of degree of **Doctor of Philosophy**.


(Shubhanga. K.N.) 15/2/22

(B. VENKATESH PERUMAL) 15/2/2022

Dr. Gururaj S Puneekar
(Chairman - DRPC)
Professor and Head of the Department
Department of Electrical and Electronics Engineering
NITK Surathkal – 575025

ACKNOWLEDGEMENTS

It gives me immense pleasure and a great sense of satisfaction to express my heartfelt gratitude to those who made this dissertation possible.

I would like to express my sincere gratitude to my professors and Head of the Department *Dr Gururaj S Punekar, Dr K N Shubhanga, and Dr B Venkatesa Perumal*, Department of Electrical and Electronics Engineering, NITK Surathkal, for their support to complete my research work.

I wish to thank my research progress assessment committee (RPAC) members *Dr. P. Parthiban*, Associate Professor, Department of Electrical and Electronics Engineering, NITK Surathkal, and *Dr. P. Sam Johnson*, Associate Professor, Department of Mathematical and Computational Sciences, NITK Surathkal, for their constructive feedback and guidance.

I thank National Institute of Technology Karnataka (NITK), Surathkal for giving me an opportunity for doing research and Ministry of Human Resource Development (MHRD), Government of India for awarding research scholarship.

I thank Jef Techno Solutions Private Limited and its management for allowing me to utilize the facilities for doing research in their lab. I thank *Mr. Nagarajan*, Head – Design, Jef Techno Solutions Private Limited for his guidance and support during my research work carried out in Jef Techno Solutions Private Limited. I thank *Dr. Selvakumar*, Assistant Professor, SRM University for his support and technical contribution in my research studies.

I would like to express my deepest gratitude towards my mom *Mrs. K R Angayarkanni Thayalan*, my brother *Mr. Surendar Thayalan*, my wife *Mrs Gayathiri*, my daughters *Ms. Kaniha Angayarkanni* and *Ms. Karthika Angayarkanni* for their love and patience which kept me going in this journey. I would like to thank my friend *Dr. N Karthik*, who supported and encouraged me continuously with unconditional love.

Finally, I thank God for given strength during all my struggling period of this journey.

ABSTRACT

A Grounding system is one of the most important parts of the electrical network. Grounding system is a pivotal one to ensure the risk of life in the situation of grounding faults and to guarantee the safe and reliable operation of the power system. In order to better quantify the behavior of an earth electrode subjected to a lightning current impulse, it is necessary to understand the commonly encountered scenario of ground with various layers resulting from geological stratification. Thus the proposed work introduces a better understanding of the lightning transient behavior of an earth electrode in multilayer soil and develops a simplified approach to quantifying this behavior. Multilayer soil structure studies with grounding rod buried in the earth structure analysis gives close agreement with the measured site data.

An optimization methodology is proposed to estimate the parameters of multilayer earth structure by using the hybrid Genetic Algorithm and Particle Swarm Optimization (GA-PSO). The objective function of the optimization problem is obtaining $(2N - 1)$ variables of N layer soil structure. Calculated apparent resistivity has taken as a parameter to compute the theoretical resistivity as well as the parameters of horizontal multi structure earth. It is understood that the thickness of soil's bottom layer is infinity. Steepest Descent Method (SDM) is also introduced for the estimation of Transient Ground Potential Rise (TGPR) in Substation. The SDM is also known as the gradient descent method. By using four wire Wenner method on the ground is to acquire the experimental apparent resistivity curve. With the measured experimental apparent resistivity, can compute the theoretical apparent resistivity curve and estimate the soil parameters such as a number of layers, thickness of each layer (N^{th} layer thickness is infinity) and its resistivity.

The design of Air Insulated Substation (AIS) grounding systems may become inaccurate if the average value of resistivity measured is taken in the design calculation especially when the variation of resistivity of different probe distances is more than 25%. It is suitable to use more than two soil layers in the AIS grounding system. In the second work, AIS selection of optimal system touch voltage and step voltage depends on the load to be served and the distance between the generation source and the

load. Soil Resistivity Measurements were carried out at site, by Wenner four point methods in location based on site condition. Observed that, measured soil resistivity readings in a direction were exceeding 30 percent, hence Multi-layer soil modelling chosen as recommended in IEEE 80-2013. In the AIS grounding system, number of layers, resistivity of each layer and thickness are the parameters to be estimated with the measured site data. Identifying specific areas on the grid are unsafe for touch and step voltage in AIS. Current Distribution, Electromagnetic Fields, Grounding and Soil Structure Analysis (CDEGS) software by using RESAP is used for optimizing the parameters of soil structure. Ground Potential Rise (GPR) of the substation is to be computed when the fault current is injected into the grounding grid in power frequency. The results of AIS are evaluated via the voltage levels such as step and touch with respect to earth design.

In order to minimize the required substation area and enhance the results of grounding system, Gas-Insulated Substations (GIS) is widely used, mainly in urban cities nowadays. An interpretation of the soil resistivity measurements was carried out and analyzed for GIS by CDEGS. In the event of a short circuit, earth fault current can in the surrounding buried metallic infrastructure where it will be dissipated into the soil. It is therefore legitimate to determine if this will threaten the integrity of adjacent resident facilities and become a concern to public personnel safety. At the beginning of the GIS technology, the grounding design was designed for limiting the power frequency enclosure potentials to safe levels based on the maximum expected fault-current conditions by computing touch voltage levels and step voltage levels. IEEE 80-2000 is used to design grounding system based GIS for soil models and help of software is taken for two or more than two-layer soil models. The performance of the grounding grid is heavily dependent on the soil structure. The results of GIS are evaluated via the voltage levels such as step and touch with respect to earth design.

Keywords:

Soil Resistivity, Multilayer Earth Structure, Ground Potential Rise(GPR), Step Voltage, Touch Voltage, CDEGS, GA, PSO, Air Insulated Substation (AIS), Grounding Grid, Gas Insulated Substation (GIS).

TABLE OF CONTENTS

ACKNOWLEDGEMENTS.....	i
ABSTRACT.....	ii
TABLE OF CONTENTS.....	iv
LIST OF FIGURES.....	viii
LIST OF TABLES.....	xii
LIST OF ABBREVIATIONS.....	xiv
CHAPTER 1	
INTRODUCTION.....	1
1.1 General.....	1
1.2 Power System Safety Requirements.....	3
1.3 Need for System Grounding.....	5
1.4 Function of Grounding System.....	6
1.5 Grounding System Safety Parameter Requirements.....	7
1.6 Soil Resistivity.....	8
1.7 Ground Potential Rise.....	11
1.8 Objectives of the Thesis.....	12
1.8 Organisation of the Report.....	13
CHAPTER 2	
SOIL RESISTIVITY MEASUREMENT AND STRATIFICATION OF EARTH STRUCTURE.....	15
2.1 Geological Information and Soil Samples.....	15
2.2 Soil Resistivity Measurements.....	15
2.3 Variation of Depth Method.....	17
2.4 Two Point Method.....	17
2.5 Three Point Method.....	18

2.6 Fall of Potential Method.....	20
2.7 The 62% Method.....	21
2.8 Four Point Method.....	22
2.8.1 Wenner Arrangement.....	22
2.8.2 Schlumberger or Unequally Spaced Method.....	24
2.9 Stratification of Earth Structure.....	26
2.9.1 Homogeneous Earth Structure.....	26
2.9.2 Horizontally Stratified Two Layer Earth Model.....	28
2.9.3 Three to Five Layer Earth Model	30
2.9.4 Multilayer Earth Model.....	32
2.10 Literature Survey.....	33
CHAPTER 3	
GROUNDING GRID MODELLING.....	37
3.1 Grounding Grid Modelling.....	37
3.2 Voltage Levels.....	37
3.3 CDEGS – Software.....	39
3.4 Earthing Design Analysis.....	40
3.5 Grid Conductor Sizing.....	42
CHAPTER 4	
HYBRID OPTIMIZATION AND STEEPEST DESCENT METHOD FOR OPTIMIZATION OF SOIL PARAMETERS IN MULTIPLE LAYERS OF GROUND STRUCTURE.....	47
4.1 Introduction.....	47
4.2 Four Point Method.....	48
4.3 Steepest Descent Method.....	50
4.4 Genetic Algorithm.....	51
4.5 Particle Swarm Optimization	53
4.6 Hybrid GA - PSO Technique.....	54
4.7 Results and Discussions.....	56

CHAPTER 5	
AIR INSULATED SUBSTATION (AIS) GROUNDING GRID DESIGN FOR OPTIMIZED SOIL PARAMETERS IN MULTIPLE LAYERS	63
5.1 Air Insulated Substation.....	63
5.2 Case Study1: AIS Grounding Design and Computation of Grid	
Impedance of 220/132/ 66 kV Substation	64
5.2.1 Design Parameters.....	65
5.2.2 Grid Conductor Sizing.....	66
5.2.3 Safety Criteria for 50 kg Body Weight with Surface Layer	68
5.2.4 Touch Voltage.....	68
5.2.5 Step Voltage.....	69
5.2.6 Conductor GPR.....	70
5.2.7 Touch Voltage 1m Outside Grid / Fence.....	72
5.2.8 Step Voltage 1 m Outside Grid.....	72
5.3 Case Study 2: 400 /220 kV AIS Substation Soil Resistivity.....	74
5.3.1 AIS Grounding Design and Computation of Grid	
Impedance	75
5.4 Case Study 3: 220 kV Substation.....	83
5.4.1 Soil Model.....	83
5.4.2 Grounding Design and Computation of Grid Impedance..	84
5.5 Results for 220 kV Satellite Grid.....	85
5.5.1 Conductor GPR	89
5.6 Summary.....	90
CHAPTER 6	
GAS INSULATED SUBSTATION (GIS) GROUNDING GRID DESIGN FOR OPTIMIZED SOIL PARAMETERS IN MULTIPLE LAYERS	91
6.1 Gas Insulated Substation.....	91
6.2 GIS Principles and Operation.....	93
6.3 Analysis of Grid 765 kV GIS Room Floor.....	96
6.3.1 Evaluation of Safety Inside the Grid Area.....	98

6.3.2 Evaluation of Safety in GIS Room.....	101
6.3.3 Metal to Metal Touch Voltage (GPD on 765kV GIS equipment inside the room).....	103
6.3.4 Metal to Metal Touch Voltage (GPD on 400kV GIS equipment inside the room).....	104
6.3.5 Evaluation of safety Outside Fence for Step Potential with Native soil.....	105
6.3.6 Ground Fault Analysis at GIS Equipment inside 765 kV GIS Room.....	107
6.4 Ground Fault Analysis at GIS Equipment inside 400 kV GIS Room.....	109
6.5 Very Fast Transient Over Voltages Analysis.....	113
6.6 Summary.....	127
CHAPTER 7	
CONCLUSIONS AND FUTURE SCOPE.....	129
7.1 Conclusions.....	129
7.2 Future Scope.....	130
REFERENCES.....	131
PUBLICATIONS BASED ON THESIS.....	136
CURRICULUM VITAE.....	137

LIST OF FIGURES

1.1	Explanation of Ground Potential Rise.....	2
2.1	Two Point Method of Earth Resistance Measurement.....	18
2.2	Three Point Method of Earth Resistance Measurement.....	19
2.3	Variation of Output Resistance with Electrode Position.....	21
2.4	Experimental Arrangement for Checking the Validity of Resistance....	21
2.5	Wenner Four Probe Method.....	23
2.6	Schlumberger Array Method.....	25
2.7	Horizontally Stratified Two Layer Earth Model.....	28
2.8	Multilayer Earth Structure.....	32
3.1	Touch, Step and Transferred Voltage.....	39
3.2	Screenshot of CDEGS Software Package.....	40
3.3	Current Components: at Electrode and Soil.....	43
4.1	Four Point Method.....	48
4.2	Flowchart of GA.....	52
4.3	Flowchart of Proposed GA – PSO Algorithm.....	55
4.4	Hybrid GA – PSO best fitness, scaling and Selection (Case Study 1)...	57
4.5	Hybrid GA – PSO best fitness, scaling and Selection (Case Study 2)...	60
5.1	Grid Layout – Plan View of Substation.....	67
5.2	Observing the Step and Touch Potential.....	68
5.3	Touch Voltage Inside the Grid for AIS Substation.....	69
5.4	Step Voltage Inside the Grid for AIS Substation.....	69
5.5	Conductor GPR for AIS Substation.....	70
5.6	Observation Profile 1m Outside the Grid / Fence Area for AIS Substation.....	71
5.7	Screenshot of System Information Summary.....	71
5.8	Step Voltage without Surface Layer for Substation.....	72

5.9	Step Voltage 1m Outside Grid / Fence without Surface Layer.....	73
5.10	Energization Module 400 / 220 kV Substation.....	76
5.11	Observation Profile Point of 400 / 220 kV Substation.....	76
5.12	Touch Voltage Inside the Grid for 400 / 220 kV Substation.....	77
5.13	Step Voltage Inside the Grid for 400 / 220 kV Substation.....	78
5.14	Conductor Grid for 400 / 220 kV AIS Substation.....	79
5.15	Screenshot of 400 / 220 kV Substation System Information Memory...	80
5.16	Observation Profile 1m Outside for 400 / 220 kV Substation.....	81
5.17	Touch Voltage 1m Outside Grid for AIS Substation.....	81
5.18	Step Voltage 1m Outside Grid for AIS Substation	82
5.19	Screenshot of SESCAD Drawing of 110 kV Substation.....	86
5.20	Satellite Grid Area for 220 kV Substation.....	87
5.21	Touch Voltage Grid Area for 220 kV Substation.....	87
5.22	Step Voltage Grid Area for 220 kV Substation.....	88
5.23	Conductor GPR for 220 kV Substation.....	89
6.1	Gas Insulated Substation and Grounding Area with Gravel Surface....	92
6.2	Fault Current Distribution Computation Circuit Model.....	95
6.3	Fault Current Distribution Computational Field Approach Model.....	95
6.4	3D View of 765 kV and 400 kV GIS.....	97
6.5	Perspective View of the System - 765 kV and 400 kV GIS.....	97
6.6	Evaluation of Safety Inside the Grid Area for GIS.....	98
6.7	Touch Voltage Profile in the Substation Area with Fault.....	99
6.8	Step Voltage Profile in the Substation Area with Fault.....	100
6.9	Conductor Ground Potential Rise Inside Grid.....	100
6.10	Observation Profile Inside the GIS Room.....	101
6.11	Safety Limit for Touch Voltage with in GIS Room.....	102
6.12	Safety Limit for Step Voltage with in GIS Room.....	102
6.13	Metal to Metal Touch Voltage (GPD on 765 kV GIS Equipments Inside Room).....	103
6.14	Metal to Metal Touch Voltage (GPD on 400 kV GIS Equipments Inside Room).....	104

6.15	Observation Profile with Native Soil.....	105
6.16	Step Voltage 1m Outside Grid for Native Soil.....	106
6.17	Ground Fault Analysis at GIS Room.....	107
6.18	Fault Location with Conductor Segment Number.....	107
6.19	Touch Voltage Results on 765 kV GIS Room Floor.....	108
6.20	Step Voltage Results on 765 kV GIS Room Floor.....	108
6.21	Ground Fault Analysis at 400 kV GIS Room.....	109
6.22	Ground Fault Location at 400 kV GIS Room.....	110
6.23	Touch Voltage Inside 400 kV GIS Room Floor.....	110
6.24	Step Voltage Inside 400 kV GIS Room Floor.....	111
6.25	Metal to Metal Touch Voltage (GPD on 400 kV GIS Equipments Inside Room).....	112
6.26	Screenshot of Summary of Independent Frequencies Recommend.....	114
6.27	Input Signal for Lightning Surge (Time Domain).....	114
6.28	Input Signal for Lightning Surge (Frequency Domain – Real Part).....	115
6.29	Input Signal for Lightning Surge (Frequency Domain – Imaginary Part).....	115
6.30	TGPR at Different Locations in Main Bus for Lightning Surge.....	116
6.31	TGPR at Conductor Segment Number 1017 (Main Bus 1).....	116
6.32	TGPR at Conductor Segment Number 1018 (Main Bus 1).....	117
6.33	TGPR at Conductor Segment Number 1016 (Main Bus 1).....	117
6.34	TGPR at Conductor Segment Number 189 (Main Bus 1).....	117
6.35	TGPR at Conductor Segment Number 190 (Main Bus 1).....	118
6.36	TGPR at Conductor Segment Number 432 (Main Bus 1).....	118
6.37	TGPR at Conductor Segment Number 191 (Main Bus 1).....	118
6.38	TGPR at Conductor Segment Number 192 (Main Bus 1).....	119
6.39	TGPR at Conductor Segment Number 1026 (Main Bus 2).....	119
6.40	TGPR at Conductor Segment Number 1011 (Main Bus 2).....	119
6.41	TGPR at Conductor Segment Number 1023 (Main Bus 2).....	120
6.42	TGPR at Conductor Segment Number 206 (Main Bus 2).....	120
6.43	TGPR at Conductor Segment Number 208 (Main Bus 2).....	120

6.44	TGPR at Conductor Segment Number 441 (Main Bus 2).....	121
6.45	TGPR at Conductor Segment Number 209 (Main Bus 2).....	121
6.46	TGPR at Conductor Segment Number 210 (Main Bus 2).....	121
6.47	TGPR at Conductor Segment Number 193 (Main Bus 3).....	122
6.48	TGPR at Conductor Segment Number 435 (Main Bus 3).....	122
6.49	TGPR at Conductor Segment Number 194 (Main Bus 3).....	122
6.50	TGPR at Conductor Segment Number 195 (Main Bus 3).....	123
6.51	TGPR at Conductor Segment Number 1032 (Main Bus 3).....	123
6.52	TGPR at Conductor Segment Number 1029 (Main Bus 3).....	123
6.53	TGPR at Conductor Segment Number 1035 (Main Bus 3).....	124
6.54	TGPR at Conductor Segment Number 211 (Main Bus 4).....	124
6.55	TGPR at Conductor Segment Number 438 (Main Bus 4).....	124
6.56	TGPR at Conductor Segment Number 212 (Main Bus 4).....	125
6.57	TGPR at Conductor Segment Number 207 (Main Bus 4).....	125
6.58	TGPR at Conductor Segment Number 1010 (Main Bus 4).....	125
6.59	TGPR at Conductor Segment Number 1038 (Main Bus 4).....	126
6.60	TGPR at Conductor Segment Number 1041 (Main Bus 4).....	126

LIST OF TABLES

1.1	Various Resistivity Values of Soil and Water.....	10
4.1	Case Study 1 – Experimental Investigation.....	56
4.2	Comparison of Hybrid PSO – GA Technique with GA.....	57
4.3	Comparison – Percentage of Error.....	58
4.4	Parameters of Soil Stratification Case Study 1.....	58
4.5	Case Study 2 – Experimental Investigation.....	59
4.6	Comparison of Experimental Resistivity with Computed Resistivity....	59
4.7	Parameters of Soil Stratification Case Study 2.....	61
5.1	Soil Resistivity Model for AIS Substation.....	65
5.2	Surface Layer of 3000 Ω m resistivity inside the Grid Area.....	73
5.3	Without Surface Layer – 1m Outside the Grid.....	73
5.4	Soil Resistivity Data of 400 / 220 kV substation.....	74
5.5	Surface Layer of 3000 Ω m resistivity for 75mm inside the Grid Area....	82
5.6	Surface Layer of 1M Outside the Grid.....	83
5.7	Soil Resistivity of 220 kV substation.....	83
5.8	Optimized Soil Parameter using Hybrid GA – PSO Algorithm.....	84
5.9	Soil Parameters for 110 kV AIS connected with Satellite Grid.....	89
5.10	Touch and Step Potential of 245 kV GIS connected with Satellite Grid.....	90
6.1	Fault Current Split Calculation Results.....	94
6.2	Comparison of Different Safety Criteria in GIS.....	106

6.3	Fault Analysis Comparison of Different Safety Criteria.....	113
6.4	GIS Results of TGPR at Different Segment Numbers in Main Bus.....	127

LIST OF ABBREVIATIONS

AIS	Air Insulated Substation
BEM	Boundary Element Method
CDEGS	Current Distribution, Electromagnetic Fields, Grounding and Soil Structure Analysis.
EA	Evolutionary Algorithm
ESP	Earth Surface Potential
FDTD	Finite Difference Time Domain
FEM	Finite Element Method
FFT	Fast Fourier Transform
GA	Genetic Algorithm
GIS	Gas Insulated Substation
GPR / EPR	Ground Potential Rise / Earth Potential Rise
IEEE	Institute of Electrical and Electronics Engineers
IS	Indian Standard
MoM	Method of Moments
PEEC	Partial Element Equivalent Circuit
PSO	Particle Swarm Optimization
SAM	Simulated Annealing Method
SDM	Steepest Descent Method
TGPR	Transient Ground Potential Rise

CHAPTER 1

INTRODUCTION

1.1 General

The rapid development in transportation and industrial sector need more electricity usage. In the time of expanding electrical infrastructure the electrical safety and servicing equipment are getting more importance. The electrical safety requirements also improved day by day by the various amendments introduced by the government. When expanding the electrical infrastructure, the electric power generating plant and substations itself having more high voltage apparatuses. So it is necessary to avoid equipment seller and risk of staff members during short circuit condition.

The risk is getting increased due to the infect integrity of the grounding equipments. The grounding equipment is the most essential part for reducing the risk of working employees and equipment damages. The reliability and performance of the grounding equipments always depends on its structural integrity. For example, the damage of grounding conductors may produce in corrective operation of relay circuit breaker. The malfunctioning of circuit breaker and relay operation also which affects the other protecting devices in the system. Usually the grounding equipments are buried inside the soil and mainly characteristics of grounding systems are influenced by the surrounding soil and it is a very challenging task to find the damaged elements inside the soil.

In electrical insulation the adequate grounding is the very important aspect and specifically in the protection of human beings and the operating equipments from the high voltage electrical faults. A well designed earthing or grounding system gives better outputs in the form of safety any equipment and the living beings, but that designing steps are very difficult and based on various number of factors. so substation grounding system needs more important to prevent High Voltage fault. The first substation grounding system design guide is introduced in 1961 as per the IEEE and ANSI standard 80 / 2000. After that that substation grounding system design guide design has

been revised in 1976, 1986 and 2000 for getting better results in the view of substation grounding system by the substation engineers.

When the ground fault occurs at a substation the ground current flow in the various transmission lines is mainly depends on the importance's of the specific transmission line. the fault current main flow in ground grade are the overhead transmission line and the potential rise should be controlled between as safe value so that it won't be harmful when any human being are living being heart touching the substation fence and conducting transmission line.

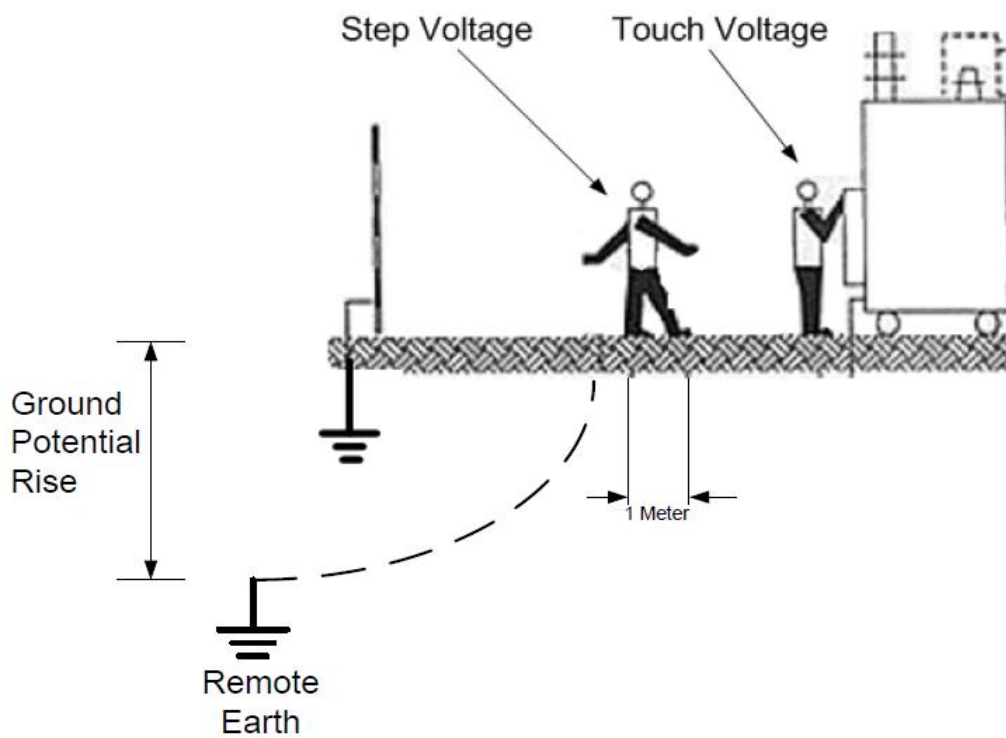


Figure 1.1: Explanation of Ground Potential Rise

The ground potential Rise is defining as the multiplication of station grounding resistance and the current flow between the surrounding earth and the ground and its explained in figure 1.1. Substation grounding system always should provide a low impedance path for allowing the fault current when the fault is occurred. The substation grounding equipments like horizontal ground electrode, vertical ground electrode, grounding mat, interconnecting cables and all the metallic structures in the substation are provide the common ground. Common grounding in a substation is also limits the

surface potential gradient of the system. Vertical grounding rods of the substation is inversely proportional to the overall resistance of the substation.

The substation ground rod resistance can be affected by the soil around the ground rod and depth of the ground electrode. The number of layers and nature of soil is different from one place to another place. Mainly increasing the length of the ground rod by twice may reduce the ground resistance by 40 percentages and increasing the diameter of the ground by twice by reduce the ground resistance only 10 percentages. The ground rod should not be installed like crowding manner and mostly the distance between the ground rods always not less than the depth of the ground rod.

The ground current flow between the various parts of the substation ground gives increase in step potential. The definition of a step potential is the difference between the surface potential when the person bridging a distance of 1 meter without contacting any other grounding path. Touch potential is defined as the surface potential difference between the person standing at the maximum recharge of 1 meter in a grounded metallic structure. The maximum safe potential of the substation is approximately 880 volts. The safe fault current dissipation can be done based on following three parameters that is ground potential rise step voltage and touch voltage. So that calculation of step voltage, touch voltage and ground potential rise needs more important in substation grounding system design.

1.2 POWER SYSTEM SAFETY REQUIREMENTS

The electric power demand is increasing day by day to satisfy the economic development of the world. The growth of electrical infrastructure also increases the size and number of the power generating plants and substations and this will lead to increase current levels in the interconnected networks. The interconnected medium and high voltage power system infrastructure requires production in touch and step voltage within the tolerable values. Especially the high voltage transmission lines and communication circuits needs more reliability among the system protection.

When lightning strike in high voltage transmission line occurring over voltage reduced by heightening the transmission line. But while lightning the transmission line it is very

difficult to maintain low impedance earthing system design. In this situation it is very difficult to maintain the continuity of supply without any effect. In the event of fault, the very high magnitude value of fault current is interrupted as fast as possible. The protective relays, circuit breakers and effective earthing systems can be used to isolate the faulty zone before affecting the human beings and electrical equipments in wide area. Nowadays by the usage of modern electronic equipments in control and protection system used to reduce the Earth potential. But the effective earthing systems always maintain the earth potential level within the tolerable limits. In the time of earth potential rise in high voltage transmission lines that affect nearby telecommunication circuits.

In the time of occurring lightning Strike if the earthing impedance value is less than the normal value means it observes the high current without affecting earth potential rise. But if the earthing impedance value is higher than the normal value means the back flashover can occur between the transmission phase conductors. When direct lightning strike the transmission line are any electrical equipment of the system can be saved by adopt adequate earthing system with an additional measure like transmission line shielding and overvoltage limiting equipments. In the time of acquiring direct lightning strike in protective zone the high current magnitude can be diverted into earthing circuit. However, in the time of short circuit fault the current can be interrupted in very quickest time period. Low impedance earthing system may help to sense the change in current very shortest time. The real temperature magnitude is a very important factor for earthing system design.

During the electrical shock time that the current tolerance value of a human body is mainly depends on earth potential rise. Normally human body can withstand lower than the value of 5 mA. But if it flows more than 5 mA it can affect the human body based on their individual wait duration of current exposure and the current magnitude value. However, the current value goes above than 200 mA to 300 mA for more than one second of time period it may give very harmful effects to the human beings as well as the living beings.

The main essential power system safety requirement is to provide good earthing system design which is used to carry electric current in normal operating condition, short circuit fault time and lightning Strike affecting time without increasing the earth potential value greater than the normal operating value. It also needs to provide step voltage and touch voltage in the time of lightning occurring in transmission lines and substations.

1.3 NEED FOR SYSTEM GROUNDING

Generally, in substation installation the grounding system or earthing system which connects the entire conductive surface for safe operation. The earthing system of the substation can connect the following parts

- Overhead transmission line towers
- Power cable sheaths
- Armours
- Transformer and reactor banks,
- cooler and radiators,
- tap changers, earthing resistors,
- earthing reactors,
- high voltage transformer neutral connections
- Metal clad switchgear assemblies and cases,
- isolators and earth switch bases
- Metal gantries and structures like wood and steel frames

The need for the substation grounding systems is to ensure the following

- Ensure safety to personnel in substations against electrical shocks.
- Provide the ground connection for connecting the neutrals of star connected transformer winding to earth (neutral earthing).

- Discharge the over voltages from overhead ground wires to earth. To provide ground path for surge arresters.
- Provide a path for discharging the charge between phase and ground by means of earthing switches.
- To provide earth connections to structures and other non-current carrying metallic objects in the sub-station (equipment earthing).

1.4 FUNCTIONS OF GROUNDING SYSTEM

The grounding system is very essential to maintain the fault current within the tolerable limit to reduce the risk of equipment failure and the living beings. Earthing system is installed along with the electrical infrastructure and its performance is to be monitored throughout the lifetime for the specific electrical network. The impressed power frequency voltage and transient voltage in the time of faulty condition can be limited by the installed an earthing system. It also used to find the appropriate fault current path to maintain the equipment safe operating limit. If the fault current at the time of short circuit fault is not maintained within the safe limit of equipment, it may produce the extensive damage of the specific equipment installed in the transmission line and also associated with the ancillary equipments like insulation breakdown and mechanical or thermal damage due to the arcing.

The main essential function of a good earthing system is always to maintaining and ensures the proper operation of the installed devices like protective relays circuit breakers and surge arresters within the safe and acceptable or tolerable limits. It also limits the potential difference across all these devices with respect to the potential reference value. During the earth fault and short circuit fault condition the earthing system should need to achieve the maximum system reliability by operating all the protective systems within the safe operating limits to minimize the fault clearing time and the resulting fault current.

In order to meet the operating requirements of the good earthing system design is also need to be monitor periodically. All the earthing system components like earthing conductors, earthing rod should be capable of transferring the fault current without

exceeding the mechanical and thermal stress of the specific electrical equipment. All the earthing system components also needs to tested and monitored before commissioning or installing and at regular time intervals to achieve better efficiency.

When the lightning Surge occurs in a transmission line, the Surge arrester conducts lightning impulse and transient surge fault currents through the low impedance earthing system to avoid the insulation breakdown and the occurrence excessive flashover voltage in the transmission line. So it is very essential to study the behaviour of the earthing system under these conditions to predict efficiency and effectiveness. The earthing system impedance is not only depending on the earthing equipments it also depends on several factors such as soil resistivity, soil permittivity and the wave front rise time based on geometry of earth electrode.

The aging of the earthing equipments affects the earthing impedance in case of corrosive action in soil. Seasonal changes in soil Resistivity and equipment corrosion due to aging of the equipment and nature of the soil will need to monitor the existing earthing system periodically to ascertain its efficiency.

1.5 GROUNDING SYSTEM SAFETY PARAMETER REQUIREMENTS

The first electrical infrastructure installations were happened in 19th century with respect to the AC current generation and distribution. At that time there were no electric laws or amendments are followed for installation and operation. The ungrounded high voltage three phase electric power system where operated in UK and Germany until 1917. The ground fault current in the ungrounded electrical system will leads to the phase to ground capacitance increase above the threshold limit. During the fall time, the persistent intermittent arcing damages the equipments and affects the living beings. Because of this reason the high magnitude over voltages are developed and it can affect the other parts and equipments of the electrical network. It leads to a problem in fault detection isolation and the arc suppression methods.

The first standard about electrical insulation was introduced in France on 1923 and it doesn't have any information about grounding system and protection systems. Still some parts of High Voltage transmission networks in worldwide operating in

underground under certain circumstances. The most common recommendation is to ground at least one neutral point of the network. So that we can able to detect, locate and clear the fault at the earliest (Jones et.al. 2011). Based on the connection between the neutral and ground the grounding system are divided into two types namely solidly grounding and impedance grounding system also can be categorized as

- Resistance type impedance grounding
- Reactance type impedance grounding and
- Resonant type impedance grounding.

In worldwide there are three grounding systems are followed and it has been accepted by many countries namely TN system, TT system and IT systems.

- In TN grounding system, the neutral of the transformer is gets grounded and the electrical system load frames are also connected to the neutral.
- In TT grounding system, the neutral of the transformer is gets grounded and the electrical system load frames are also connected to the ground system.
- In IT grounding system, the neutral of the transformer is not gets grounded and the electrical system load frames are also connected to the ground system.

1.6 SOIL RESISTIVITY

The earth or ground is not a good conductor and consequently large potential gradient produced when it carries a very high fault current and it exhibit an increase in ground potential rise (GPR). Nature of soil resistivity and other factors may vary one place to another place in the time of electrical installation. The high voltage substation ground impedance value may range from 0.05 ohm to 1 ohm and the magnitude of ground fault currents may range from 5 kA to 30 kA as per the IEEE guide for safety in AC substation grounding.

The soil resistivity and ground resistance of the electrode may vary based on the following factors.

1. Soil type
2. Moisture content available in the soil
3. Salt content available in the soil
4. Temperature of the ground or soil
5. Injected signal frequency
6. Input current wave shape
7. Number of layers in the soil
8. Soil density in that place
9. Depth of the ground electrode
10. Seasonal variation
11. Surface topography
12. Objects nearby the ground electrode

Generally, the resistance of any material is depends on its atomic structure and it can be calculated from the following equation.

$$R = \frac{\rho * l}{a} \quad (1.1)$$

where,

‘ ρ ’ is the specific resistivity of the conducting material

‘ l ’ is the length of the conducting material

‘ a ’ is the area of cross section of the conducting material

Table 1.1 various resistivity values of soil and water [8]

Type of Soil or Water	Typical Resistivity Ωm	Usual Limit Ωm
Sea water	2	0.1 to 10
Clay	40	8 to 70
Ground well and Spring water	50	10 to 150
Clay and Sand mixture	100	4 to 300
Shale, Slates, Sandstones etc.	120	10 to 100
Peat, Loam and Mud	150	5 to 250
Lake and Brooke Water	250	100 to 400
Sand	2000	200 to 3000
Moraine Gravel	3000	40 to 10000
Ridge Gravel	15000	3000 to 30000
Granite	25000	10000 to 50000
Ice	100000	10000 to 100000

As per the above equation the resistivity of the soil can be defined as opposite side resistances in the cube of soil with a dimension of 1 meter. The variation in the soil resistivity is mainly depends on the type of the soil present in the specific location. The soil resistivity will gets increasing with respect to the temperature decreasing from 25 degrees centigrade to deliver than zero degrees centigrade. For example, in winter season the Frozen soil has very high resistivity value.

The table 1.1 shows the various soil resistivity values in different grounding system designs. Soil resistivity changes with the climatic conditions such as temperature, percentage of moisture content in the soil and percentage of salt content in the soil. Since water is a good conductive and electrolytic will influences the grounds resistivity

with respect to the moisture content. the moisture content may vary from 0 % to 18 %. Usually the soil has the moisture content value of more than 40 %. So the large quantity of water does not imply the soil resistivity value to be very low. Compared to various metals the soil conductivity is extremely very poor value. In the soil structure the conductivity of upper soil layer is always greater than the lower soil layers. Presley the topmost layer is having very high conductivity of soil and it carries most of the current to an electrode. For shallow grounding electrodes the temperature will gets increase when resistivity of the soil getting decreased at very low temperature level that groundwater can freeze and increase the soil resistivity. If the water from the soil is gets evaporated the resistivity of the soil also can be increased. The stability of the grounding system enhanced by increasing the electrode depth. Apart from the electrical safety the grounding system should need the corrosion resistant and mechanical strength for carrying the maximum fault current.

1.7 GROUND POTENTIAL RISE

The ground potential Rise is defined as the voltage difference between the remote earth and the grounding system. when the lightning stroke or Phase to earth fault occurring time the electrical potential rise increase in the surrounding soil and grounding system may result hazardous touch and step voltage values. The initial grounding system design can be based on the ground potential rise and it can be calculated from the following equation

$$U_E = R_E * I_E \quad (1.2)$$

where,

U_E is the measured resistance to earth in ohms

I_E is the fault current to earth in A

The permissible value of the touch voltage maximum potential rise of human can with stand during an earth fault. According to NEK 440: 2011 electric law the permissible step voltage is mainly depends on the current through the heart during a fault condition, maximum permissible current through the human body and the body impedance value.

The permissible touch voltage is a function of fault occurring time and it reduces with increasing the time value.

The permissible touch voltage value varies with time intervals in fault occurring time. The duration of fault is mainly depending on protection system and it automatically in the touch voltage limitation. As per the standard IEEE 80, permissible touching voltages can be increased by adding additional resistances. The permissible touching voltage can be increased by applying and insulating surface in a substation. Potential touch voltage can be less than the permissible touch voltage when the ground potential rise during Earth fault is lesser than the two times of permissible touch voltage. The maximum permissible touch voltage can be calculated from the following equation.

$$R_E = \frac{U_{TP}}{I_E} \quad (1.3)$$

where,

R_E is the maximum permissible earth resistance in ohms

U_{TP} is the potential touch voltage in volt

I_E is the earth current in Ampere

1.8 Objectives of the Thesis

The overall objectives of this work is to obtain a better understanding of the lightning transient behaviour of an earth electrode in multilayer soil and develop a simplified approach to quantifying this behaviour.

1. By implementing optimization techniques and estimate the parameters such as number of layers, thickness and its resistivities to get better agreement with the measured apparent resistivity.
2. To decrease the ground resistance by adding/reducing the length of the ground rods based on realizing the multilayer soil structure.

3. To compute the frequency response of surrounding soil when subjected to lightning impulse and soil ionization and to model the transient analysis of grounding system in multilayer soil structure.

1.9 ORGANISATION OF THE REPORT

The thesis is organized into seven chapters. This section provides information about the major contribution of each chapter.

Chapter 1 presents brief introduction about the Power System Grounding.

Chapter 2 outlines the conventional measurement of soil resistivity methods along with physical structure of soil. This chapter also explores the Mathematical modelling for Schlumberger, two point and three point methods for stratification of earth structure problem, and that can be solved by an Optimization problem.

Chapter 3 deals with substation grounding system with grid modelling. The design and construction procedure of grounding system can be implemented for various fault current level, and the output performance is evaluated with conventional measured values.

Chapter 4 highlights the estimation of soil parameters in various soil structures and for various number of layers like two, three and multi-layer structure. The simulation of multi-layer soil structure with various soil parameters is carried out. The obtained simulation results are a comparison between traditional two layers, three layer and multi-layer with and without conventional measured earth resistance value.

Chapter 5, the Air Insulated Substation modelling is done using step voltage and touch voltage values and soil parameters for the grounding system is carried out with lesser computational effort.

Chapter 6, the role of Gas insulated substation modelling and installation of grounding Devices with step voltage and touch voltage is discussed. The optimal system modelling and fault analysis of substation device are investigated.

Chapter 7 summarizes the conclusions obtained from the results and future scope of this project.

CHAPTER 2

SOIL RESISTIVITY MEASUREMENTS AND STRATIFICATION OF EARTH STRUCTURE

2.1 Geological Information and Soil Samples

The geological information of the area is very important for design and analysis of the electrical substation. If the soil investigations and geological information of the place is used to understand the behaviour of the soil, rock condition and if it is inadequate, it may lead to failure of the project, delaying of the project and over cost. Hence, the investigation of soil is should be part of the substation design process. Soil sampling is used to find the characteristic of the consent soil. From the conventional soil sampling techniques, we can collect only the soil information and appraisal of data but for the assessment and representation in the ground beneath of the site cannot be known. During site characterization in current soil sampling techniques, a site conceptual model is developed and it's used for the selection and implementation of remedial actions is gathered.

Typical site characterization actions include calculation of the past expenditures of property, site reconnaissance and collection and analysis of environmental samples. The geotechnical investigation of the place consists of surface exploration and subsurface exploration of a site. Surface exploration will include geologic mapping, geophysical methods and photogrammetry of the place. Subsurface exploration usually involves in-situ tests and laboratory test. The mostly used in situ tests are standard penetration and cone penetration tests and mostly used laboratory tests are plasticity test, particle size analysis test etc.

2.2 Soil Resistivity Measurements

The electrical performance of the earth can be found by using the equivalent soil model. The equivalent soil model is a set of obtained soil resistivity measurements. If the measured set of soil resistivity results unrealistic values means, then it needs adequate background investigations. The adequate background investigations may include the

data related to geological metrological and geographical information of the specific area. For example, in geological data which includes soil layer and thickness of the layer. Namely the thickness of the layer gives the retention properties of the all layers. If any variation is found in the upper layer resistivity, then the soil resistivity is taken as a comparison of recent rainfall value against the average seasonal value.

This investigation is used to find the soil model and ground grid resistance determinations through the measurement of soil resistivity. Generally, the soil resistivity measurement can be done by measuring the voltage difference between the two inner potential props in the ground when injecting current. When the potential probe and adjacent current probe are close to each other it indicates the surface soil characteristics through the soil resistivity measurements. However, it requires more number of measurements to achieve it. The average deep soil characteristics of the area can be found by keeping the probes too far away from each other. By doing so the average deep soil characteristics can be found for much larger area. Generally, in practice the adjacent current probe and potential probe are kept based on the same order of magnitude.

However, it is preferable to extend the measurement technique for several times with maximum grounding system dimension. This procedure is used to find the exact soil model when it has more than one layer present in the specific area. But for the soil resistivity measurement the probe spacing can also be decided with respect to the maximum available area which is interfering bare buried conductors.

The soil resistivity measurement test can be affected by various factors such as length of the cable required probe tip measurement technique efficiency, cost and the interpretation of measured data. The various tests can be used for measuring the soil resistivity of the ground in world wide. Among all, the following methods are the mainly considered methods such as

1. Variation of Depth Method
2. Two – Point Method

3. Three – Point Method

- a. Fall of potential Method
- b. The 62% Method

4. Four – Point Method

- a. Wenner Array Method and
- b. Schlumberger Palmer or Unequally Spaced Method.

In homogeneous isotropic ground model, the resistivity is constant. But in non-homogeneous isotropic ground models the spacing of the electrode is vary and the different value of soil resistivity is measured in earth surface or upper layer. By using the above methods, the apparent resistivity and soil model calculation of the soil can be found. This reinforces the requirement for an accurate soil model.

2.3 Variation of Depth Method

In this variation of depth method, the soil resistivity can be measured by passing the current through the earth electrode and the potential between the Earth electrode and the test electrode can be recorded for the calculation of apparent resistivity. In this method the measurement has been taken for many times for different electrode depth. By using an earthed electrode, the depth of the electrode can be increased at each time of measurement. The recorded value will reflect the variation in apparent soil resistivity value with an increased depth of electrodes. This method is time taking method and the driving of the long rods is not practical. So mostly four point methods are used for the soil measurements at large volume.

2.4 Two Point Method

The two-point method of soil resistivity measurement technique is shown in figure 2.1. In this method the total resistance of the unknown soil and axillary Earth can be

measured. The metallic water pipe in close vicinity is used as an axillary Earth. In this method the soil resistance measurement can be done between single rod driven earth electrode and metallic water pipe. The resistance half the metallic water pipe or axillary Earth is assumed to be the order of 1 Ohm. So the value of axillary earth resistance is assumed to be negligible when compared to the unknown Earth electrode. This two-point method mainly is not suitable for measurement of low resistance soil. This method also can be used for the rough estimation of soil resistance value and not for the accurate measurement.

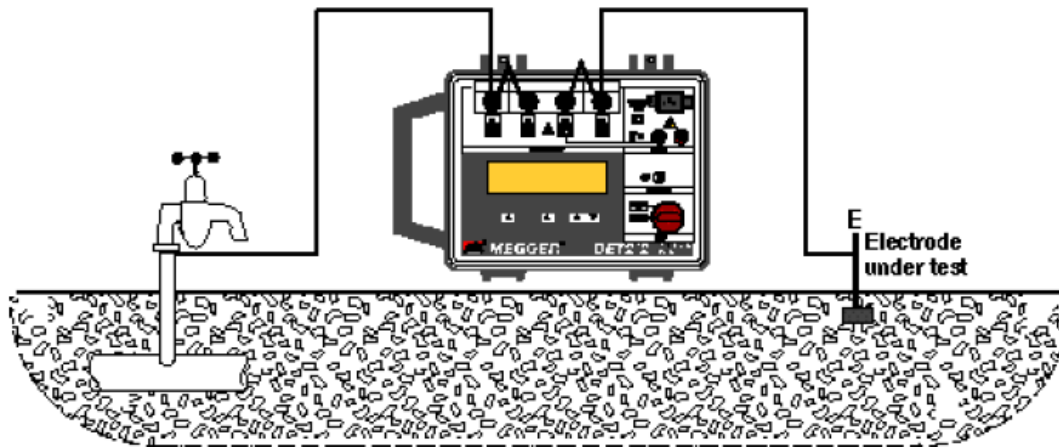


Figure 2.1 Two-point method of earth resistance measurement

2.5 Three Point Method

Three-point method of soil resistivity measurement uses two test electrodes and the resistance of that is R_1 and R_2 . The testing Earth electrode resistance is taken as R_1 . Each pair of electrode resistance can be measured and calculated by the following equations.

$$R_{12} = R_1 + R_2 \quad (2.1)$$

$$R_{13} = R_1 + R_3 \quad (2.2)$$

$$R_{23} = R_2 + R_3 \quad (2.3)$$

Solving the above equations, we get

$$R_1 = \frac{R_{12} + R_{13} - R_{23}}{2} \quad (2.4)$$

where,

- R_1 - Earth electrode resistance
- R_2, R_3 - Test electrode resistance
- R_{12} - Resistance between Earth electrode and Test electrode 1
- R_{13} - Resistance between Earth electrode and Test electrode 2
- R_{23} - Resistance between Test electrode 2 and Test electrode 1

Figure 2.2 shows the three-point method arrangement. If the magnitude of earth electrode is lesser than the two test electrode means this method will not give the accurate results. In this three-point method of soil resistivity technique, the spacing between two test electrodes should be maintained more than 5 metres. This method also is not suitable for the large area earthing systems measurements.

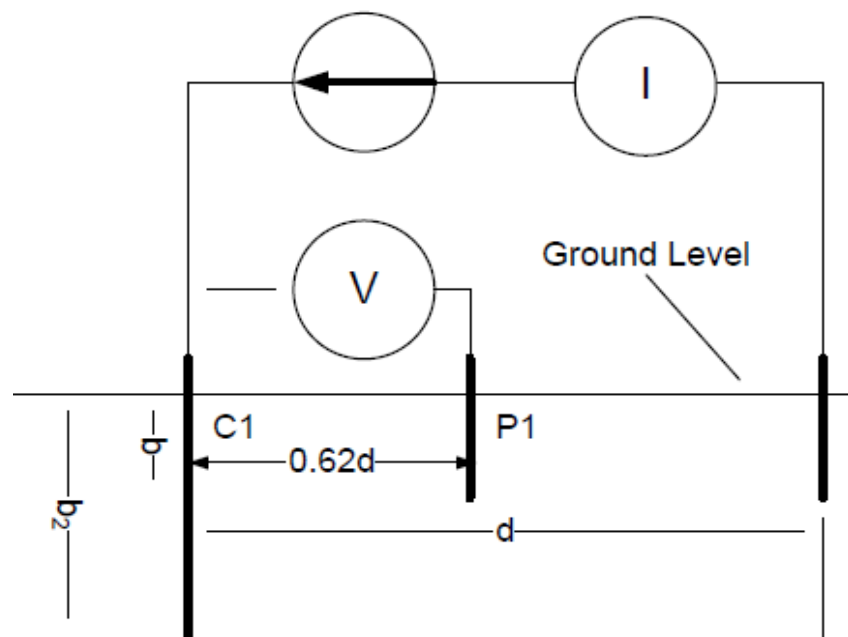


Figure 2.2 Three-point method of earth resistance measurement

2.6 Fall of potential method:

The most commonly used earth resistance is three point (Fall of potential method) method and it measures the earth resistance between the electrode and true earth. This Fall of potential method is derived from the four-point soil resistivity measurement method. This three-point method (Fall of potential method) includes two electrically independent electrodes and one earth electrode and its shown in above figure. Usually it's named as Potential electrode, current electrode and earth electrode. By applying the AC current to the electrode we can able to measure the voltage at the outer electrode circuit. By using the applied current (I) and measured output voltage (V), we can able to find the soil resistance in simple way using ohms' law. But when measuring the output voltage, based on the placement of test electrodes the soil resistance value also will get varied and it's shown in figure 2.3.

When measuring the output voltage, if the electrodes are closely placed means the resistance areas are overlapped each other and it will lead to steep variation in the soil resistance value. But if the electrodes are correctly positioned means the resistance areas are not gets overlapped and we are getting a flat output resistance value. To avoid this problem, it is advisable to take some set of measurement for ensuring the test accuracy. Because of this problem, it will not be used for the measurement for large earthing installation system. In practical the test electrode is driven by 30-meter depth and the current electrode is driven by 50-meter depth. But the potential electrode is placed in between the test and current electrode (between 30m to 50m depth).

The accuracy of fall of potential method will get increased by doing two additional measurements,

1. In first measurement the potential electrode (P) moved 10% from the original position and its given in figure 2.4
2. In second measurement it moved a distance of 10% closer to its original position like figure 2.4

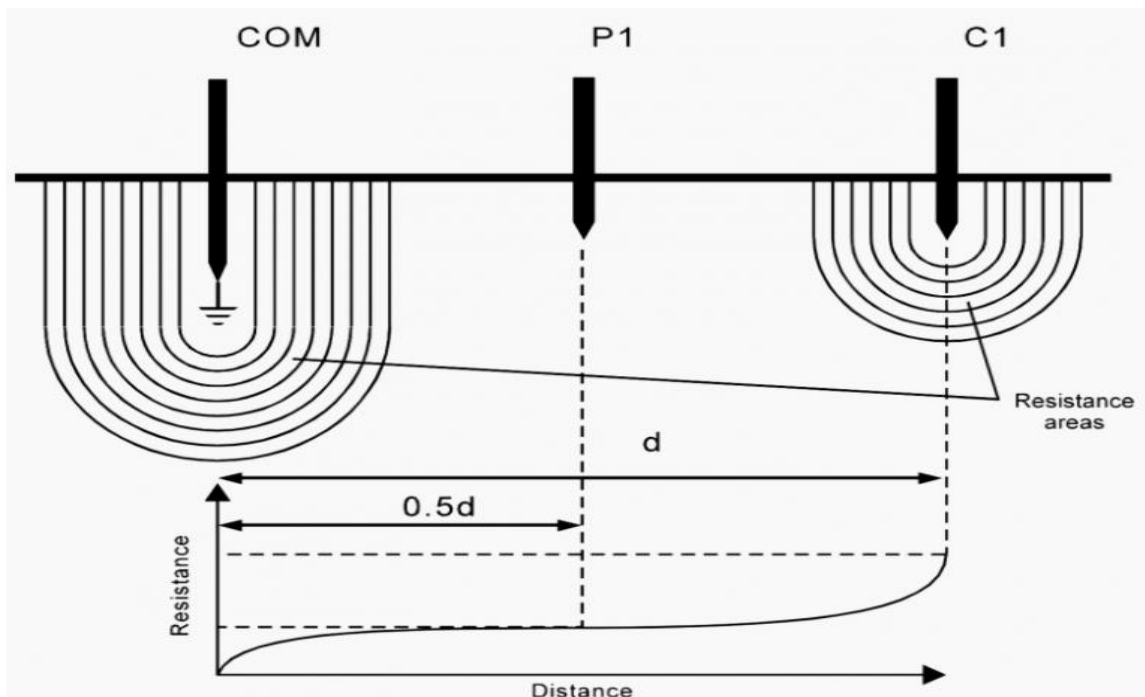


Figure 2.3 Variation of output resistance with electrode position

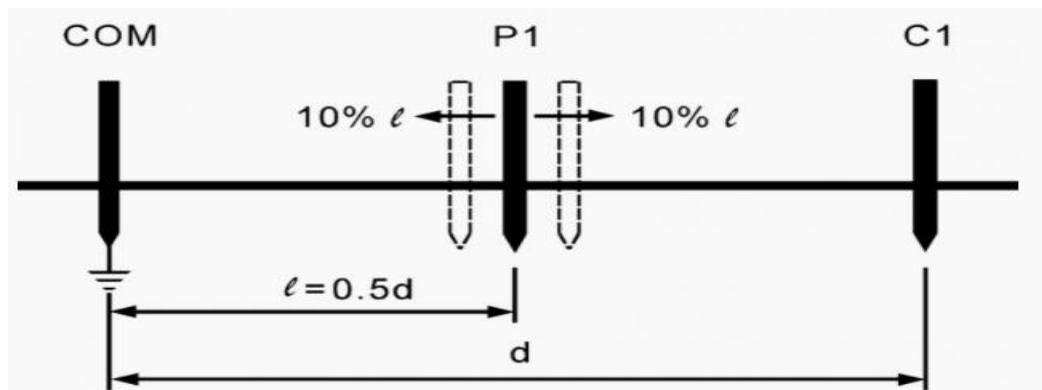


Figure 2.4 Experimental Arrangement for Checking the validity of resistance

2.7 The 62% Method

In this method the medium sized earthing systems will be used and its slightly more than the fall of potential method of measurement. The positioning of the outer stake separation into the earth electrode is 62% in this method. But in the fall of potential method, it was 50%. Because of this reason only it can be called as 62% method of soil measurement. All the other test stake locations are considered as straight line from the

other structures. This method also repeated from the original positions of electrode into $\pm 10\%$ movement. The main disadvantage with this method is that the theory on which it is based relies on the assumption that the underlying soil is homogeneous, which in practice is rarely the case.

2.8 Four Point Method

In four-point method, there are four small sized electrodes used at same depth in the earth and it is driven by same height and equally spaced electrodes in straight line of the earth surface. The soil resistivity mainly affects with the amount of salt content and moisture content available in the soil. Soil resistivity measurements will also be affected by existing nearby grounded electrodes. Buried conductive objects in contact with the soil can invalidate readings if they are close enough to alter the test current flow pattern. This is particularly true for large or long objects.

2.8.1 Wenner Arrangement

The Wenner array method consists of four collinear electrodes with equally spaced distance. Among the four electrodes the outer two electrodes are the current electrodes and the inner two electrodes are the potential electrodes. The current electrode also called as source electrodes and the potential electrode or inner electrode in a Wenner array method is called as receiver electrodes. The Wenner array method is also called as Wenner 4 probe method. In this method the spacing between the all four groups are varied for each test. But the spacing between the adjacent probes are maintained remains constant. The average resistivity of the soil is measured in between the two Centre are inner probes depth equal to the spacing between adjacent probes. If we want to measure the average soil resistivity for maximum depth, we should increase the probe spacing. The main advantage of the Wenner array method is the calculation of apparent resistivity of the soil is very simple. In this method a very small current magnitude is enough to measure the output potential differences between the probes. The figure 2.5 shows the Wenner four probe method experimental diagram.

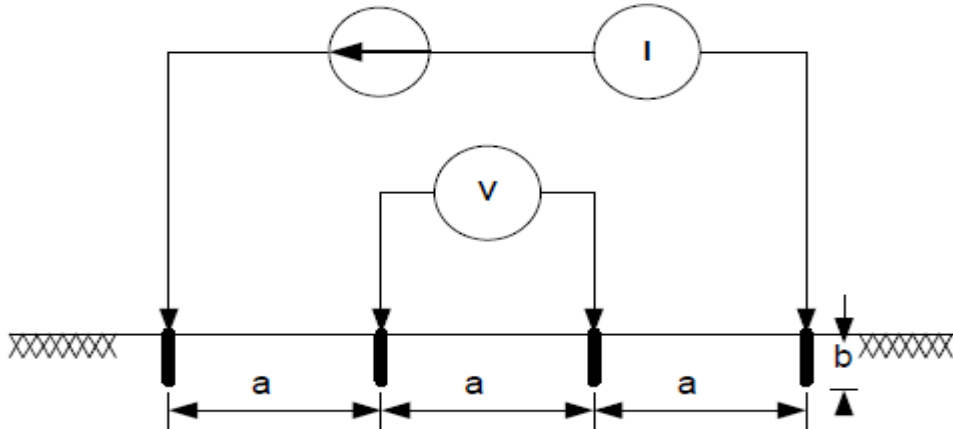


Figure 2.5 Wenner four probe method

If the spacing between the four probes is higher than the penetration or depth of the probe means the apparent resistivity calculation. If the spacing of the electrodes and the depth or penetrations of the probe is equally means the Apparent resistivity calculation is,

$$\rho = \frac{4\pi aR}{1 + \frac{2a}{\sqrt{a^2 + 4b^2}} - \frac{2a}{\sqrt{4a^2 + 4b^2}}} \quad (2.5)$$

$$\rho = \frac{4\pi aR}{n} \quad (2.6)$$

where, the number of layers 'n' varies from 1 and 2, depends on the ratio between the a & b.

When $a < b$,

$$\rho_a = 4\pi aR \quad (2.7)$$

If $a > b$, then

$$\rho_a = 2\pi aR \quad (2.8)$$

where,

- ρ_a - Apparent resistivity in ohm-meter
- a - Spacing between the probes in meter
- b - Penetration of the probe in meter
- R - Measured resistance in ohms

If a=b, then

$$\rho_a = \frac{4\pi a R}{1 + \frac{2a}{\sqrt{a^2 + 4b^2}} - \frac{a}{\sqrt{a^2 + b^2}}} \quad (2.9)$$

The above equation is used for the calculation of apparent resistivity of the soil which is having more than one layer. This equation is developed by Wenner for multi-layer earth structure and it's also called curve fitted equation.

2.8.2 Schlumberger Palmer or Unequally Spaced

The Schlumberger array method also consists of four collinear electrodes for soil resistivity measurements. The outer two electrodes are called as source or current electrodes and the inner two electrodes are called as receiver or potential electrodes like a Wenner array method. But the potential or receiver electrodes are placed with less distance compared to the current electrodes. So that, to this method is also called as an equally spaced soil resistivity measurement technique. Here the probes are moved four to five times for each position of the inner or receiver electrodes. This reduction in probe moment minimizes the lateral variation effect in the soil resistivity test results. So that the maximum time can be saved compared to the Wenner array method. The lower voltage readings can be taken from the array of results. The figure 2.6 shows the soil resistivity measurement setup by using Schlumberger array method.

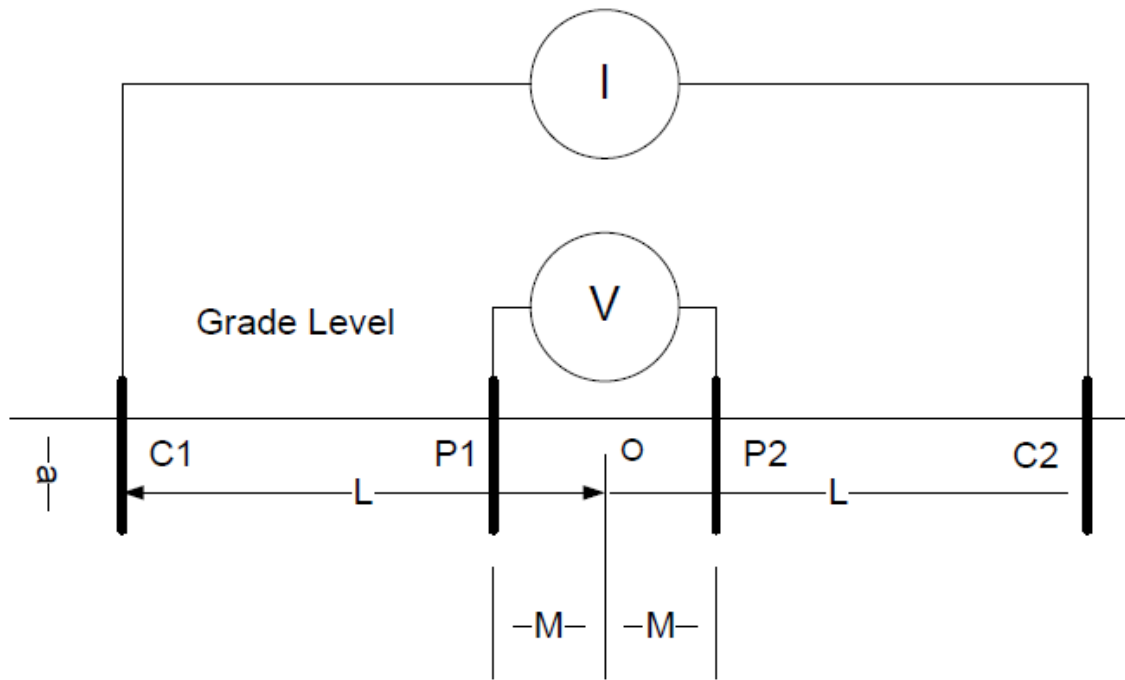


Figure 2.6 Schlumberger array method

The Schlumberger array is more Complex compared to Wenner array method because the spacing between the source and receiver probes are not equal. The following equation is used to determine the apparent soil resistivity by using Schlumberger array method.

$$\rho_a = \frac{\pi L^2 R}{2M} \quad (2.10)$$

Where,

- ρ_a - Apparent resistivity in ohm-meter
- L - Spacing between the outer probes and centre line in meter
- b - Spacing between the inner probes and centre line in meter
- R - Measured resistance in ohms

2.9 STRATIFICATION OF EARTH STRUCTURE

Soil monitoring by using soil resistivity is followed for many of the civil and electrical engineering applications. The substation safety in short circuit condition is mainly depend on the design of grounding grids. Designing of the substation grounding grids depends on the calculation of soil surface electric potential and grounding resistance corresponding to the depth of the soil. For designing the grid, we need to calculate or obtain the exact representation or characteristics of the soil is very important. The exact representation of the soil is derived from the measurements of various soil parameters.

The most of the projects related to grounding is done by the combination of horizontal and vertical spaced ground conductors. The number of soil layers are calculated based on the soil resistivity and thickness of the specific soil layer. If the soil has more thickness in the surface area with low resistivity means it is preferable to use horizontal conductors for grounding. In the thin soil surface cases we can use the horizontal conductors for grounding and for the measurements Wenner method are mostly used. By considering the Soil electric potentiality and thickness we can divide the modelling of the earth structure into three categories namely

- a) Homogeneous Earth Structure
- b) Non- Homogeneous Earth Structure
 - i) Two-layer Model
 - ii) Three to five-layer model
 - iii) Multi-layer model

2.9.1 Homogeneous Earth Structure

In homogeneous earth structure the isotropic earth structure is centrifugally symmetric and measured electrical potential all over the place an insulated electrode is homogeneous. The specific resistivity of the soil is calculated from the measured Voltage, current and resistance. The value of the specific resistivity of the soil in homogeneous earth structure is same in all the places. But, Current density of the

homogeneous earth structure soil decreases with respect to depth. The measurement of potential difference and specific resistivity of the homogeneous earth structure is given figure 2.8. Depth of penetration of current is mainly depend on the spacing between current and potential electrodes. The potential gradient of the homogeneous earth structure soil is calculated from the potential drop between any two points on the soil surface. But in homogeneous earth structure the value of dV/dr is negative because the voltage may decrease with respect to the current flow in electrodes.

When there is small change in soil specific resistivity there should be uniform soil model is used for getting better grounding system. The potential distribution of the hemi spherical shape of grounding device is calculated from the simple potential distribution formula, which is

$$v = \frac{I\rho}{2\pi r} \quad (2.11)$$

where,

‘I’ is the current flowing through grounding electrode into the earth

‘ ρ ’ is the specific resistivity of the soil

‘r’ is the radius of the hemi spherical grounding device

The grounding resistance of the hemi spherical grounding device is,

$$R = \frac{v_0}{I} = \frac{\rho}{2\pi r_0} \quad (2.12)$$

Assuming the soil with isotropic and homogeneous resistivity ρ , and the current source is ‘ I_0 ’. The current density at the surface of the earth is,

$$i = \frac{I_0}{4\pi S^2} \quad (2.13)$$

The electric field is

$$E = \rho i \quad (2.14)$$

Accordingly, the potential of the earth is

$$-grad V = \frac{\rho i}{4\pi S^2} \quad (2.15)$$

The basic potential equation in homogeneous and isotropic earth structure is

$$V_0 = \frac{\rho_0 I}{2\pi} \int_0^\infty e^{-\lambda|z|} J_0(\lambda x) d\lambda \quad (2.16)$$

The potential is measured in any point of homogeneous earth structure electrode with flow of 'I' current.

Where,

ρ_0 – Specific resistivity

$J_0(\lambda x)$ - First order Bessel function

2.9.2 Horizontally Stratified Two Layer Earth model

In horizontally stratified two-layer earth model contains the two layer of earth structure and it is shown in figure 2.7. In two-layer earth model includes three parameters namely first layer (upper layer) soil resistivity ρ_1 and the lower layer (bottom layer) soil resistivity ρ_2 and the depth h_1 of the first layer.

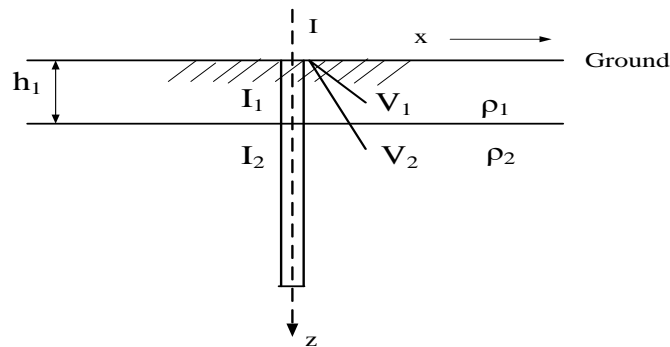


Figure 2.7 Horizontally Stratified Two Layer Earth model

The potential of Horizontally Stratified Two Layer Earth model in any point is

$$V_1 = V_0 + V'_1 \quad (2.17)$$

$$V_2 = V_0 + V'_2 \quad (2.18)$$

where,

V_0 - Homogeneous earth potential

ρ_0 - Homogeneous earth resistivity

According to the basic equation of homogenous earth structure

$$V_0 = \frac{\rho_0 I}{2\pi} \int_0^{\infty} e^{-\lambda|z|} J_0(\lambda x) d\lambda \quad (2.19)$$

First order equation is

$$V_1' = \frac{\rho_0 I}{2\pi} \int_0^{\infty} \{f_1(\lambda)e^{-\lambda|z|} + g_1(\lambda)e^{\lambda|z|}\} \times J_0(\lambda x) d\lambda \quad (2.20)$$

Second order equation is

$$V_2' = \frac{\rho_1 I}{2\pi} \int_0^{\infty} \{f_2(\lambda)e^{-\lambda|z|} + g_2(\lambda)e^{\lambda|z|}\} \times J_0(\lambda x) d\lambda \quad (2.21)$$

We have considered,

Let $|z| = z$, since the direction of z axis is considered as positive value.

The first equation is derived with respect to first layer and second order equation is derived with respect to second layer parameters. In the second order equation, unknown $f_2(\lambda)$ and $g_2(\lambda)$ are calculated by considering the following boundary constraints.

- 1) As $z \rightarrow -$, $V_2 \rightarrow 0$
- 2) At $z = 0$, $\frac{\partial V_1}{\partial z} = 0$
- 3) At $z = h$, $V_1 = V_2$
- 4) At $z = h$, $(\frac{1}{\rho_1})(\frac{\partial V_1}{\partial z}) = (\frac{1}{\rho_2})(\frac{\partial V_2}{\partial z})$

By solving the above two functions with boundary constraints, we get

$$f_1(\lambda) = \frac{k_1 e^{-2\lambda h}}{1 - k_1 e^{-2\lambda h}} \quad (2.22)$$

$$g_1(\lambda) = f_1(\lambda) \quad (2.23)$$

where,

$$k_1 = (\rho_2 - \rho_1)/(\rho_2 + \rho_1)$$

In two layers earth potential $V_2(x)$ is calculated as,

$$V_2(x) = \frac{\rho_1 I}{2\pi \cdot x} [1 + F_2(x)] \quad (2.24)$$

where,

$$F_2(x) = 2 \cdot x \cdot \int_0^{\infty} \frac{k_1 e^{-2\lambda h}}{1 - k_1 e^{-2\lambda h}} J_0(\lambda \cdot x) \cdot \partial \lambda \quad (2.25)$$

' k_1 ' – reflection factor from the first layer to second layer.

' k_1 ' is given by

$$k_1 = \frac{\rho_2^- \rho_1}{\rho_2^+ \rho_1}$$

2.9.3 Three to Five Layer Earth Model

In soil structure have more than two layers, the potential calculation is derived from the same voltage equation and for the horizontally stratified three to five soil layer earth structure is follows the given boundary constraints

- The lowest bottom layer potential z goes from infinity to zero
- The flow of current in earth surface is considered as zero
- The potential difference of the layer is same for either side of the boundary
- The current flow between the two different layers are considered as continuous.

Based on the above boundary constraints, the horizontally stratified three to five-layer model is derived below,

For the two layer of earth structure case

$$f_1(\lambda) = g_1(\lambda) = \frac{k_1 e^{-2\lambda h_1}}{1 - k_1 e^{-2\lambda h_1}} \quad (2.26)$$

where,

$$k_1 = \frac{\rho_2^- \rho_1}{\rho_2^+ \rho_1}$$

for third layer

$$f_1(\lambda) = g_1(\lambda) = \frac{k_{31} e^{-2\lambda h_1}}{1 - k_{31} e^{-2\lambda h_1}} \quad (2.27)$$

where,

$$k_{31} = \frac{k_1 + k_2 e^{-2\lambda h_2}}{1 + k_1 k_2 e^{-2\lambda h_2}}$$

$$k_2 = \frac{\rho_3 - \rho_2}{\rho_3 + \rho_2}$$

for forth layer

$$f_1(\lambda) = g_1(\lambda) = \frac{k_{41} e^{-2\lambda h_1}}{1 - k_{41} e^{-2\lambda h_1}}$$

where,

$$k_{41} = \frac{k_1 + k_{42} e^{-2\lambda h_2}}{1 + k_1 k_{42} e^{-2\lambda h_2}}$$

$$k_{42} = \frac{k_2 + k_3 e^{-2\lambda h_3}}{1 + k_1 k_3 e^{-2\lambda h_3}}$$

$$k_3 = \frac{\rho_4 - \rho_3}{\rho_4 + \rho_3}$$

for fifth layer,

$$f_1(\lambda) = g_1(\lambda) = \frac{k_{51} e^{-2\lambda h_1}}{1 - k_{51} e^{-2\lambda h_1}}$$

where,

$$k_{51} = \frac{k_1 + k_{52} e^{-2\lambda h_2}}{1 + k_1 k_{52} e^{-2\lambda h_2}}$$

$$k_{42} = \frac{k_2 + k_{53} e^{-2\lambda h_3}}{1 + k_1 k_{53} e^{-2\lambda h_3}}$$

$$k_{42} = \frac{k_3 + k_4 e^{-2\lambda h_4}}{1 + k_3 k_4 e^{-2\lambda h_4}}$$

$$k_3 = \frac{\rho_5 - \rho_4}{\rho_5 + \rho_4}$$

2.9.4 Multilayer Earth Model

For the designing of multi-layer earth model the parameters like potential differences, soil resistivity and each layer thickness are considered. The potentiality of each layer and electric field is varied according to the depth of the soil structure and is given figure 2.8. the figure shows the horizontally stratified N layer earth structure and the multi-layer model is derived from the continuation of three to five-layer model.

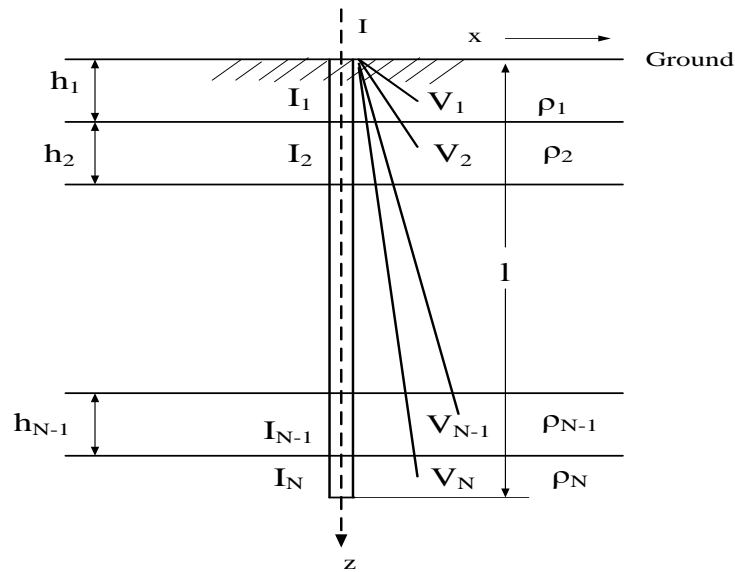


Figure 2.8 Multi-layer earth structure

In multi-layer model the voltage at any point x is derived at the current value of 'I' in surface electrode is given following equation

$$V_N(x) = \frac{\rho_1 I}{2\pi x} [1 + F_N(x)] \quad (2.28)$$

where,

$$F_N(x) = 2 \cdot x \cdot \int_0^{\infty} \frac{K_{N1} e^{-2\lambda h_1}}{1 - K_{N1} e^{-2\lambda h_1}} J_0(\lambda \cdot x) \cdot \partial \lambda$$

and

$$k_{N1} = \frac{k_1 + K_{N2} e^{-2\lambda h_2}}{1 + k_1 K_{N2} e^{-2\lambda h_2}}$$

$$k_{N2} = \frac{k_2 + K_{N3}e^{-2\lambda h3}}{1 + k_1 K_{N3}e^{-2\lambda h3}}$$

$$\dots \dots k_{NS} = \frac{k_S + k_{NS+1}e^{-2\lambda h(S+1)}}{1 + k_S k_{NS+1}e^{-2\lambda h(S+1)}}$$

$$k_{NN-2} = \frac{k_{N-2} + K_{NN-1}e^{-2\lambda h(N-1)}}{1 + k_{N-2} K_{NN-1}e^{-2\lambda h(N-1)}}$$

$$K_{NN-1} = k_{N-1}$$

In addition,

$$k_1 = \frac{\rho_2 - \rho_1}{\rho_2 + \rho_1} \dots \dots k_S = \frac{\rho_{S+1} - \rho_S}{\rho_{S+1} + \rho_S}$$

$$k_{N-1} = \frac{\rho_N - \rho_{N-1}}{\rho_N + \rho_{N-1}}$$

2.10 LITERATURE SURVEY

In this section, the conventional literatures related to the estimation of soil parameters by using the measurement of the earth resistivity and impedances are investigated. Many soil resistivity based techniques are proposed for the estimation of number of soil layers and for better grounding systems and it is under active area of research for the system grounding. First, a review of homogenous and non-homogenous earth system with two-layer earth structure case is analysed. Then, investigations on three to five-layer soil structure is discussed. Finally, the multi-layer earth structure is analysed for the determination of ground potential rise in order to design better grounding system.

R. L. Smith-Rose et.al., proposed various electrical properties of the earth for different frequency levels. The measurement was taken for the frequency range of 50 cycles to 200 million cycles per second. The measurement of soil resistivity and reactance for the various range of frequencies like 100 to 10000 kilo cycles per second. From the measured data with different depth level the resultant curves are drawn for different frequencies. From the results the author concluded that the alternating at the soil surface may penetrate up to a depth of 20 meters (over 60 ft.).

H. G. Taylor et.al., examined the constraints of the alternating current loading capacity by using the earth electrodes under three different conditions like long duration loading, short duration overloading and long duration overloading. In long duration loading condition the current flow through the earth is large and it's not enough to disturb the continuous supply. But in the short and long duration overloading condition the protective gear may get operating. In long duration overloading condition it also leads to the failure of the protective gear and its get earthed through the tuned reactance coil at any one phase of the supply.

H.R. Armstrong was presented the grounding electrode performance test at various methods, like model method, resistance and voltage gradients for multiple rod electrodes, sparking gradient method, current distribution in extended multiple rod method, filed test and current capacity of electrodes in various soils. From the results current carrying capacity of the soil was calculated for simple and multiple electrode cases.

F. Dawalibi et.al., explained the soil characteristics through parametric analysis for various ground fault currents. The results are analysed in direct earth connection or coupling method. The results are given both theoretical and practical value in self and mutual impedance of underground and overhead substation conductors.

R. Caldecott et.al., investigated the interpretive techniques of the soil resistivity measurement techniques. The test was conducted at various places with two-layer soil structure. The various parameters of the soil like height and specific resistivity of the soil layers are calculated and verified in both the theoretical and practical values. The practical test was done by the electrolytic tanks and this device is constructed for finding the characteristics of the grounding grid model. The most of the tests are carried out under 1.0-meter diameter hemispherical return electrode and this return electrode may use to limit the maximum probe depth and spacing between the electrodes in this proposed method.

Magdy F. Attia et.al., suggested time domain induced polarization method for modelling the earth structure as a different layer. The method was done by using Direct Current and the layers are assumed as horizontally stratified. In this numerical

algorithmic method, the soil various soil characteristics like chargeability, DC resistivity and thickness of each layer. The numerical examples are used to find the calculated value of the substation soil parameters and characteristics.

Damir Cavka et.al., compared the soil parameters like soil conductivity and resistivity for different models in different frequency levels. The models are developed with curve fit expressions for the calculation of relative permittivity and of the soil and resistivity. The measured experimental data was compared with six different electrical soil models like Scott, smith Longmire, messier and Visacro – Alipio methods. The soil electrical models causality is tested by Kramers – Kronig relationship. All the soil models are tested with the lightning current at two cases namely a simple horizontal electrode and realistic grounding electrode with wind turbine system. The obtained results are compared with all six different models and it shows that the Visacro – Alipio expression model gives better results among other models.

Jinliang He et.al., calculated grounding resistance value for various substation equipment's like grounding grids and tower footing resistances. While calculating the maximum value ground fault current and maximum hazardous touch and step voltages are considered. The fault current division factors are calculated for different seasonal conditions with different top layer soil resistivity values. For this analysis two substations are considered and both are connected with the transmission lines without neutral and other connecting transmission lines. The analysis was done for vertical and horizontal grounding rods. By comparing both the methods the vertical grounding rod method is giving better results in various seasonal condition.

Wesley Pacheco Calixto et.al., proposed a 3-D soil stratification methodology for finding the soil characteristics in a substation. In this method the exact substation grounding system was developed by using the 3-D soil resistivity calculation method. The proposed 3-D soil resistivity calculation method is sub modelled into squared subareas and a geo electrical prospection method. The soil stratification results like number of layers, soil resistivity, height of the layer and spacing between the electrodes are achieved by the Wenner's method and genetic algorithm.

F. H. Slaoui et.al., designed substation grounding system for the high voltage substation and power distribution and transmission system. The multi-layer earth structure is a realistic representation of the actual earth structure. The Soil characteristics are estimated based on a set of practical measurements of soil resistivity. Inversion method is used here for the soil parameter calculation. The input for the inversion method soil resistivity calculation is from Schlumberger measurements.

P.J. Lagace et.al., estimated the soil parameters for the place with some of observations. The proposed model was developed for the horizontal multi 'N' number of layers with different depth and horizontal layers. The various soil parameters and apparent soil resistivity are calculated by using the electrostatic images. The proposed model was developed as a nonlinear function and the resultant soil layer depth and resistivity's are calculated. The electrostatic images are giving better efficiency with considering sensitivity factor. The proposed results are compared with practical measured results for various two-layer earth structure.

Hyung Soo Lee et.al., proposed the grounding performance for multi-layer soil structure in uniform and horizontally stratified soil. The developed model is mainly depending on the structure of the available soil structure and height for producing better and efficient results. In the absence of ground of rod condition the resultant soil resistivity value is very high in nature. At this condition the top layer of the soil surface may have high in value. But the better efficiency is achieved when the top layer of the soil surface may have very less in value.

In order to better quantify the behaviour of an earth electrode subjected to a lightning current impulses, it is necessary to understand the commonly encountered scenario of ground with various layers resulting from geological stratification. Once this knowledge has been obtained it may then be applied in design of efficient earthing and lightning protection systems.

CHAPTER 3

GROUNDING GRID MODELLING

3.1 Grounding Grid Modelling

The primal design objective is to obtain a minimal earth resistance of grounding the grid of a substation. Nevertheless, the latest designs procedures are equipped with control of step as well as touch potential within the prescribed range. The design of the grounding system primarily relies on the soil resistivity model that is chosen for grounding the substation soil. The three types of models that are widely deployed are uniform model, two or twin layers and multi-layered model. A more precise soil model can be designed by employing appropriate measurement strategy for quantising the soil resistivity. The design of such grounding system may turn out to be inaccurate if mean resistivity used in calculations is with more than 25% variation resistivity at different probe distances. Hence, the two-layer soil models become a natural choice.

Computer software is employed to design of grounding system. This will indeed improve the accuracy. At the same time, there is a demand to construct empirical formulas to estimate the required design parameters. These empirical works eventually aid the design engineers to approximate the design parameters of the grounding systems. This chapter will concentrate on Air Insulated Substation (AIS) grounding grid design and proceed in the following manner:

- Data analysis using CDEGS software
- Modelling the soil resistivity with appropriate number of layers
- Simulating the fault current from the collected data
- Isolating the unsafe grid areas that are dangerous for touch as well as step potentials.

3.2 Voltage Levels

The choice of the optimal voltage levels totally relied on the load to be offered and also on the gap between generation the load and source. It can be witnessed that large power plants are generally situated at larger distances from load centres in order to handle the

fuel supplies, source of energy, cooling strategies, costs at the sites, environmental factors and availability. For the above mentioned causes, a high 765 kV voltages are used for transmission. Further the transmission system at the substations offers bulk power that operate in the voltages range of 69 to 765 kV.

Multiple elements inspire the choice of appropriate type of substation pertaining to any application. The selection criteria depend on voltage level, environmental considerations, load, limitations at site space, and transmission-line. Tremendous effort is required in determining the equipment cost, labour, and land. The major expenses at the substations are mainly dependent on the count of power transformers that are deployed, circuit breakers, and uncoupling the switches and associated structures with their foundations. Apart from this the choice of insulation levels as well as the coordination practices also impacts the cost, where Extra High Voltage (EHV) deserve a special mention. The high voltage in the design can be reduced through two levels of voltages as mentioned below:

Touch Voltage: The preliminary distinction between the touched object and the ground point occurs when ground currents flow through it. This is defined as maximum potential difference between an earthed metallic structure that is capable to be touched and ground point during fault current flow. A generic measure is to maintain 1m between the ground point and metallic structure.

Step Voltage: This is the measure in the change in surface potential that is felt by a person at a 1m distance without touching any other objects that are grounded. This can be further explained as maximum difference in the potential between the feet during the flow of a fault current.

Ground Potential Rise (GPR): This is defined as the maximum electrical potential attained by a grounding grid of the power substation with respect to a remote grounding point which is presumed to be anywhere at remote earth's potential. The GPR is same as the product of maximum grid current and grid resistance.

Mesh voltage (E_{lm}): This is the maximum touch voltage within the limits of the ground grid mesh.

Metal-to-metal touch voltage (E_{mm}): This is a measure of the potential change among metallic structures or objects within the range of substation site that is bridged either by direct hand-to-feet or hand-to-hand contact.

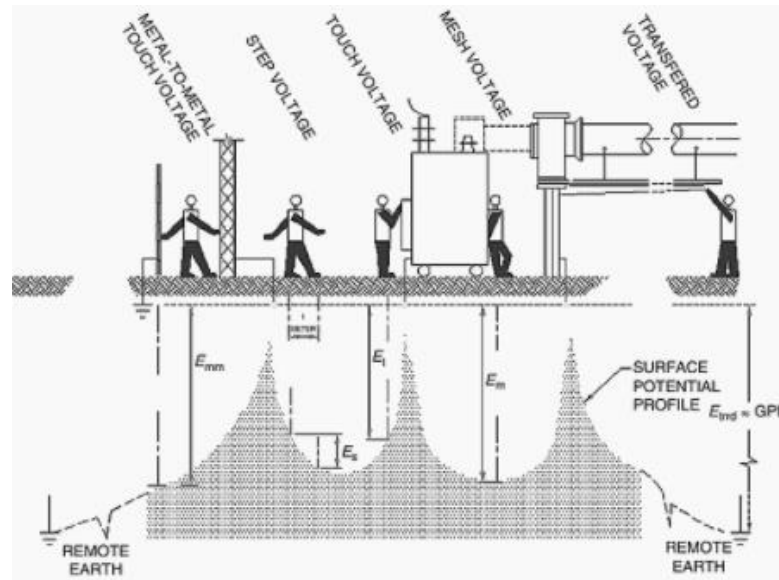


Figure 3.1 Touch, Step and Transferred Voltages

Figure 3.1 clearly displays the above-mentioned phenomena. To reduce the potentials to the permissible values of currents flow in human body, to confirm the electrical safety, and to confine the electrical interference with any other third-party equipment, the AIS should be offered with an appropriate earthing system that connects all the non-live metallic installation parts. The common elements can be metallic structures, surge arresters, earthing switches, switchboard enclosures, motors, metallic fences. And transformers rails.

3.3 CDEGS – SOFTWARE

CDEGS software is primarily designed to deeply investigate the issues involved in grounding and earthing process. The following are the main modules in CDEGS:

MALZ: This module analyses the complete frequency domain efficacy of the buried conductor networks, estimates the earth as well as the conductor potentials, longitudinal current distribution and leakage current distribution.

SESCAD: This is a program to edit or view 3-D networks of grounding conductors, interference of AC, and transient or lightning studies.

RESAP: This finds the equivalent earth structure models that is selected based on soil resistivity data.

CDEGS is a computer-based electrical engineering software that models the program based on IEEE 80.

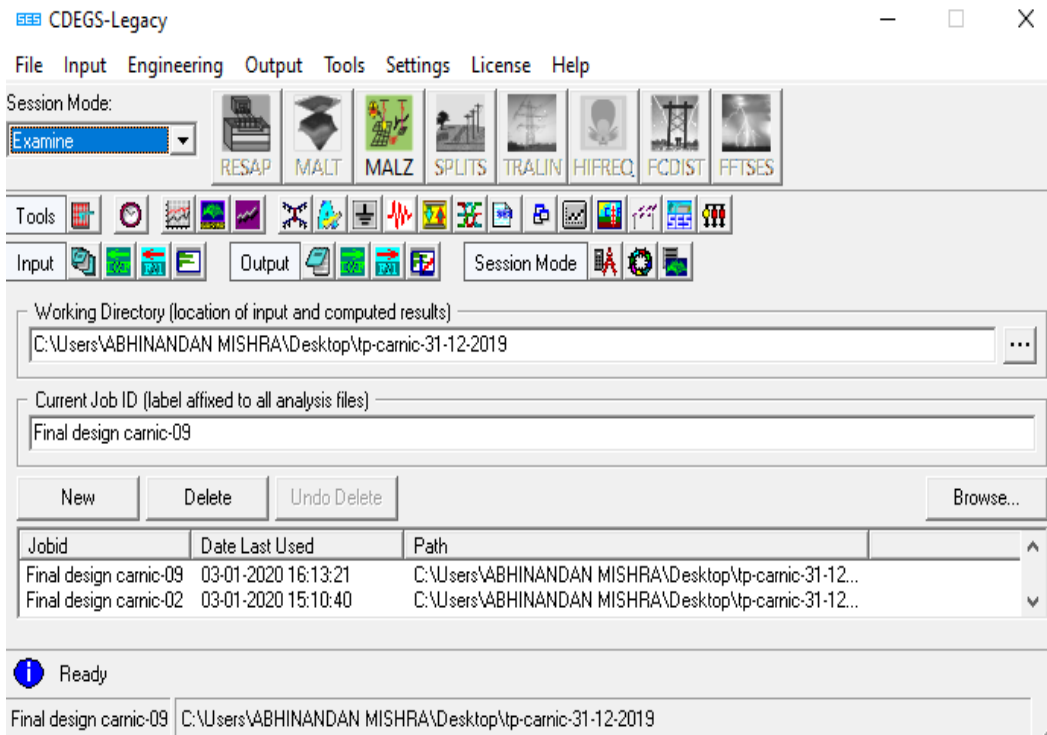


Figure 3.2. Screenshot of CDEGS Software Package

The snapshot of the CDES software package is displayed in figure 3.2. The **Current Distribution, Electromagnetic Fields, Grounding and Soil Structure Analysis (CDES)** is an integrated software tools pertaining to engineering design to analyse the issues in earthing and grounding process, electromagnetic fields and its interference.

3.4 EARTHING DESIGN ANALYSIS

Earthing design analysis is proceeded as:

Step 1: Soil Resistivity

Soil Resistivity analysis module (RESAP) analyses and interprets soil measurement data to obtain appropriate soil model. More than one soil model can be selected for detailed study from those secured from all the measurement traverses with explanation about the choices. It is predicted that more than one more soil layers may be demanded

in the computer model to sufficiently represent the medium of grounding process. The graphical representations of apparent resistivity and the computer apparent resistivity curve for every measurement traverse can be provided that effectively demonstrates chosen soil models in the context of soil's electrical property.

Step 2: Computation of grid impedance and grid design for grounding

MALZ engineering module that is Frequency-dependent, accounts for longitudinal voltage drop in conductors, accounts for circulating currents, shall be used.

- a. With SESCAD program, Main grid shall be modelled as first step at required depth of burial. The grid will generally cover entire substation.
- b. The grid conductor size shall be calculated as per standard IEEE80-2013

Step 3: Analysis of fault current distribution

FCDIST, a more simplified module for fault current distribution is employed for computing the distribution of fault current. The step and touch voltages in grounding network are directly related to fault magnitude that is discharged into the soil by the underlying grounding network. Hence it is paramount important to estimate the ratio of discharged fault current in grounding grid. The same ratio can be determined from the graph according to the standards of IEEE 80 2013.

Step 4: Analysis of Grid with Fault Current

The grid so designed as per Step 2 shall be energized with fault current arrived as per Step3. Touch and Step potential shall be computed by defining safety criteria and the results shall be compared with thresholds safety limits determined based on the Standard IEEE80-2013.

Step 5: Safety Criteria and Safety evaluation

Safety Threshold Limit shall be generated as per Standard IEEE80-2013 by defining,

- a. Surface soil, that is a crushed rock with wet resistivity of 3000 Ohm-m to a thickness of 75mm to 200 mm. Underlying soil (subsurface) resistivity is taken automatically from Soil model. (Step1)
- b. Fault clearing time

c. Body weight. Tolerable limit for touch and step shall be calculated for 50Kgs and 70Kgs.

d. X/R Ratio.

3.5 Grid Conductor Sizing

Calculated grid conductor sizing as per IEEE std. 80 – 2000 and input data (Properties of Steel referred as per Item 09 Table 1 of IEEE std. 80-2013).

- (i) Conductor Material – Steel
- (ii) System Voltage, V – 132 kV
- (iii) Fault Current I_f – 16 kA
- (iv) Fault Duration, t_c – 3 sec.
- (v) Maximum Allowable Temperature, T_m – 620°C
- (vi) Ambient Temperature, T_a – 50°C
- (vii) Thermal Coefficient Resistivity at reference Temperature, α_r – 0.0016
- (viii) Resistivity of Ground Conductor, ρ_r – 15.9 $\mu\Omega$ -cm.
- (ix) Thermal Capacity Factor, TCAP – 3.28 J/cm³. °C
- (x) K_0 ($=1/\alpha_0$) – 605

To calculate the conductor as per the standard IEEE 80 – 2013 is,

$$A = \frac{I_f}{\sqrt{\frac{TCAP}{t_c \alpha_f \rho_r} \ln\left(\frac{K_0 + T_m}{K_0 + T_a}\right)}} \quad 3.1$$

After solving equation 3.1,

Calculated Conductor Size – 308 sq.mm

Conductor Size Equivalent Diameter – 20 mm

Corrosion allowance for thickness – 2.25 mm

Hence, minimum size required will be 22.25mm

Thus, diameter of steel conductor – 25 mm

A brief review of the empirical studies is carried out to gain in depth understanding of properties of the soil when subjected to high impulse currents.

B.R.Gupta et al. (1980) proposed an empirical formula that analyses the impulse impedance of the underlying grounding grid. The validity of proposed analytical method is examined using model tests. The primary finding from this study that there is no profound impact can be observed from the soil ionization on the impulse impedance in grounding process at high voltage substation.

R.Verma and D.Mukhedkar (1981) analysed the response of grounding grid when it is subjected to ramp impulses inputs as well as double exponential waves. The result of this investigation is the impulse impedance escalates to higher values at initial stage and then gradually reduces to reach steady state. The high initial value of impulse impedance is not only raise the earth surface potential also affects the insulator flashover at towers. Hence, the grounding grid should be designed in such a way that it must maintain low impulse impedance with grid inductance as a major factor.

S.Visacro (2007) presented some important aspects of transient behaviour of grounding system. The first aspect is that the termination to earth exercises three effects namely resistive, capacitive and inductive. Figure 3.4 portrays the circuit that effectively represents the existing components in the soil as well as electrode.

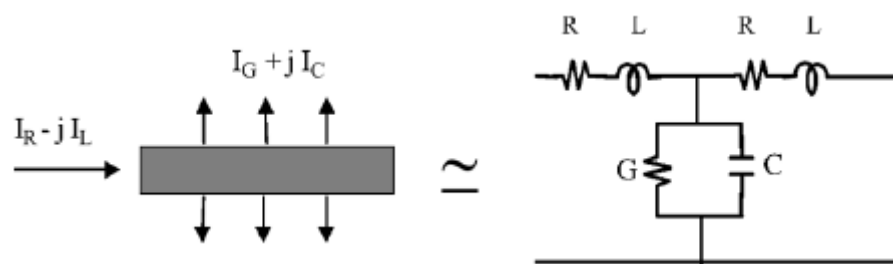


Figure 3.4 Current Components: at Electrode and Soil

The current comprises of two major components: First is the leakage transversal current (I_T) that directly spreads into soil along with transversal current (I_L) that is transferred to the residual length of the electrode used. Second the existing longitudinal current triggers internal losses to the conductor used at the same time develops a magnetic field in and around the electrode. Figure 3.3 depicts a series resistance (R) with the inductance (L), where RL branch is accounted for the effects. Both the parameters

experience a significant drop in the voltage along the electrode when the current flows through it.

The leakage current develops an electric field in the soil, which is considered as a medium with permittivity ϵ and resistivity ρ . This ultimately determine the conductive flow and also the capacitive currents that flows through the soil. The ratio of conductive current and capacitive currents is independent of electrode geometry.

The impulsive grounding impedance is closely related to current waveform as well as parameters that are observed at front time. These two aspects vividly describe the two grounding behaviours, namely (1) soil or medium behaviour when imposed with electromagnetic phenomenon and (2) electromagnetic coupling that occurs between the entire grounding components which includes the propagation effects. The former relies only on soil properties, but the latter is heavily influenced by the configuration geometry of the electrodes used.

Jinliang He et.al (2008, 2011 & 2012) investigated the characteristics of lightning impulses and breakdown delay of the frozen soil. Apart from this, the transient characteristics of grounding are also determined from the impulse breakdown. This proves that the impact of soil ionization with the electrodes that are grounded are to be taken into consideration in for achieving better accurate lightning protection. Breakdown of the soil impulse cause a delay which eventually decreases with the increase in the applied impulse voltage. Generally, this delay experienced during the soil breakdown is eventually greater when the soil moisture is high, or soil temperature is low, or at larger soil density. The detailed experimental analysis reveals that the breakdown of soil subjected to the impulse can be claimed as electrical process not as thermal process. This is due to the electrical breakdown generated by the voids among the underlying soil particles. Further, the impulse breakdown delay imposes strong influence on lightning protection mechanism of the transmission line at low voltage levels.

S.Visacro et.al (2009) analyses the transient behaviour of the existing grounding systems that rectifies the basic aspects of these systems when subjected to lightning

currents. The detailed result analysis reveals that when subjected to fast current wave, the impulsive grounding impedance denoted as Z_P of the shorter electrodes is considerable lesser than its corresponding low frequency resistance (R_{LF}) at the same time, the electrodes that are longer than the length will possess resistance values that are very much lesser than the impulsive impedance. The ratio (Z_P/R_{LF}) of the experiments are comparatively less than the numerical simulation of the electrodes that are relatively shorter than the estimated effective length. S.Visacro et.al (2011, 2012 & 2013) also examined the impact of frequency in soil characteristics with variety of electrodes with the grounding grid.

F.E. Asimakopoulou et.al (2010) examined the properties of the grounding system in terms of fault current that differs from the steady state. It can be seen that when higher current is subjected into the grounding system, the impedance declines due to ionization. This forms the soil's critical electric field.

A numerical and experimental investigation is done by Jing Li et.al (2011) about the grounding electrode impulse against the dispersal regularity of the current by including the transient ionization. Electromagnetic field is due to the surge current that flows in the grounding system embedded in the soil is totally time varying. This study integrates the finite element method and finite difference time domain for determining the transient soil ionization. The leakage of high impulse current into the soil is due to soil ionization. This space – time varying soil resistivity approach is mainly deployed for simulating the ionization of soil ionization by varying the time.

An extensive numerical analysis is performed using the single vertical rod. High magnitude current is essential to find the soil ionization phenomenon. At higher current magnitudes, FEM analysis pertaining to grounding soil and GPR is found at varying current magnitudes. It is evident that resistance value declines as the current magnitude increases. Hence it is quite essential to analyse the breakdown soil properties. The results reveals that there is an agreement among the measured and numerical analysis.

To smoothen the non-regularity in current dispersal the ground electrode is used as a shield between the grounding conductors. Further, the decline in resistivity of the soil

can be attributed to the ionization caused due to direct Touch Voltage. However, the ionization of soil that immediately surrounds the grounding electrode alters the distribution of current resulting in the formation of Step Potential. Hence it becomes quite essential to consider the ionization of soil as well as the non-uniform leakage in the current distribution when estimating the grounding system.

N.M.Nor et.al (2013) exhibited the results of impulse characteristics of an earthing system through FEM. The outcomes portray that during transients, the impulse resistance display different values than when subjected to DC. This obviously decreases with the magnitude of current. A greater reduction can be witnessed at higher DC earth resistance. Also, it can be sensed that a 2 – rod earthing systems exhibits better, or larger reduction in resistance than the 4 rods. The FEM simulation reveals that, the Electromagnetic coefficient relies on earthing systems. Hence, it is evident that the process of ionization occurs at reduced voltage or currents with higher earth resistance.

M. Mokhari (2015) formulated an improved circuit model of grounding electrode that considers the current rise rate and soil ionization. The nonlinear resistance along with computed inductance change when lightning current parameters are altered. Hence, A more accurate voltage response can be achieved.

CHAPTER 4

HYBRID OPTIMIZATION AND STEEPEST DESCENT METHOD FOR OPTIMIZATION OF SOIL PARAMETERS IN MULTIPLE LAYERS OF GROUND STRUCTURE

4.1 Introduction

A pre-requisite for design and installation of grounding systems is soil structure analysis. Field simulations using circuits achieve proximity to established grounding systems when soil structures and characteristics are estimated and where computed parameters represent soil's electrical departments. Real time practices approximate multilayer soil structures in horizontal stratifications and compare apparent resistivity curves with experimentally observed apparent resistivity curves.

The estimations of soil's parameters and closeness of optimized parameters to measured data is critical to the erection of grounding grids. The projected horizontal soil parameters reflect its non-uniform stratification. Ideal Wenner technique is generically used for measuring apparent soil resistivity and the computed values are compared to theoretical apparent resistivity data. Soil's behavior can be quantified when measured and computed values are close to each other. Assumptions that soil is isotropic in nature created issues in the model's tests which revealed that the examined sites were not homogenous in nature.

Comprehending soil structures needs studying multiple soil layers and investigating upper soil layers alone is not sufficient for conclusive assessments. The study analyses of multilayer soil structures are based on grounding rods buried in the soil which are viewed in close accordance with observed site data. The comparative estimates may be based on a multitude of techniques including Quassi Newton method, Complex image approaches, SDMs (Steepest Descent Methods), GAs (Genetic Algorithms) DEs (Differential Evolutions) and PSOs (Particle Swarm Optimizations). This chapter proposes a hybrid method where a combination of GAs and PSOs called (GA-PSO)

which results in optimized estimations of multi layered soil structures. This work also uses SDMs for estimating TGPRs (Transient Ground Potential Rises) in Substations.

4.2 Four Point Wenner

The Wenner 4-point tests are used for determining soil resistivity. In these tests four spikes are driven into the ground in a straight line and equidistant from each other. A specified current is passed between probes or electrodes at the wire's ends. Potential differences between spikes that occur during soil resistance referred to as potential probes are measured. Experimental arrangement to determine the soil resistivity is shown in figure 4.1.

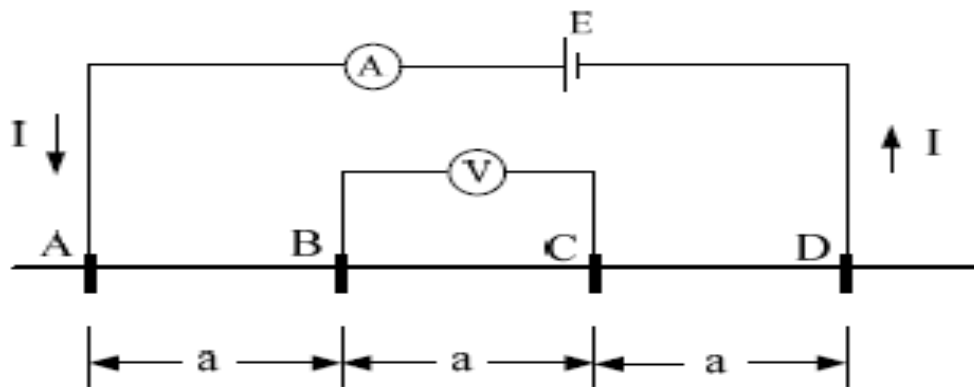


Figure 4.1 - Four Point Method

Electrical interferences cause registration of undesired signals. The presence of metallic items in the electrical line also results in poor quality readings. The clearance between pins and nearby metallic structures should at least be equal to their pin spacing.

A four-terminal channel is created where resistances are dependent on uniform spacing of gaps 'a' between the four electrodes. The setup's resistances are measured using terminals 'A' and 'D' as current electrodes while 'B' and 'C' as voltage electrode terminals. Electricity is passed into the earth via 'A' which returns via 'D' to the circuit. The voltage electrode terminals compute potential drops in ground voltages that are studied. The remaining applied current 'I' and potential drop 'V' produces a resistance 'R' which is used for obtaining apparent resistivity curve experimentally using Ohm's law. It is depicted using equations 4.1 to 4.8 and explained. Equation (4.1) defines the observed apparent resistivity curve,

$$\rho_a^m = 2\pi aV/I \quad (4.1)$$

Where ‘a’ stands for the distance between consecutive electrodes. When homogeneity/Isotropic earth are assumed, a point’s potential ‘ V_0 ’ can be depicted as equation (4.2),

$$V_0(x) = \frac{\rho_0 I}{2\pi} \int_0^\infty e^{-\lambda|z|} J_0(\lambda \cdot x) \cdot \partial\lambda \quad (4.2)$$

where ‘ J_0 ’ represents Bessel function. For electrodes situated on the earth’s surface with two layers, potential $V_2(x)$ is computed using Equations (4.3) and (4.4),

$$V_2(x) = \frac{\rho_1 I}{2\pi x} [1 + F_2(x)] \quad (4.3)$$

$$F_2(x) = 2 \cdot x \cdot \int_0^\infty \frac{k_1 e^{-2\lambda h}}{1 - k_1 e^{-2\lambda h}} J_0(\lambda \cdot x) \partial\lambda \quad (4.4)$$

Where, ‘ k_1 ’ is the reflection of the upper layer (first) on the lower layer (second) and can be computed using Equation (4.5),

$$k_1 = \frac{\rho_2 - \rho_1}{\rho_2 + \rho_1} \quad (4.5)$$

Multiple structures of earth’s layers (n) are optimized for resistivity ($\rho_1, \rho_2, \dots, \rho_n$), thickness (h_1, h_2, \dots, h_{n-1}) where thickness of the nth layer is considered infinite. The electrode point binding multilayered earth point x ’s potential $V_n(x)$ can be depicted as Equations (4.6) and (4.7),

$$V_n(x) = \frac{\rho_1 \cdot I}{2\pi x} [1 + F_n(x)] \quad (4.6)$$

$$F_n(x) = 2 \cdot x \cdot \int_0^\infty \frac{k_{N_1} e^{-2\lambda h}}{1 - k_{N_1} e^{-2\lambda h}} J_0(\lambda \cdot x) \partial\lambda \quad (4.7)$$

and when $1 < i < n - 1$ is true, factors of reflection coefficients can be computed using Equation (4.8),

$$k_i = \frac{\rho_{i+1} - \rho_i}{\rho_{i+1} + \rho_i} \quad (4.8)$$

4.3 Steepest Descent Method

Steepest Descent Method (SDM) also known as gradient descents are one of the earliest approaches for minimizing generic nonlinear functions. CDEGS RESAP module optimizes soil resistivity data using SDMs, SAMs (simulated annealing methods), and Marquardt methods. These three approaches were benchmarked for obtaining maximized characteristics of three site soil measurements separately where SDMs in comparison to other two theoretical implementations of software modules, showed best close matches of apparent resistivity curves. Accuracy was fixed to 0.0025 p.u, step size to 0.0001 and iteration count was set to 500. Cauchy proposed using gradients to solve nonlinear equations shown in Equation (4.9)

$$f(x_1, \dots, x_n) = 0 \quad (4.9)$$

Where, f represents real-valued continuous function that has positive values within certain limits. It works on a simple principle that continuous functions decrease, at least in the initial stages when a step is turned towards negative gradient direction.

Assuming the minimum of function $f(x) : R^n \rightarrow R$ has to be obtained where $x \in R^n$ and gradients of f are denoted by $g_k = g(x_k) = \nabla f(x_k)$, then minimizations are computations along given search directions, d_k (refer equation 4.10)

$$x_{k+1} = x_k + \alpha_k d_k, k = 0, 1, \dots, n \quad (4.10)$$

and step length, α_k selection based on Equation (4.10) can be depicted as Equation (4.11),

$$\alpha_k = \arg \min_{\alpha} f(x_k + \alpha d_k) \quad (4.11)$$

The arguments for function's minimum for SDM in the search direction is $d_k = -\nabla f(x_k)$. SDMs have two key computational advantages that of simplicity of programme constructions with minimal storage spaces required, $O(n)$. The important part is computation of step length, k , and gradient in searches.

Algorithm 4.3.1. SDM

Given an initial $x_0, d_0 = -g_0$ and a convergence tolerance tol

For $k=0$ to $maxiter$ do

Set $\alpha_k = \arg \min \phi(x) = f(x_k) - \alpha g_k$

$$x_{k+1} = x_k - \alpha_k g_k$$

Compute $g_{k+1} = \nabla f(x_{k+1})$

If $\|g_{k+1}\|_2 \leq tol$ then

 Converged

End if

End for

4.4 Genetic Algorithm

GAs are heuristic searches that imitate the processes of natural evolution. They are frequently employed in generating helpful optimization solutions and search issues. GAs form a part of wider class of EAs (Evolutionary Algorithms), which resolve optimization issues using methods based on natural evolution like inheritances, mutations, selections, and crossovers. GAs use chromosomes/genomes which get encoded for generating optimized candidate solutions. Solutions in GAs are traditionally expressed in binary as strings of 0s and 1s. Evolutions normally begin from populations of randomly created individuals and gradually improve over generations. Individual fitness is evaluated during generations where multiple stochastically selected individuals based on their original/modified fitness values result in generation of new populations which are subsequently utilized in ensuing iterations. Typically, when the algorithm ends on achieving highest possible generations, a guarantee that satisfactory solutions are found may not exist. Solutions are commonly represented as n-bit arrays. The fundamental advantage of genetic representations is easy matches due to set sizes, allowing easy crossover procedures. Figure 4.2 depicts the overall process of GAs.

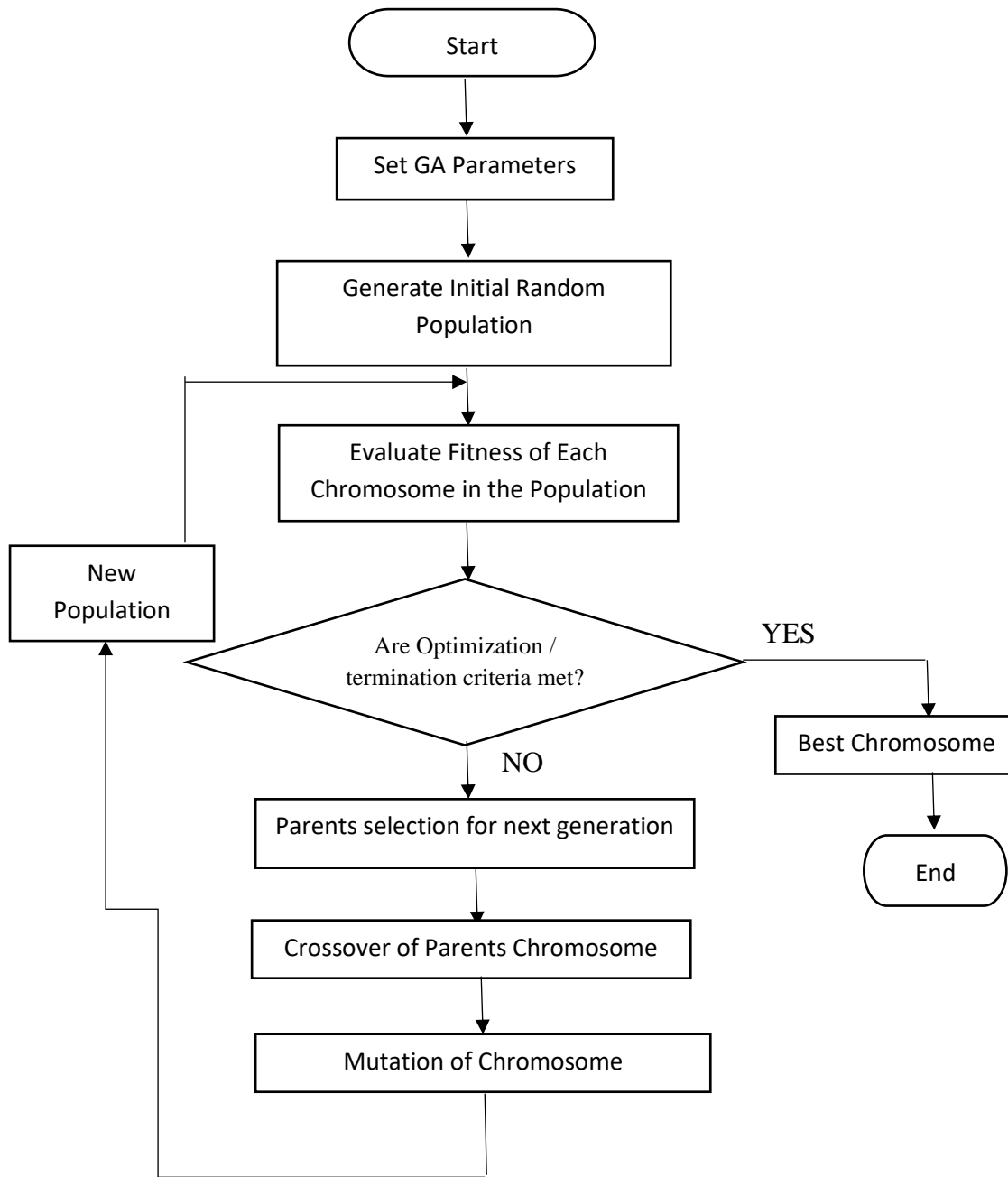


Figure 4.2 Flow Chart of GA

GA's fitness functions define genetic representations which are then used to evaluate quality of represented solutions. The population sample solutions are also at random, but improving them using the steps of mutations, crossovers, inversions, and selections.

Initialization: A large number of individual solutions are produced at random in the establishment of an initial population whose size is determined by the nature of the problem though thousands of potential answers may exist. Traditionally, GA's

population is produced at random, encompassing all conceivable solutions (search space) and are rarely seeded for discovery of optimum solutions.

Selection: This process selects individuals based on their fitness value strengths for breeding new generations. Selection approaches may also prioritize best options.

Reproduction: This stage is creation of second generation population of solutions using genetic operators of crossover (re-combinations) and/or mutations on parents of the previous generation. These resulting children exhibiting their parental traits are generated until required number of children (solutions) is reached. The children generated from two parents may result in better quality when more parents are involved in the reproduction process. The chromosomes of the children differ from their original generations improving population's average fitness values, since finest organisms of generations breed new generations though a small fraction of solutions may be less fit. Although crossovers and mutations are most well-known genetic operators, additional operators like regroupings, colonization / extinctions, and migrations can also be used in GAs.

4.5 Particle Swarm Optimization

PSOs are computational approaches that optimize solutions by iteratively attempting to enhance candidate solutions specific to defined quality measures. They solve issues by generating possible solutions (particles) and then moving these particles based on their position and velocity in defined search-spaces. The movements of these particles are restricted towards their best local positions, but can also be guided towards best global positions within search spaces. When better places are discovered by other particles they are updated in the search space. Thus, swarm's attention is directed towards the best options. PSOs are metaheuristic in the sense that they make little or no assumptions about the issue to be solved and work well within very vast spaces for finding potential solutions. Furthermore, PSOs do not use gradients of problem being optimized and hence do not require optimization issues to be differentiable like other traditional optimization methods like gradient descents or quasi-newton methods. In the context of PSOs, the term convergence often refers to two distinct definitions:

- The found solutions of search spaces converge (Stability) to a location that might be the optimal location

- The solutions may also converge into local optimum values best p or swarm's best known location g independent of the swarm's actions

In PSOs, the sequence of solution's convergences was where investigations resulted in the choice of PSO settings that can induce swarm particle convergences to a point while preventing the particles from divergence. According to Pedersen, PSOs are oversimplified as they assume swarms with just one particle and fail to consider stochastic variables resulting in best location p of the particle and best position g of the swarm being of constant value throughout optimizations. PSO's convergence to local optimums have been investigated and it has been demonstrated that PSOs require adjustments to ensure discovery of local optimums. As a result, Empirical data is still needed to determine PSO's convergence capabilities, though it can be addressed using techniques which constructs converging exemplars for PSOs by making better use of knowledge already learnt in the connection between p and g. PSO's overall performance can improve with quicker global convergences, greater solution qualities, and better resilience of objectives, though such analyses do not provide theoretical proofs.

4.6 Hybrid GA-PSO System

GAs are approaches which deal obligated and unconstrained challenges. Their computations are based on trademark choices and driven by organic progresses. GAs estimates have been successful in redesigning numerous aims and self-assured constraints. GA computations are well-hybridized using numerous approaches and heuristics. PSOs are computer processes that solve issues by iteratively attempting to find better potential courses of actions for a given measure of important values.

PSOs solve problems by generating a large number of possible courses of action, referred to as particles which move around in the solution space. Each particle's movement is guided by its nearest best known position in addition to best known spots in the targeted solution space and which are revived when better positions are discovered by other particles. A swarm's layer counts 'N' are predicted by experimental measurements of apparent resistivity ρ_{exp} from which infection points 'p' are also obtained making $N = p+1$. This starting values are used to compute remaining required parameters. Optimization's objective function obtains $(2N - 1)$ variables from soil structure's N layers. Thus, with the obtained N, ρ_i and h_i , values Sunde's algorithm is

used to get the inverse process. F_n (fitness function) for T pairs of soil resistivity in electrodes separation can be depicted as equation (4.11),

$$F_n = \sum_{i=1}^T \frac{|\rho_{ai}^{exp} - \rho_a^{exp}|}{\rho_{ai}^{exp}} \quad (4.12)$$

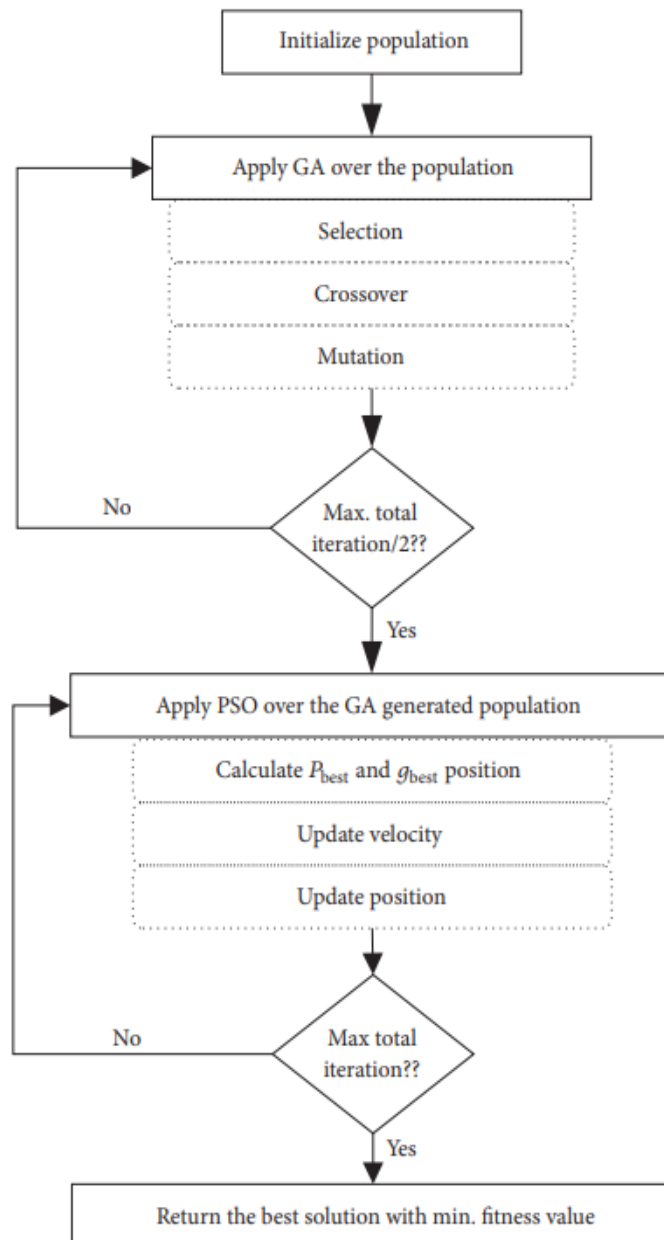


Fig. 4.3 – proposed GA – PSO Flow Chart

where ρ_{ai}^{exp} stands for soil's i^{th} experimental measured resistivity, 'a' separates two electrodes while ρ_a^{The} soil resistivity obtained from computations. Theoretically, apparent resistivity computed using GAs can be depicted as Equation (4.13),

$$\rho_{ai}^{The} = \rho_1 \cdot [1 + 2 \cdot F_n(a) - F_n(2 \cdot a)] \quad (4.13)$$

By solving equation (4.12) and (4.13) can compute the theoretical resistivity.

4.7 Results and Discussions

Case Study 1: The apparent resistivity was determined utilizing the four wire- Wenner technique using observed earth resistance. The calculated apparent resistivity was used to calculate the theoretical resistivity as well as the characteristics of the horizontal multi-structured earth. Table 4.2 lists experimental apparent resistivity values from literature as case study 1.

Table 4.2. Case Study 1 - Experimental Investigation

a(m)	Apparent Resistivity
1.0	10484.43
2.0	10786.84
4.0	8104.34
8.0	11308.53
16.0	12036.63

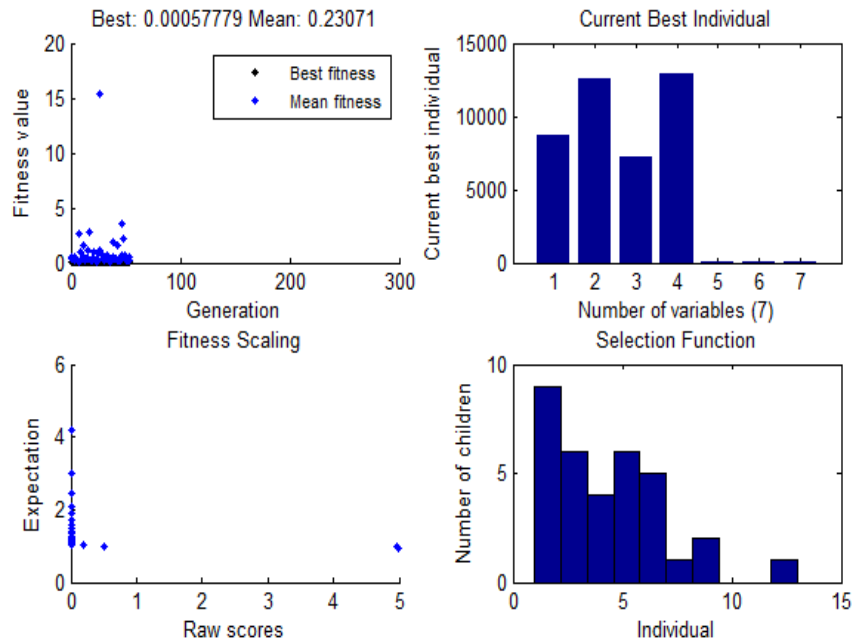


Figure 4.4. Hybrid Ga Best Fitness, Individual, Scaling, And Selection [Case Study 1]

Table 4.3. Comparison of Hybrid PSO – GA Technique withGA

a(m)	Apparent Resistivity	GA	GA-PSO
1.0	10484.43	10746.74	10792.08
2.0	10786.84	9717.28	10982.34
4.0	8104.34	8102.28	8206.32
8.0	11308.53	11277.01	11301.01
16.0	12036.63	11786.48	12121.73

Figure 4.4 depicts selected individuals, highest fitness amongst selected individuals, current best individuals and average distances. Table 4.3 list the comparative values of the proposed Hybrid GA–PSO scheme with GAs. Table 4.4 lists experimental soil deviation values of the proposed Hybrid GA–PSO scheme with GAs. It can be seen that

values of GAs vary between 0.02-9.9% while the proposed scheme in comparison shows variations between 0.06 % to 2.9 %. These higher values imply proposed GA-PSO approach agrees better agreements with actual measurements.

Table 4.4. Comparison – Percentage of Error

a(m)	Apparent Resistivity	Error GA (%)	Error GA-PSO (%)
1.0	10484.43	2.5	2.9
2.0	10786.84	9.9	1.8
4.0	8104.34	0.02	1.25
8.0	11308.53	0.28	0.06
16.0	12036.63	2.1	0.71

Table 4.5. Parameters of Soil Stratification Case Study 1

Layer	GA	GA-PSO
ρ_1	9964.37	8662.688
ρ_2	9693.47	12550.803
ρ_3	21658.56	7160.554
ρ_4	15862.48	12954.477
h_1	1.29	1.29
h_2	1.17	1.348
h_3	1.03	1.353
h_4	inf	inf

Table 4.6. Case Study – Experimental Investigation

a(m)	Apparent Resistivity	a(m)	Apparent Resistivity
1.0	214	20.0	250
3.0	256	30.0	225
5.0	273	50.0	210
10.0	307	80.0	186
15.0	284		

Table 4.7. Comparison of Experimental Resistivity with Computed Resistivity

a(m)	Apparent Resistivity	Hybrid GA	Error Hybrid GA-PSO (%)
1.0	214	216.17	3.12
3.0	256	262.14	2.4
5.0	273	291.87	6.9
10.0	307	322.12	4.9
15.0	284	281.66	0.82
20.0	250	244.85	2.06
30.0	225	219.63	2.38
50.0	210	197.18	6.10
80.0	186	196.0	5.37

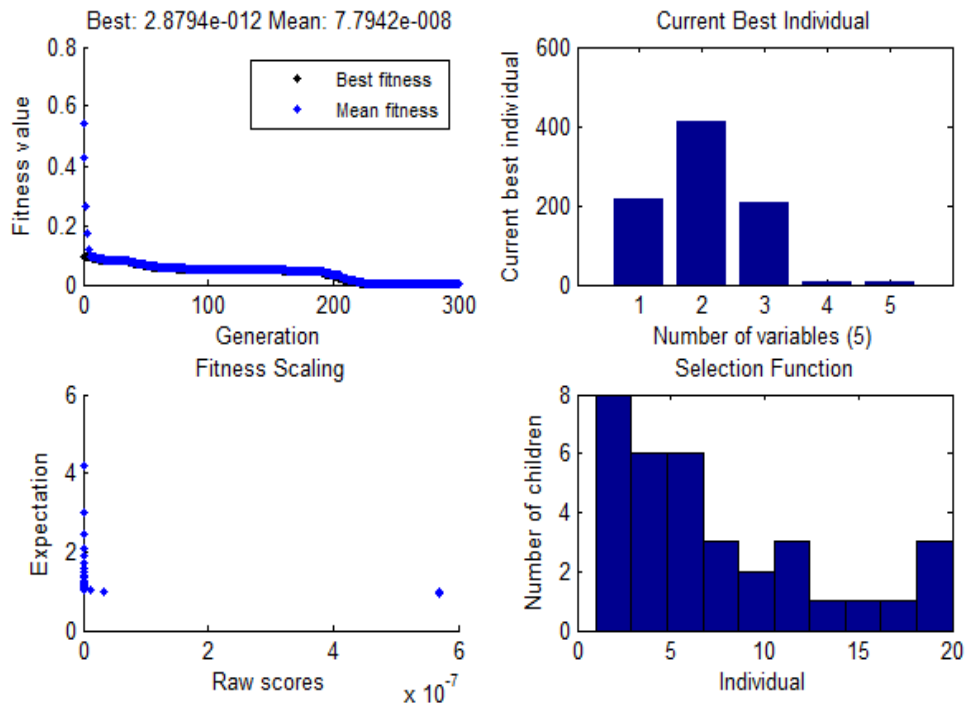


Figure 4.13. Hybrid GA Best Fitness, Individual, and Selection [Case Study 2]

Table 4.5 lists values of four optimized layers obtained from horizontal multi-layer stratifications of soil. The topmost layer’s resistivity was found to be $9964.37 \Omega.m$ with a thickness of 1.29 M and correspondingly second, third and fourth layers resistivities and thickness were found to be $9693.47 \Omega.m / 1.17 M$, $21658.56 \Omega.m / 1.03 M$ and $15862.48 \Omega.m / \text{infinity}$ respectively.

Case Study 2: The experimental apparent resistivity in the literature is chosen as case study 1 in Table 4.6. The thickness of the earth’s lowest layer is infinite in both cases 1 and 2.

Table 4.7 shows comparative values of proposed hybrid GA–PSO with GA in terms of divergences from experimental results. Figure 4.13 depicts the optimal fitness, people, scaling, and case study 2 selection using the suggested hybrid algorithms.

The optimal stratification of soil layers for Case Study 2 is shown in Table 4.8. Computed result shows there are three layers in the earth. The resistivity of first layer is $214 \Omega.m$ and its thickness is 6.793 M. Resistivity and thickness of second layer is

409.736 Ωm and 7.449 M. The bottom layer resistivity is 208.092 $\Omega\text{.m}$ and its thickness is infinity.

Table 4.8. Parameters of Soil Stratification Case Study 2

Layer	GA	GA-PSO
ρ_1	196.9	214
ρ_2	351.7	409.736
ρ_3	185.2	208.092
h_1	1.7	6.793
h_2	8.4	7.449
h_3	INF	INF

The number of layers N , the resistivity of all layers, and the thickness of the first layer to $N - 1$ layers were all modified in this study, which presented a strategy and numerical demonstration for the technique of soil stratification into flat multi layers utilizing a Hybrid GA-PSO. The soil's lowest layer is supposed to be infinitely thick. It was proposed that this technique presents which are suitable for soil stratification into horizontal multilayer, in addition to optimizing a number of layers.

The importance of soil models and ground potential rise in substation grounding has also been discussed. To highlight the differences and effect of soil models on ground potential rise, three various soil profiles were studied: high, medium, and low soil resistivity. After increasing 0.15 m surface layer thickness and 5000 Ohm – m, step voltage is safe for all three sites without adjusting the grounding grid design. However,

even after adding the maximum 0.15 m surface layer required by the standard, the contact voltage is not safe in all three locations.

As a result, the grounding grid must be altered, either by expanding the grid or by burying the grounding rods deeper into the grid's problematic corners.

CHAPTER 5

AIR INSULATED SUBSTATION (AIS) GROUNDING GRID DESIGN FOR OPTIMIZED SOIL PARAMETERS IN MULTIPLE LAYERS

5.1 Air Insulated Sub-stations (AIS)

Modern current methods in sub-stations maintain step and touch potentials below acceptable levels as soil resistivity model used in sub-station soils which can be uniform or two layered or multi-layered affect grounding system designs. Hence, the basic aim of this work is to minimize earth resistances in grounding grids of sub-stations in its proposed design. A proper technique measuring soil resistivity can result in accurate soil models being created. Designs using average observed values of resistivity in grounding system designs may be erroneous, specifically when resistivity variance between probe distances is more than 25% and in these conditions two layered soil models are considered appropriate

Sub-stations, also known as AISs, are Power System components that control step up/down voltage levels of transmissions or distributions using many types of equipment. Any sub-station's heart is its transformer which alters voltages without affecting frequencies. Examples of sub-station elements can include circuit breakers, instrument transformers (current/potential transformers), isolators, and lightning arresters.

In AIS, switchgears, bus bars, and other equipments installed outside in switchyards stand exposed. AIS use porcelain or composite insulators with/or bushings to isolate main circuit's ground potential. AIS are made up of entirely air-insulated technology components including circuit breakers, disconnect switches, surge arrestors, instrument/power transformers, capacitors and bus bars. These elements are connected using stranded flexible conductors, tubes, or buried power cables. AISs are globally the most common type of sub-stations accounting to more than 70%.

Power generations in India use 11kV of power generation stations where power transmissions of produced voltages are less cost effective due to rising losses. Hence, sub-stations are used to step up transmission voltages of generating stations. When voltage levels have to be raised for transmissions to long distances, second sub-stations are used in their step up operations. These high power transmissions cannot be used directly by consumers (domestic or industrial), making distributions through sub-stations a significant alternative as they get down voltages to distribution friendly levels like 440 V, 3.3 kV, 6.6 kV, or 11 kV based on consumer types.

Stations generating power may share it with sub-stations. Transformers receive inputs from many protective and measurement devices and the input voltages are subsequently stepped up or down for distribution of electricity or transportation through protected metering equipments. Though, high voltage sub-stations in the range of 132 kV can be operated manually, the equipments in these sub-stations are automatic for safety. Sub-stations use bus systems for consistency and seamless functioning. They are equipped with control rooms and control panels which monitor sub-stations and take required actions when needed.

Sub-stations or switching stations are connection and switching points for power generation sources, transmissions, distributions where step-up and step-down transformers are an important part of these transmission or distribution networks. The main design goal of sub-stations is to deliver highest level of dependability and flexibility while meeting system's requirements and reducing overall investments.

5.2 Case Study 1: AIS Grounding Design and Computation of Grid Impedance of -220/132/66 kV AIS Substation

The soil resistivity data of the AIS sub-station is discussed in table 5.1. The grid conductor material is selected as Steel. The size of the grid conductor was arrived as per Standard IEEE80-2013. The grid conductor shall be buried at a depth of 600 mm below $EL\pm 0.00$ (FGL) and covers the entire sub-station area. The grid's perimeter is defined as outer most conductors which reside at least 1 meter outside fence's edge to eliminate the risk of excessive touch voltage for people standing outside. The electrode

quantities are obtained from the data shared with us and modelled accordingly in the MALZ computation module. It is understood that the entire sub-station area is spread with crushed stone/gravel with resistivity 3000 Ohm-m for a depth of 75mm and the same is considered for safety criteria computation.

Table 5.1. Soil Resistivity Model of AIS Sub-station

S. No.	Spacing of Electrode in m	Soil Resistivity in Ohm m				Average Soil Resistivity in Ohm m
		Location1	Location2	Location3	Location4	
1	0.5	17.1	12.23	9.69	25.51	16.63
2	1	14.07	17.72	14.98	29.72	19.12
3	2	19.98	25.88	24.31	43.16	28.33
4	3	23.65	29.97	28.84	49.76	33.06
5	5	31.73	36.44	37.07	64.08	42.33
6	10	48.69	53.09	62.2	87.33	62.83
7	15	50.42	58.9	62.67	90.47	65.62
8	20	43.35	54.66	49.63	98.01	61.41
Average Soil Resistivity						41.10

5.2.1 Design Parameters

Length & Width of Grid: Refer to grid layout.

Soil Resistivity: Two-layer soil model.

Grid Fault current & Duration for conductor Sizing: 14.64 kA/1 sec

Split Factor – 0.45

Fault Current – 6.588kA

Fault Clearing time for touch & Step potential: -1 Sec

Conductor Size: 75x10 GI Flat

Depth of grid: 600 mm

Vertical rods: 60mm dia GI Pipe (3-Meter-Deep) – 31 No's

90mm dia GI Pipe (3-Meter-Deep) – 58 No's

100mm dia MS Pipe (3-Meter-Deep) – 54 No's

- 50mm dia GI Pipe (3-Meter-Deep) – 21 No's
- 40mm dia MS Rod (3-Meter-Deep) – 10 No's
- 40mm dia MS Pipe (3-Meter-Deep) – 6 No's
- 40mm dia GI Pipe (3-Meter-Deep) – 11 No's
- 75mm dia GI Pipe (3-Meter-Deep) – 01 No's
- 120mm dia MS Pipe (3-Meter-Deep) – 01 No's

Surface Soil Resistivity & Thickness: Gravel (3000 Ohm – meter) & 75mm Thickness.

5.2.2 Grid Conductor Sizing

The material and size of various parts of earthing used have a major impact on lives of sub-stations as they to transport and dissipate earth fault current without causing fires or explosive threats to the region. The cross-sectional area and diameter of conductors are computed as below:

Input Data (Properties of GI referred as per Item 09 Table 1 of IEEE std. 80-2013).

- (i) Conductor Material – GI
- (ii) Fault Current I_f – 14.64 kA
- (iii) Fault Duration, t_c – 1 second
- (iv) Maximum Allowable Temperature, T_m – 419°C
- (v) Ambient Temperature, T_a – 50°C
- (vi) Thermal Coefficient Resistivity at reference Temperature, α_f – 0.0032
- (vii) Resistivity of Ground Conductor, ρ_r – 20.1 $\mu\Omega$ -cm.
- (viii) Thermal Capacity Factor, TCAP – 3.9 J/cm³. °C
- (ix) K_0 (=1/ α_0) – 293

To calculate the conductor as per the standard IEEE 80 – 2013 is,

$$A = \frac{I_f}{\sqrt{\frac{TCAP}{t_c \alpha_f \rho_r} \ln\left(\frac{K_0 + T_m}{K_0 + T_a}\right)}} \quad 5.1$$

After solving equation 5.1,

Calculated Conductor Size – 220 sq.mm

Corrosion allowance – 15.0 %

Minimum size of conductor required as per calculation =253 sq.mm

Conductor in service= $75 \times 10 = 750 \text{ sq.mm}$

Hence it is to be noted that the Size of the conductor in service at sub-station is sufficient to carry the fault current of 14.64kA for 1sec. The SESCAD model developed from the sub-station and the point of energization is shown below in Figure 5.1.

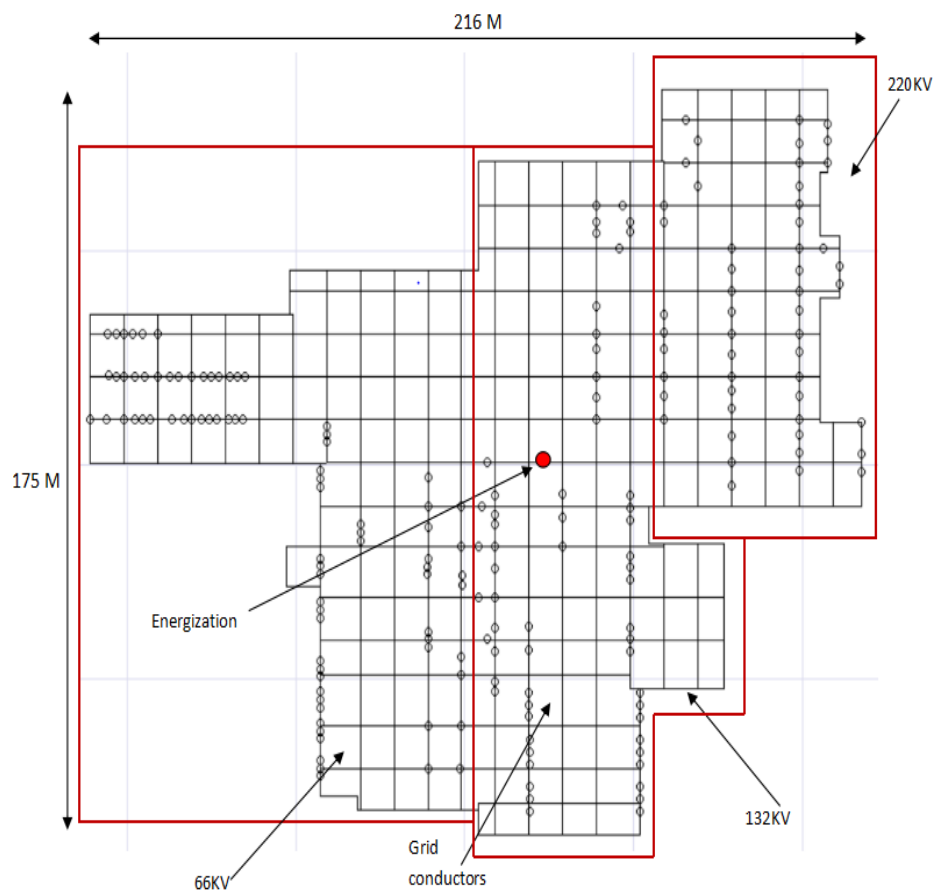


Figure 5.1. Grid Layout- Plan View of Sub-station

The observation profile points for observing the step and touch potentials are shown below in Figure 5.2.

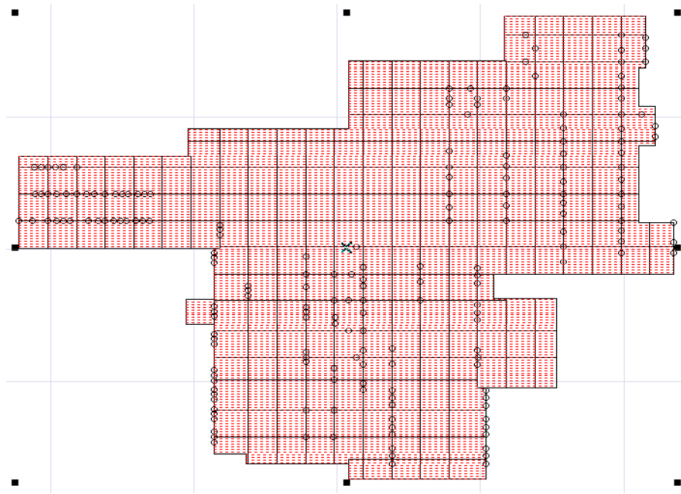


Figure 5.2. Observing the Step and Touch Potentials

5.2.3 Safety Criteria for 50kg body weight with surface layer

One of the important aspects of earthing system designs in accordance with IEEE Std 80-2013 is the determination of safety limits of touch and step voltages using functional parameters given below

- Magnitude of permissible body current (IB)
- Duration of shock current (ts)
- Resistance of current flow path through human body consisting of body resistance (RB) and resistance of feet (Rfoot)
- X/R Ratio

The following snapshot shows the safety limits for Step and Touch potential voltage with a surface layer of 3000 Ohm-m for 75mm thickness.

5.2.4 Touch Voltage

The potential difference between an accessible earthed conductive component and the earth surface potential at the place where a person stands with his hands in touch with an earthed part is known as Touch Voltage. The touch voltage profile in the sub-station region when the fault is simulated is shown in the software snapshot below. The contact voltage inside the grid of the AIS sub-station is shown in Figure 5. 3.

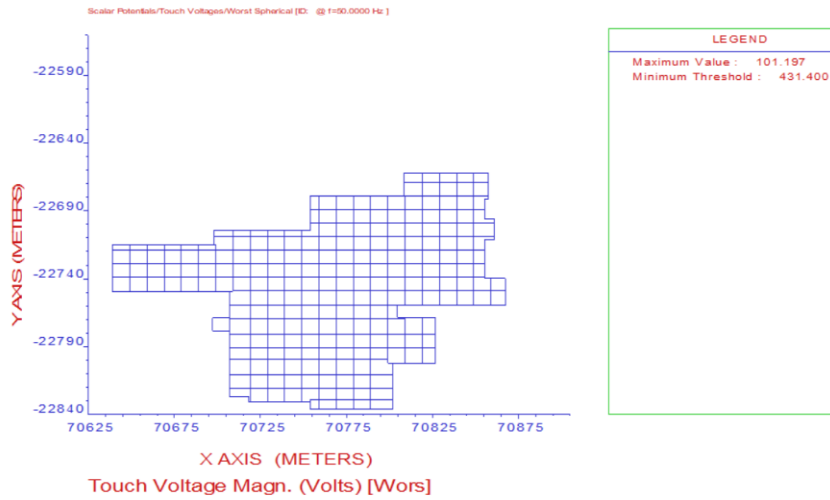


Figure 5.3. Touch Voltage Inside the Grid for AIS Sub-station

Threshold: 431.40 V; Attained: 101.197 V

It is observed that the touch potentials inside the grid area are within the tolerable limits.

5.2.5 Step Voltage

The difference in potential between two earth surface points that are 1 m apart is known as step voltage. A person traversing a distance of 1 m (standard step size) without contacting any item that is earthed is to this voltage. The contact voltage of AIS sub-station grid is shown in Figure 5.4.

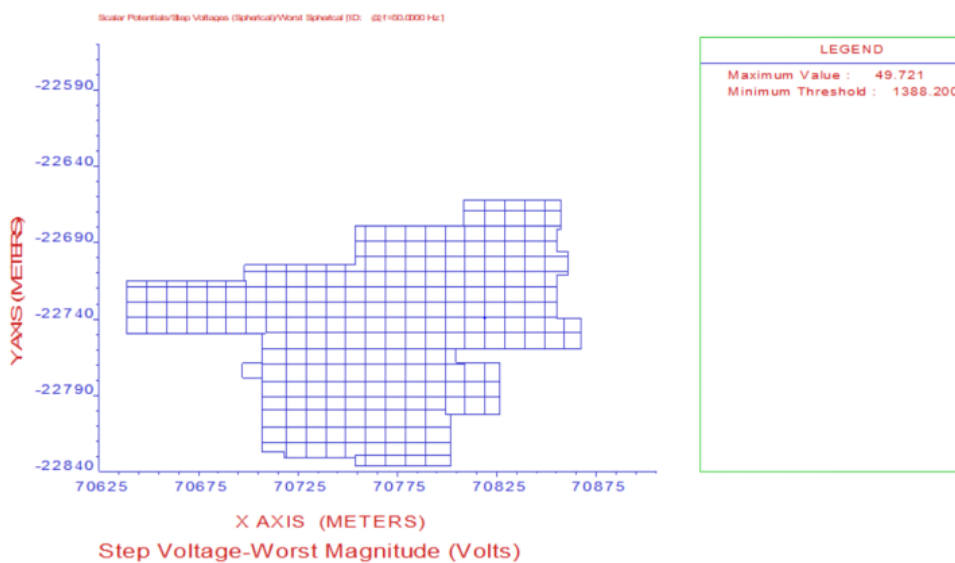


Figure 5.4. Step Voltage Inside the Grid for AIS Sub-station

Threshold: 1388.20 V

Attained: 49.721 V

It is observed that the step potentials inside the grid area are within the tolerable limits.

5.2.6 Conductor GPR

The highest voltage reached by an earth electrode in relation to a distant earthing point at the potential of remote earth or reference earth in a station is known as ground potential rise. Figure 5.5 shows the conductor GPR of the sub-station under study. Figure 5.6 Shows the observation of 1 M outside the fence / grid area.

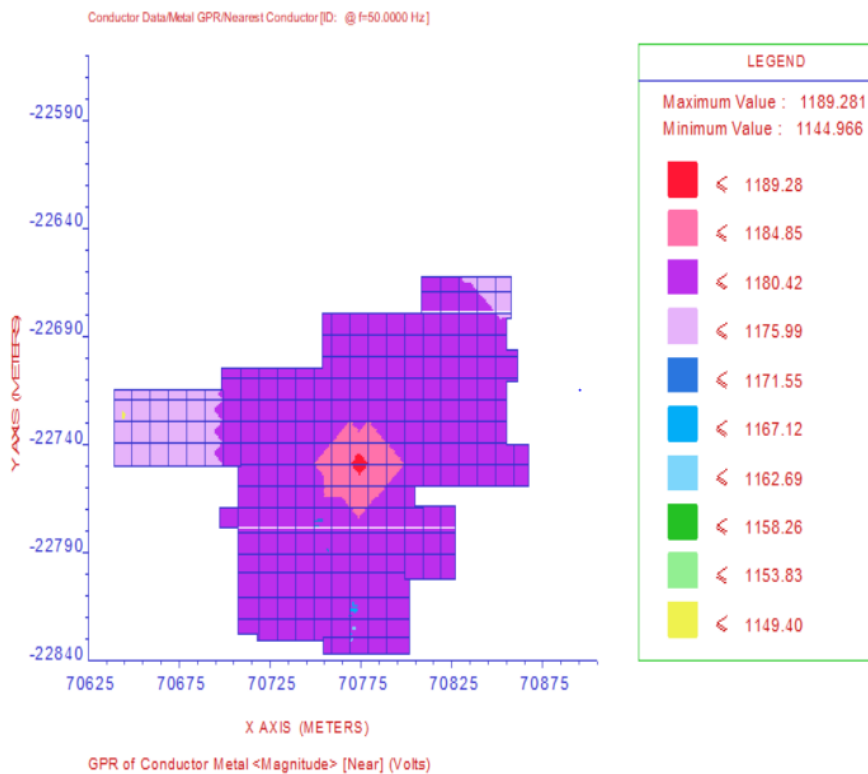


Figure 5.5. Conductor Ground Potential Rise for AIS Sub-station

Minimum GPR: 1144.966 V; Maximum GPR: 1189.281 V

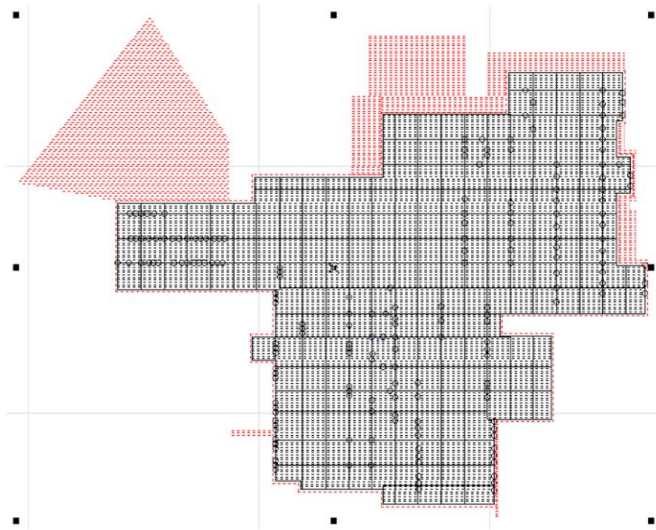


Figure 5.6. Observation Profile 1m Outside the Grid/Fence Area for AIS Sub-station

```

DATE OF RUN (Start)= DAY 30 / Month 3 / Year 2018
STARTING TIME= 18:43:54:00

=====< M A L Z          ( SYSTEM INFORMATION SUMMARY ) >=====

Run ID.....:
System of Units .....: Metric
Earth Potential/Magnetic Field Calculations : Potentials
Number of Energization Source Busses .....: 1
Current Injected in Reference Source Bus....: 6588 Amps
Energization Scaling Factor (SPLITS/FCDIST/specified)... 1.0000
Number of Original Conductors .....: 275
Number of Frequency Values to be Analyzed...: 1
Power Source Frequency.....: 50.000 Hertz
Impedance Values are Based On.....: 50.000 Hertz
Total Length of Conductor Network.....: 5597.4 meters

CHARACTERISTICS OF MEDIA SURROUNDING NETWORK
=====
AIR LAYER : Resistivity.....: 0.100000E+13 ohm-meters
             Relative Permittivity...: 1.00000
             Relative Permeability...: 1.00000

|>>> SOIL TYPE : Multi-Layer Horizontal

LAYER RESISTIVITY |----- RELATIVE -----| THICKNESS
No. (ohm-meter)  Permittivity Permeability (meters)
-----|-----|-----
1  15.6855      1.00000      1.00000      1.14897
2  70.9680      1.00000      1.00000      Infinite

Case Number.....: 1
Frequency for This Case.....: 50.000 Hertz
GPR of Reference Source Bus (# 1)....Magn...: 1189.940 Volts
Angle..: 0.5966500E-01 degrees

Impedance of Grounding System.....Magn...: 0.1806223 Ohms
Angle..: 0.5966500E-01 degrees

```

Figure 5.7 Screen Shot of System Information Summary

Impedance of the grounding system is calculated to be 0.1806 Ohms.

5.2.7 Touch Voltage 1m outside grid/fence

The below snapshot describes the touch voltage 1m outside grid / fence without surface layer shown in figure 5.8.

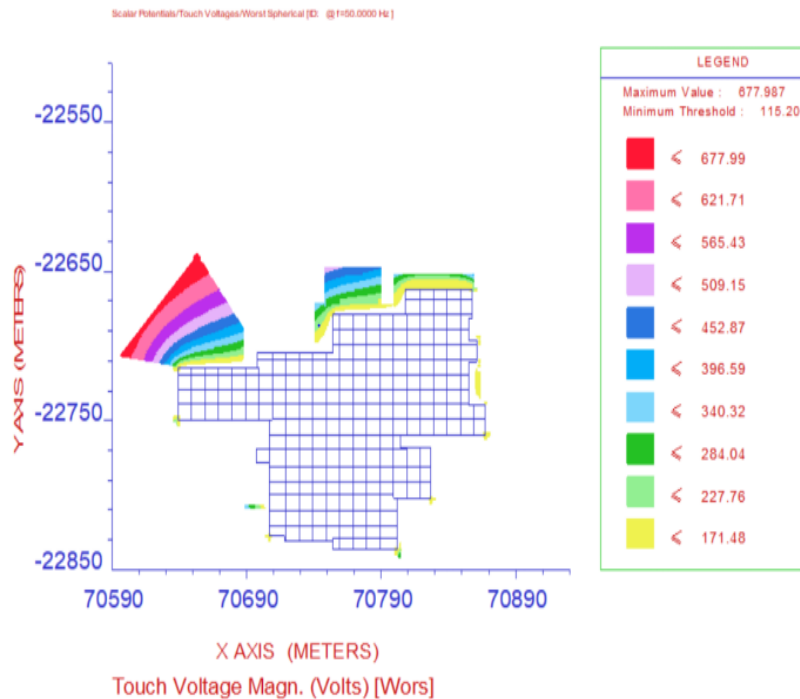


Figure 5.8. Step and Touch Voltage without Surface Layer for AIS Sub-station

Threshold: 115.20 V; Attained: 677.987 V

It is observed that the touch potentials are not within the tolerable limits.

5.2.8 Step Voltage 1m outside grid/fence

The below snapshot describes the step voltage 1m outside grid/fence without surface layer shown in Figure 5.9.

Threshold: 123.50 V; Attained: 49.721 V

It is observed that the step potentials are within the tolerable limits. The grid was modelled and analysed by injecting a fault current of 6.588kA (14.64 kA with split factor of 0.45) in the following scenarios. With surface layer of 3000 Ohm m resistivity

for 75mm inside the grid area (See Table 5.2). Without any surface layer above native soil, 1m outside the grid/fence area is shown in Table 5.3.

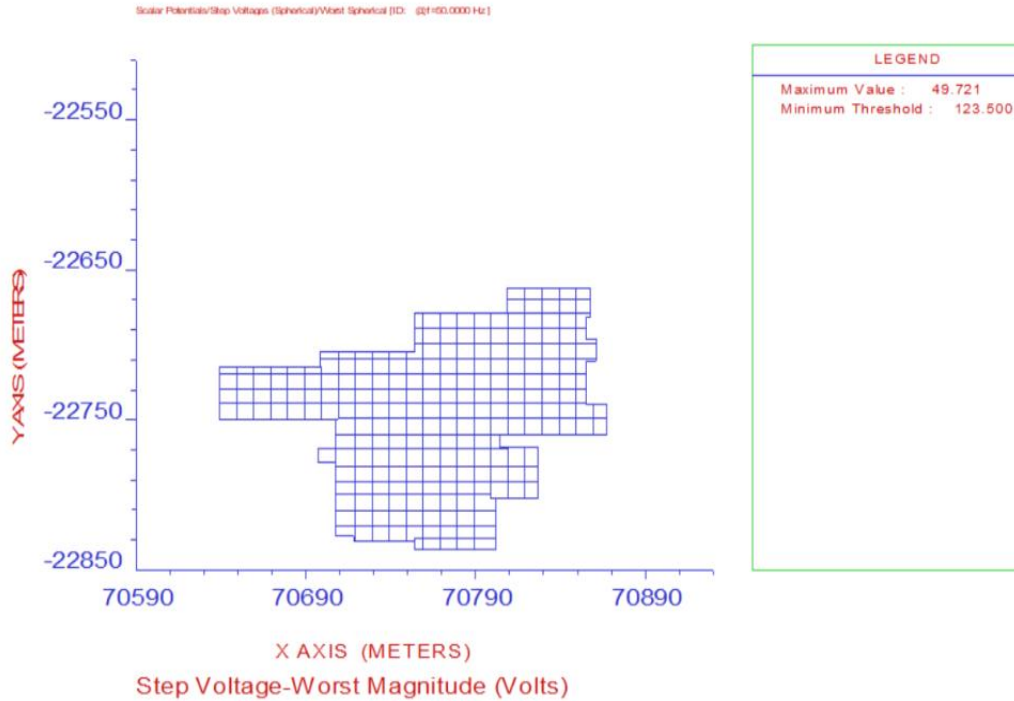


Figure 5.9. Step Voltage 1m Outside Grid/Fence Without Surface Layer for AIS Substation

Table 5.2. Surface layer of 3000 Ohm m resistivity - 75mm inside the grid area

Parameters	Tolerable Values (Safe Limit)	Attained Values
Touch Voltage	431.40 V	101.197 V
Step Voltage	1388.20 V	49.721 V
GPR	1189.281 V	
Impedance	0.1806 Ohms	

Table 5.3. Without surface layer - 1m outside the grid

Parameters	Tolerable Values (Safe Limit)	Attained Values
Touch Voltage	115.20 V	677.987 V
Step Voltage	123.50 V	49.721 V

5.3 Case Study 2: 400 / 220 kV AIS SUB-STATION- SOIL RESITIVITY

The resistance of earth electrode, earth electrode potential rise, and earth surface potentials that affect magnitude of dangerous voltages, are directly proportional to electrical resistivity of soil. Therefore, it is recommended that electrical resistivity of soil should be properly measured and analysed to determine soil resistivity model for design of grid earth electrode. The soil resistivity model of 400 / 220 kV sub-station is discussed in the table 5.4.

Table 5.4. Soil Resistivity Data of 400 / 220 kV Sub-Station

S. No.	Spacing of Electrode in M	Soil Resistivity in Ohm M				Average Soil Resistivity in Ohm M
		Location1	Location2	Location3	Location4	
1	0.5	52.69	54.89	88	72.56	67.04
2	1	59.57	69.04	96.65	53.31	69.64
3	1.5	35.14	56.68	-	41.79	44.54
4	2	21.7	62.45	136.33	37.51	64.50
5	3	11.5	46.65	151.44	40.9	62.62
6	5	2.1	44.13	212.66	35.81	73.68
7	10	2.87	30.16	109.31	38.32	45.17
8	12	-	-	94.61	-	94.61
8	15	14.14	23.09	59.37	17.43	38.40
Average Soil Resistivity						62.24

Soil parameters optimized by using hybrid GA – PSO technique, inspected soil site is two layered soil model. Top layer resistivity is 49.97 Ω m and bottom layer resistivity is 29.48 Ω m and the thickness of top layer is 8.47 M.

5.3.1 AIS Grounding Design and Computation of Grid Impedance

The grid conductor material is selected as Steel. The size of the grid conductor was arrived as per Standard IEEE80-2013. The grid conductor shall be buried at a depth of 600 mm below EL±0.00 (FGL) and covers the entire sub-station area. To protect individuals from standing inside high contact voltage areas, perimeter of grids are defined so that the outermost conductors are positioned at least 1 metre outside the grid fence's border. The electrode quantities are obtained from the data shared with us and modelled accordingly in the MALZ computation module. It is understood that the entire sub-station area is spread with crushed stone/gravel with resistivity 3000 Ohm-m for a depth of 75mm and the same is considered for safety criteria computation.

Design Parameters

Length & Width of Grid: Refer to grid layout.

Soil Resistivity: Two-layer soil model.

Grid Fault current /Duration for conductor Sizing: 42.1 KA/1 sec

Split Factor – 0.65

Fault Current – 27.365kA

Fault Clearing time for touch & Step potential: 1 Sec

Conductor Size: 40mm Dia MS rod

Depth of grid: 600 mm

Vertical rods: 32mm Dia MS Pipe (3 M Deep) – 9 No's

100mm Dia GI Pipe (3 M Deep) – 43 No's

40mm Dia GI Pipe (3 M Deep) – 171 No's

32mm Dia GI Pipe (3 M Deep) – 4 No's

Surface Soil Resistivity & Thickness: Gravel (3000 Ohm – Meter) & 75mm Thickness.

The SESCAD model developed from the sub-station and the point of energization is shown in Figure 5.10. The observation profile points for observing the step and touch potentials are shown in Figure 5.11.

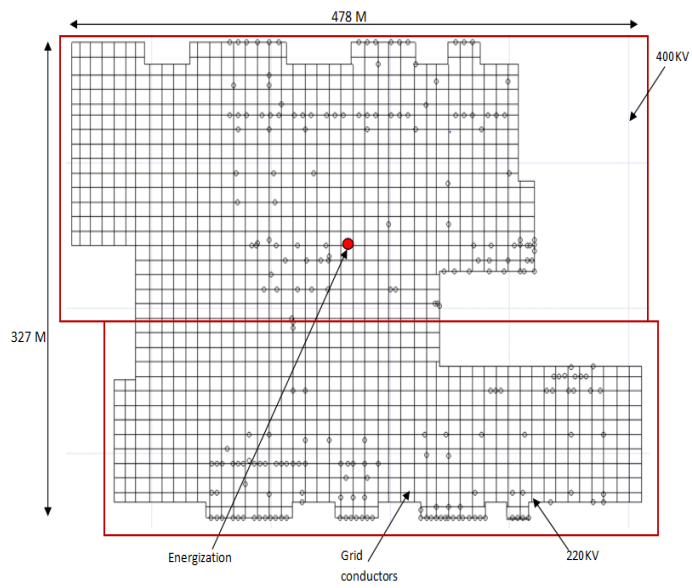


Figure 5.10. Energization Module 400 / 220 kV Sub-Station

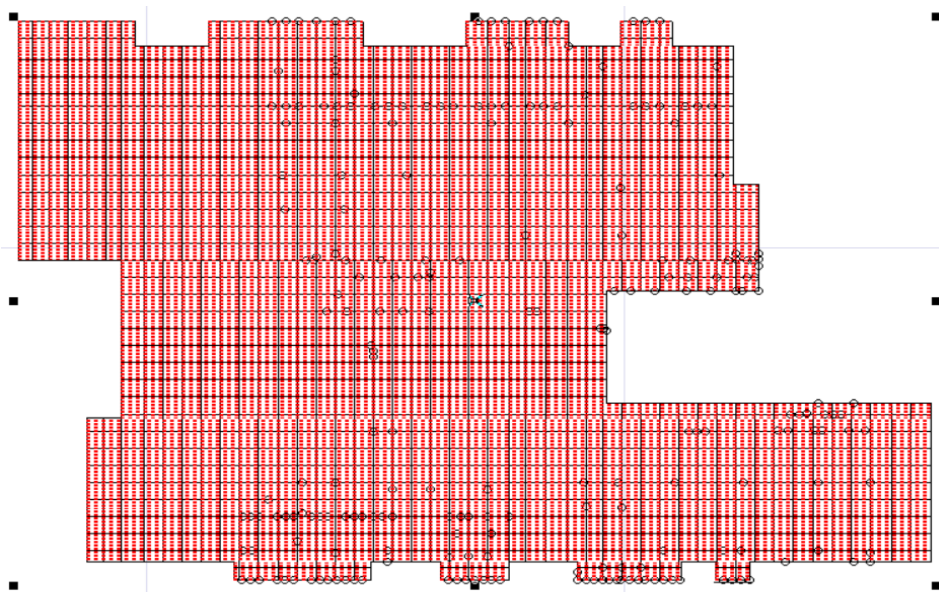


Figure 5.11. Energization Module of 400 / 220 kV Sub-Station

One of the important aspects of earthing system designs in accordance with IEEE Std 80-2013 is the determination of safety limits of touch and step voltages using functional parameters given below

- Magnitude of permissible body current (IB)
- Duration of shock current (ts)
- Resistance of current flow path through human body consisting of body resistance (RB) and resistance of feet (Rfoot)
- X/R Ratio

Safety limits for Step and Touch potential voltage with a surface layer of 3000 Ohm-m for 75mm thickness.

Touch Voltage

The potential difference between an accessible earthed conductive component and the earth surface potential at the place where a person stands with his hands in touch with an earthed part is known as Touch Voltage. The below snapshot from software shows the touch voltage profile in the sub-station area when the fault is simulated (See Figure 5.12).

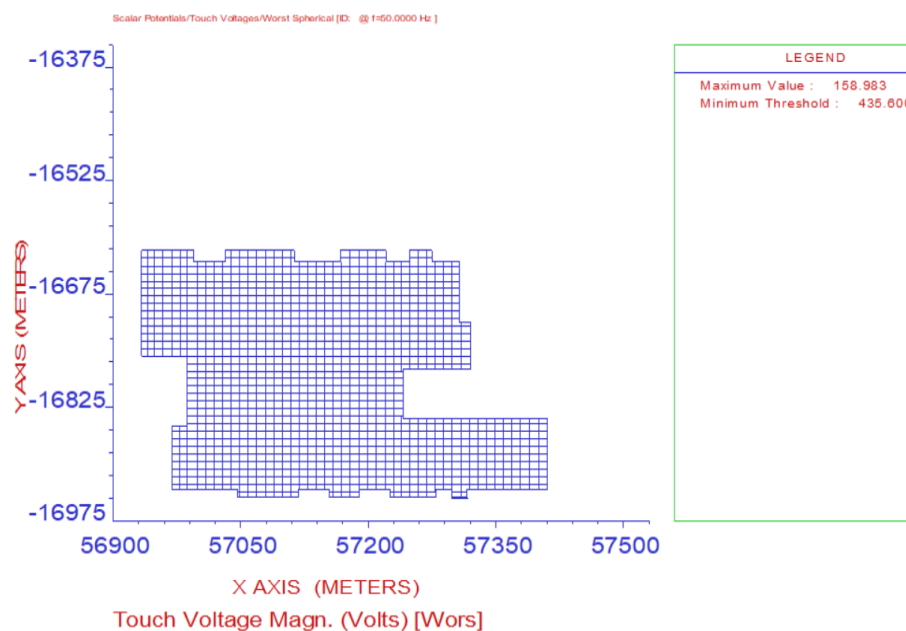


Figure 5.12. Touch Voltage Inside the Grid for 400 / 220 kV Sub-Station

Threshold: 435.60 V; Attained: 158.983 V

It is observed that the touch potentials inside the grid area are within the tolerable limits.

Step Voltage

The difference in potential between two earth surface points that are 1 m apart is known as step voltage. A person traversing a distance of 1 m (standard step size) without contacting any earthed item will be exposed to this voltage (Refer Figure 5.13).

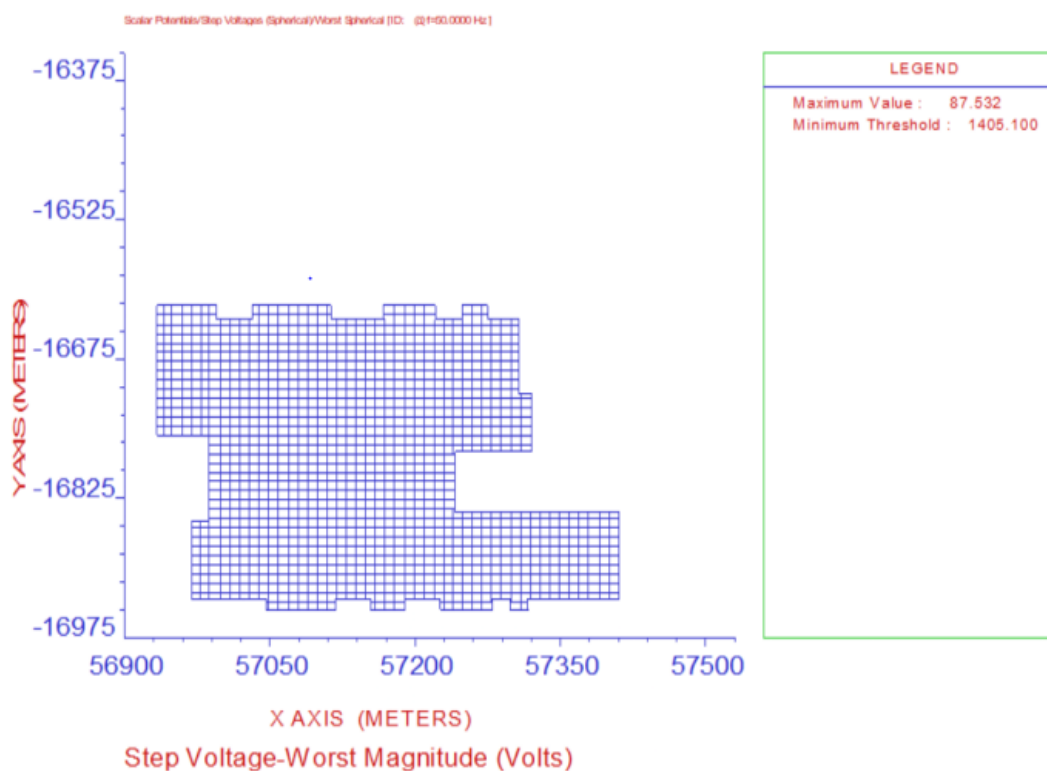


Figure 5.13. Step Voltage Inside the Grid for 400 / 220 kV Sub-Station

Threshold: 1405.10 V

Attained: 87.532 V

It is observed that the step potentials inside the grid area are within the tolerable limits.

Conductor GPR

The highest voltage reached by an earth electrode in relation to a distant earthing point at the potential of remote earth or reference earth in a station is known as ground potential rise (Refer Figure 5.14). The following layout snapshot describes the observation profile 1m outside the grid/fence area shown in figure 5.15.

Minimum GPR: 1000.689 V

Maximum GPR: 1137.842 V

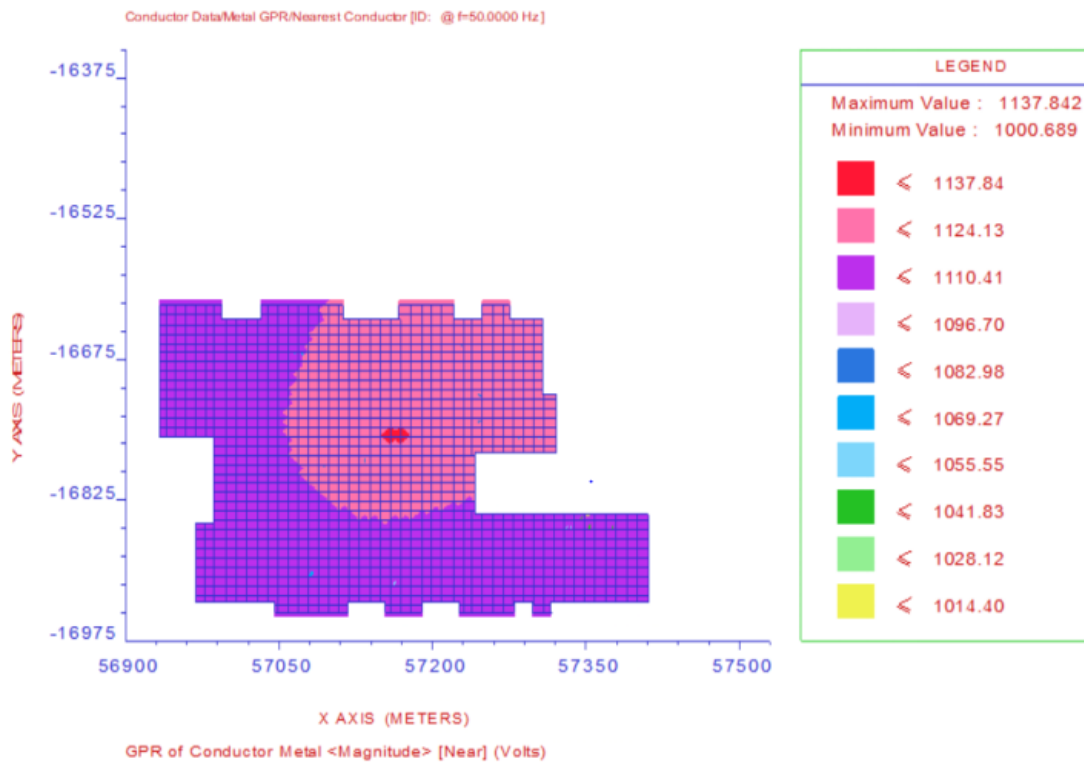


Figure 5.14. Conductor Grid for AIS Sub-Station

System Information Summary

```

DATE OF RUN (Start)= DAY 30 / Month 3 / Year 2018
STARTING TIME= 12:16:14:63

===== < M A L Z          ( SYSTEM INFORMATION SUMMARY ) > =====

Run ID.....:
System of Units .....: Metric
Earth Potential/Magnetic Field Calculations : Potentials
Number of Energization Source Busses .....: 1
  Current Injected in Reference Source Bus....: 27365 Amps
Energization Scaling Factor (SPLITS/FCDIST/specified)...: 1.0000
Number of Original Conductors .....: 372
Number of Frequency Values to be Analyzed...: 1
Power Source Frequency.....: 50.000      Hertz
Impedance Values are Based On.....: 50.000      Hertz
Total Length of Conductor Network.....: 25303.      meters

CHARACTERISTICS OF MEDIA SURROUNDING NETWORK
=====
AIR LAYER : Resistivity.....: 0.100000E+13 ohm-meters
            Relative Permittivity..: 1.00000
            Relative Permeability..: 1.00000

|>>> SOIL TYPE : Multi-Layer Horizontal

LAYER RESISTIVITY |----- RELATIVE -----| THICKNESS
  No. (ohm-meter)  Permittivity Permeability (meters)
-----|-----|-----|-----
  1  59.9777      1.00000      1.00000      8.47143
  2  29.6059      1.00000      1.00000      Infinite

Case Number.....: 1
Frequency for This Case.....: 50.000      Hertz
GPR of Reference Source Bus (# 1)....Magn...: 1140.587      Volts
                                         Angle.: 0.2681471      degrees

Impedance of Grounding System.....Magn...: 0.4168051E-01 Ohms
                                         Angle.: 0.2681471      degrees

```

Figure 5.15. Screenshot of 220 kV Substation computational information

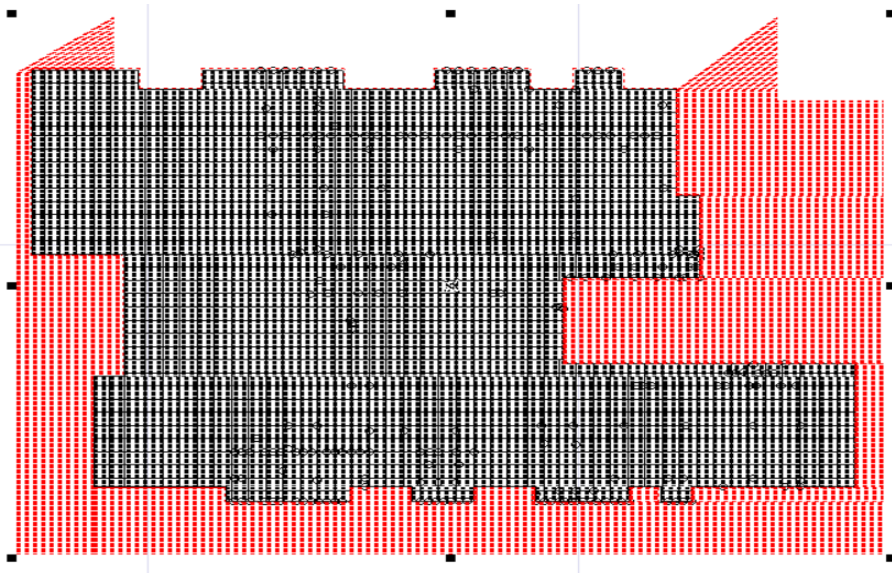


Figure 5.16. Observation Profile 1m Outside for 400 / 220 kV Sub-Station

Touch Voltage 1m outside grid/fence

The below snapshot describes the touch voltage 1m outside grid/fence without surface layer displayed in figure 5.17.

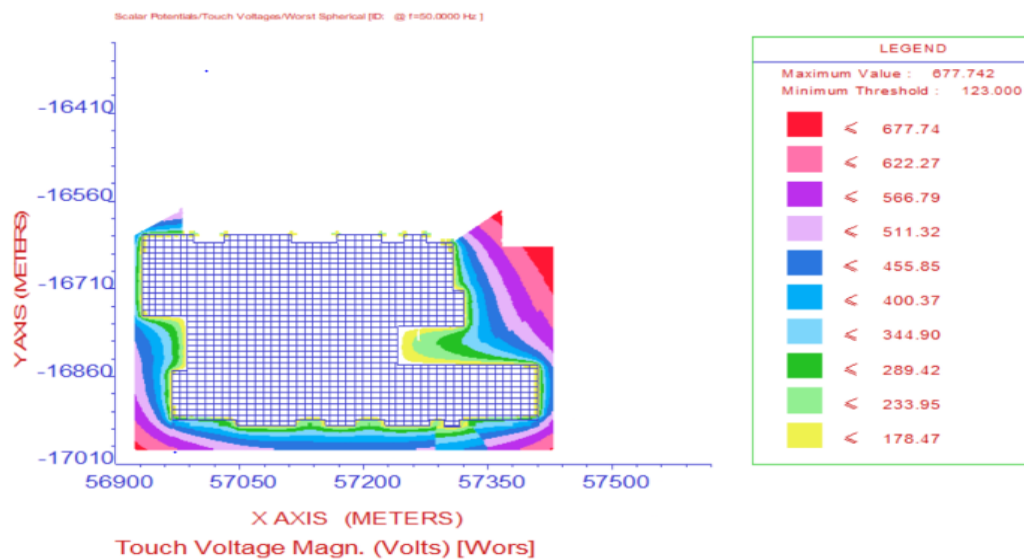


Figure 5.17. Touch Voltage 1m Outside Grid for AIS Substation

Threshold:123.0 V; Attained: 677.742 V

It is observed that the touch potentials are not within the tolerable limits.

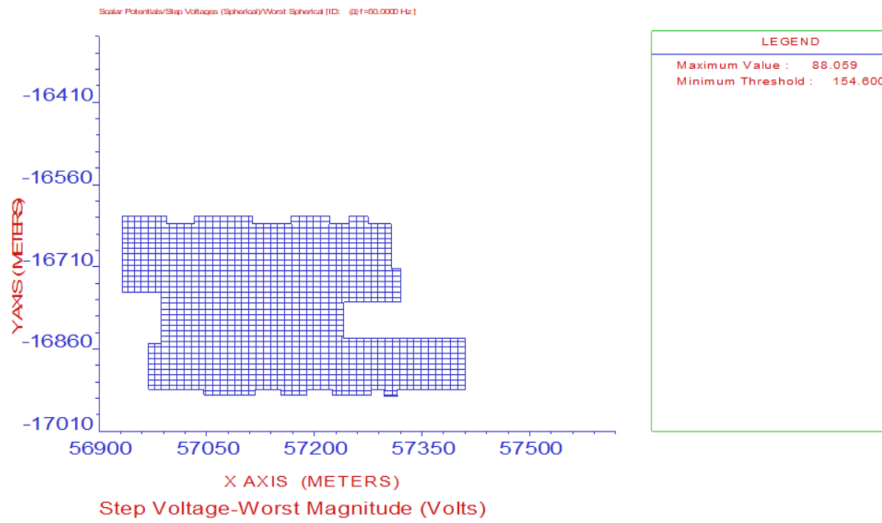


Figure 5.18. Step Touch Voltage 1m Outside Grid for Sub-Station

Step Voltage 1m outside grid/fence

The below snapshot describes the step voltage 1m outside grid without surface layer (See Figure 5.18).

Threshold: 154.60 V

Attained: 88.059 V

It is observed that the step potentials are within the tolerable limits. The grid was modelled and analysed by injecting a fault current of 27.365kA (42.1kA with split factor of 0.65) in the following scenarios. With surface layer of 3000 Ohm m resistivity for 75mm inside the grid area shown in Table 5.5. Table 5.6 shows without any surface layer above native soil, 1m outside the grid / fence area.

Table 5.5. Surface Layer of 3000 Ω m Resistivity for 75 mm Inside the Grid Area

Parameters	Tolerable Values (Safe Limit)	Attained Values
Touch Voltage	435.6 V	158.983 V
Step Voltage	1405.1 V	87.532 V
GPR	1137.842 V	
Impedance	0.0416 Ohm	

Table 5.6. Surface Layer of 1m Outside the Grid Area

Parameters	Tolerable Values (Safe Limit)	Attained Values
Touch Voltage	123.0 V	677.742 V
Step Voltage	154.6 V	88.059 V

5.4 Case Study 3 – 220 kV Substation

Soil resistivity calculated in the 220 kV substation is tabulated as below.

Table 5.7. Soil Resistivity for 220 kV Substation

S. No.	Spacing of Electrode (L) in M	Soil Resistivity $\rho = 2\pi LR$ in Ohm M		Average Soil Resistivity in Ohm M
		Location1	Location2	
1	0.5	85.45	56.86	71.155
2	1	63.21	69.24	66.225
3	2	33.55	49.26	41.405
4	3	-	31.29	31.29
5	5	8.17	6.91	7.54
Average Soil Resistivity				43.52

5.4.1 SOIL MODEL

The following soil resistivity measurements was taken from Soil Resistivity report for developing the Soil Model using GA – PSO algorithm using MATLAB software. After optimization it is evident that the site is three layered model and soil parameters are shown in Table 5.8.

Table 5.8 Optimized Soil Parameters using Hybrid GA – PSO Algorithm

Three Layer Model		
Layer	Resistivity in Ohm.m	Thickness in m.
Top Layer	71.48	1.63
Middle Layer	51.92	0.25
Bottom Layer	1.50	Inf
Error Percentage – 8.49%		

5.4.2 Grounding Design and Computation of Grid Impedance

Screen shot of the earthing grid configured in the software is shown. The grid conductor material is selected as Copper. The size of the grid conductor was arrived as per Standard IEEE80-2013. The grid conductor shall be buried at a depth of 600 mm/ below EL±0.00 (FGL) and covers the entire sub-station area. The electrode quantities are obtained from the data shared with us and modelled accordingly in the MALZ computation module. The entire sub-station area is concrete with resistivity of 100 Ohm-m for a depth of 100mm for open switchyard and 10000 Ohm-meter & 100mm Thickness is considered for safety criteria computation.

Design Parameters

Design parameters for designing the three layered soil model of 220 kV substation is discussed below,

Soil Resistivity: Three-layer soil model.

Grid Fault current & Duration for conductor Sizing: 50 KA/3 sec

Fault clearing time for touch & Step potential: 1 Sec

Conductor Size: Refer the Grid layout

Depth of grid: 600 mm

Surface Soil Resistivity & Thickness: Concrete (100 Ohm – Meter) & 100mm Thickness for Open switchyard, 10000 Ohm-meter & 100mm Thickness for Asphalt.

Conductor Sizing

Earthing systems that transport and dissipate earth fault currents without causing fires or explosive dangers in the region in its service lifetime is directly dependent on the designed materials and sizes of its system parts. The diameter of the conductor is found by multiplying the area of the cross section by the diameter of the conductor.

Input Data (Properties of Copper referred as per Item 09 Table 1 of IEEE std. 80-2013)

- (i) Conductor Material – Cu
- (ii) Fault Current I_f – 50 kA
- (iii) Fault Duration, t_c – 3 second
- (iv) Maximum Allowable Temperature, T_m – 433.2°C
- (v) Ambient Temperature, T_a – 50°C
- (vi) Thermal Coefficient Resistivity at reference Temperature, α_r – 0.00393
- (vii) Resistivity of Ground Conductor, ρ_r – 1.72 $\mu\Omega$ -cm.
- (viii) Thermal Capacity Factor, TCAP – 3.4 J/cm³. °C
- (ix) K_0 (=1/ α_0) – 234

Calculated conductor size using equation 5.1, $A = 418$ sq.mm

5.5 RESULTS FOR 220KV SATELLITE GRID

A result of 220 kV satellite grid with safety criteria is discussed in the following section.

Safety Criteria for 50kg body weight with surface layer

One of the important aspects of earthing system designs in accordance with IEEE Std 80-2013 is the determination of safety limits of touch and step voltages using functional parameters given below

- Magnitude of permissible body current (IB)
- Duration of shock current (ts)
- Resistance of current flow path through human body consisting of body resistance (RB) and resistance of feet (Rfoot)
- X/R Ratio

The following snapshot shows the safety limits for Step and Touch potential voltage with a surface layer of 10000 Ohm-m for 100mm thickness.

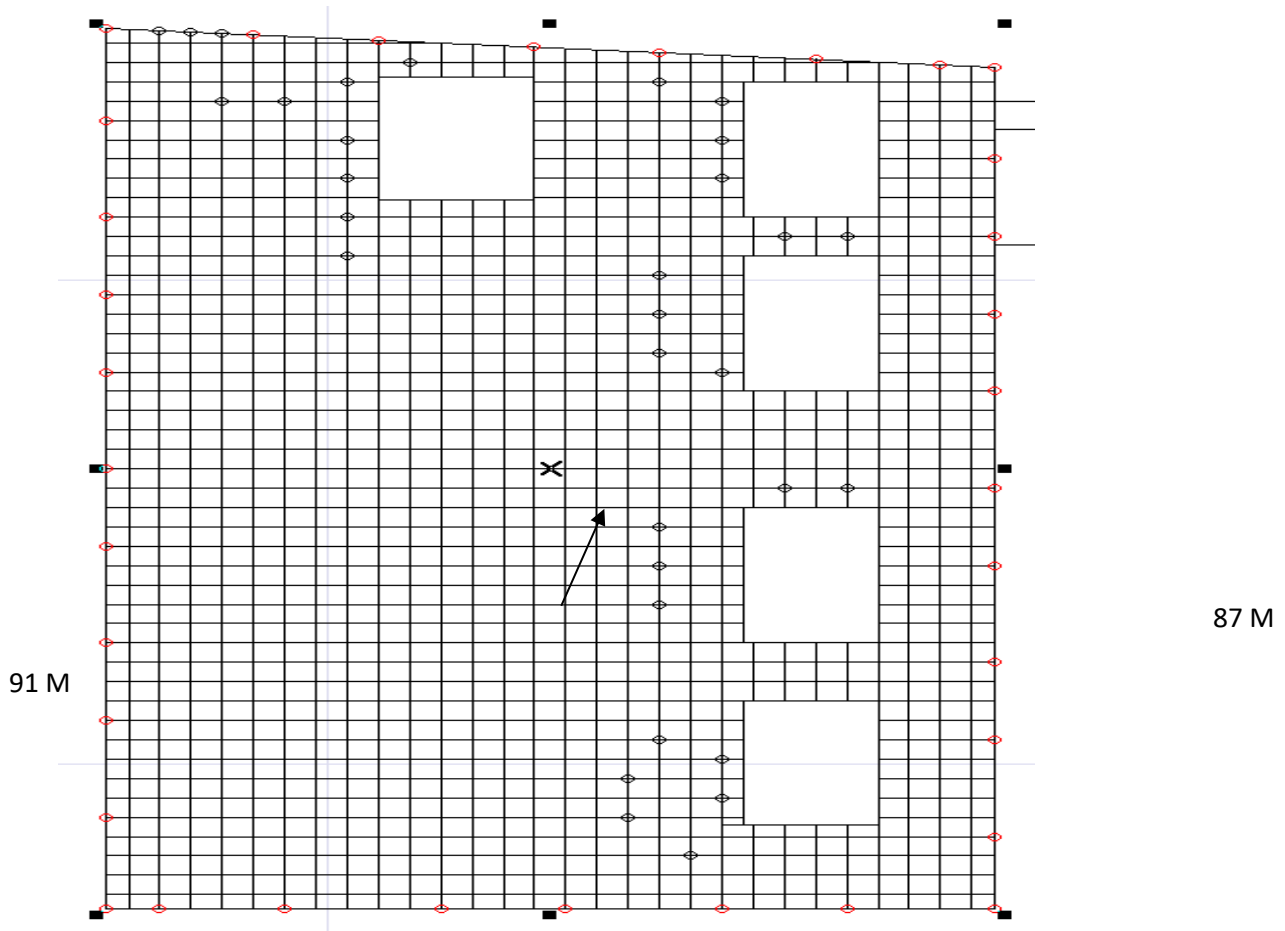


Figure 5.19 Screenshot of SESCAD Drawing of 110kV Substation

○ M Long Electrode - 30mm diameter Pipe electrode - 32 No's

Grid - 2 x 0.2 Sq. inch Conductor

○ M Long Additional Electrode - 17.2 mm diameter copper-bonded steel Rod with
100 mm

The below snapshot shows the observation profile inside the grid area (See Figure 5.20).

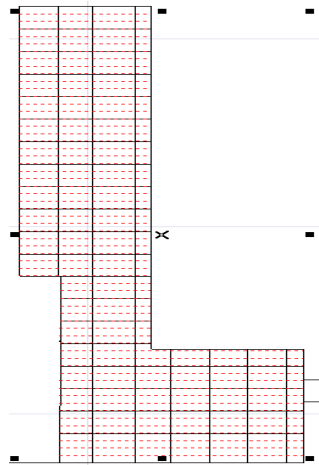


Figure 5.20. Satellite Grid Area for 220 kV Substation

Touch Voltage (with asphalt road)

The potential difference between an accessible earthed conductive component and the earth surface potential at the place where a person stands with his hands in touch with an earthed part is known as Touch Voltage. The below snapshot from software shows the touch voltage profile in the sub-station area when the fault is simulated (See Figure 5.21).

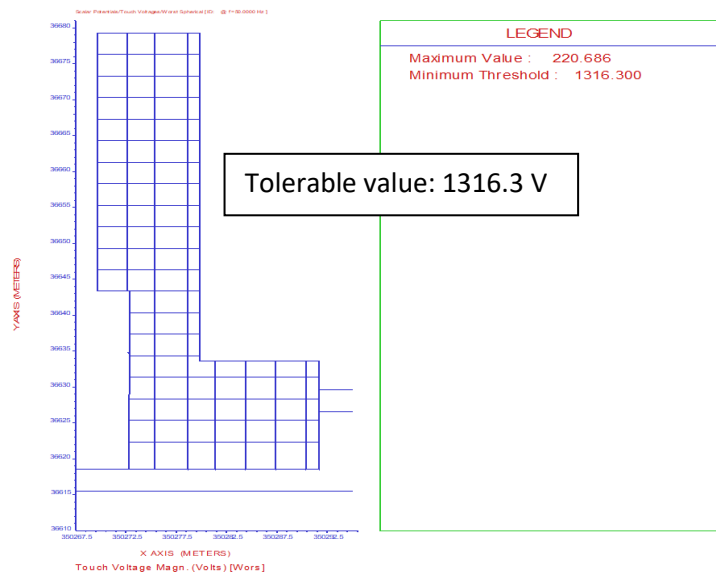


Figure 5.21. Touch Voltage Grid Area for 220 kV Substation

Results achieved by Touch Voltage with attained value as 220.686 V, and Threshold Value as 1316.300 V. It was observed that grid area's touch potential is within permissible limits.

Step Voltage (with asphalt road)

The difference in potential between two earth surface points that are 1 m apart is known as step voltage. A person traversing a distance of 1 m (standard step size) without contacting any earthed item will be exposed to this voltage (Refer Figure 5.22).

Results achieved by step voltage with attained value as 56.694 V, and Threshold Value as 4927.800 V. It is observed that the step potential inside the grid area is within the tolerable limits.

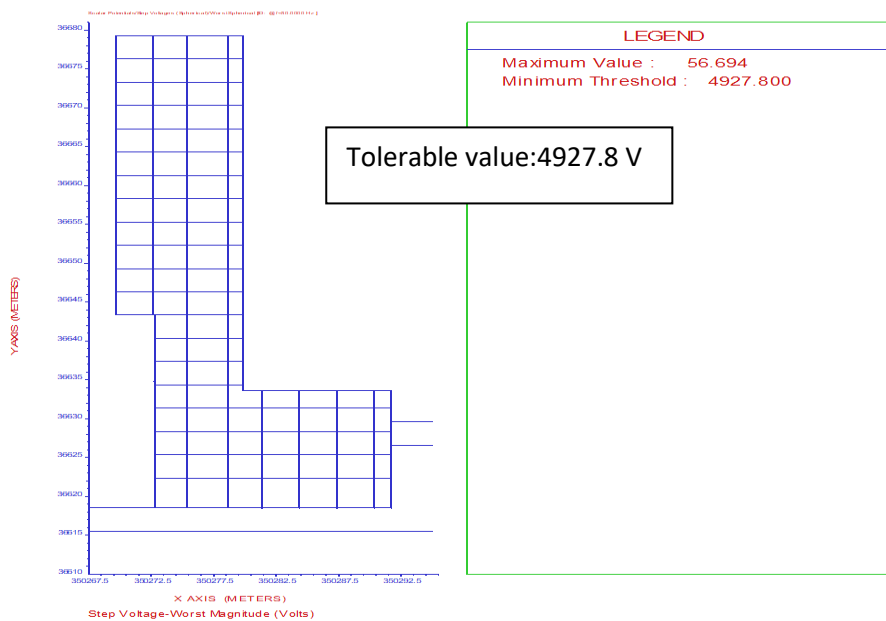


Figure 5.22. Step Voltage Grid Area for 220 kV Substation

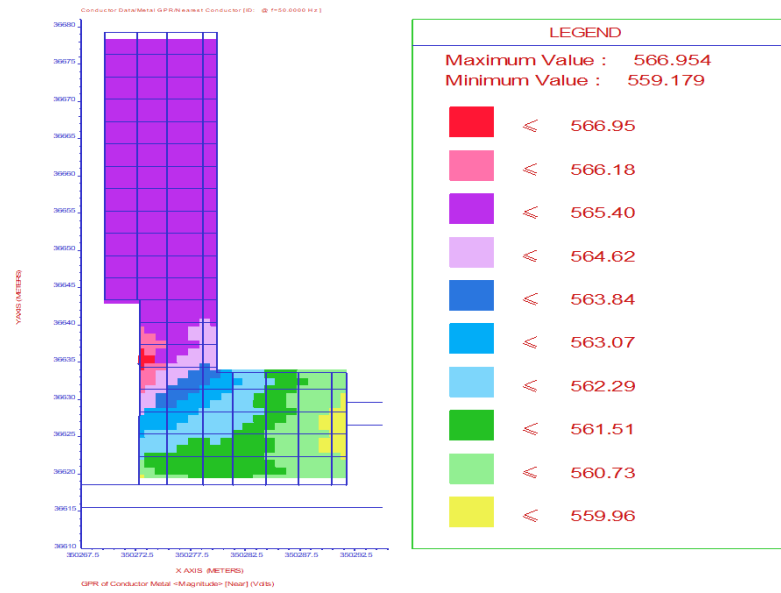


Figure 5.23. Conductor GPR for 220 kV Substation

5.5.1 Conductor GPR

The highest voltage reached by an earth electrode in relation to a distant earthing point at the potential of remote earth or reference earth in a station is known as ground potential rise (Refer Figure 5.22).

Table 5.9. Soil Parameters for 110 kV AIS Connected with Satellite Grid

Parameters	Tolerable Value	Attainable Value
Touch Voltage inside 110 kV AIS Grid	128.8 V	82.101 V
Step Voltage inside 110 kV AIS Grid	177.7 V	93.118 V
Touch Voltage inside 220 kV Satellite Grid	1316.2 V	220.686 V
Step Voltage inside 220 kV Satellite Grid	4927.9 V	56.694 V
Grid Impedance	0.0115 Ohms	

Results achieved by GPR with maximum value as 566.954V, and minimum value as 559.179 V. It is observed that the step potential inside the grid area is within the tolerable limits. Satellite Grid for 220kV GIS was proposed & interconnected with

existing 110kV AIS & 245kV GIS grid. Injected the Fault current of 50kA in the satellite grid & analysed the Touch & step potential in 220kV satellite grid and existing 110kV AIS & 245kV GIS grid and found to be safe (See Table 5.9).

Table 5.10. Touch & Step Potential of 245 kV GIS Connected with Satellite Grid

Parameters	Tolerable Value	Attainable Value
Touch Voltage inside 245 kV GIS Grid	1316.3 V	894.908 V
Step Voltage inside 245 kV GIS Grid	4927.8 V	253.789 V
Touch Voltage inside 220 kV Satellite Grid	1316.3 V	631.897 V
Step Voltage inside 220 kV Satellite Grid	4927.8 V	161.819 V
Grid Impedance	0.0284 Ohms	

Scenario – 2:

Satellite Grid for 220kV GIS was proposed & interconnected with existing 245kV GIS grid. Injected the Fault current of 50kA in the satellite grid & analyzed the Touch & step potential in 220kV satellite grid and existing 245kV GIS grid and found to be safe (See Table 5.10).

In both the Scenario's we found that the touch & step potentials are well within the limits & Grid impedance is less than 1 ohm.

5.5 SUMMARY

This chapter detailed on a soil model with precise design for an air-insulated substation's grounding system. For two or more layered soil models, IEEE80-2013 provides directions for designing their grounding systems which were executed in this work using software. In terms of earth design, the outcomes of AISs were assessed using voltage levels like step and touch voltages.

CHAPTER 6

GAS INSULATED SUB-STATION (GIS) GROUNDING GRID DESIGN FOR OPTIMIZED SOIL PARAMETERS IN MULTIPLE LAYERS

6.1 Gas Insulated Substation

Grounding systems are critical components in power system sub-stations as they prevent excessive voltages or voltage overshoots and thus ensure safety. These systems are also closely related to electrical grid's stability, integrity and operational safety of sub-stations and nearby regions. Soil resistivity models for sub-station soils affecting grounding systems include uniform, two layered or multi-layered models. Accurate soil models can be defined based on proper measurements of soil resistivity. When observed resistivity's average values are made a part of design, it results in erroneous computations specifically, when the variance between probe distance's resistivity is more than 25% and in such instances, two layered soil models are most appropriate. Further, empirical studies can help design engineers in their sub-station grounding system parameter estimations for two layered or multi-layered soil resistivity models.

Hence, a proper sub-station grounding system needs to be designed, tested, and implemented for ensuring sub-station employee protection in addition to extending the life of sub-station equipments and infrastructure. GISs (Gas Insulated Sub-stations) are frequently used in urbanized areas as they occupy lesser space and also enhance aesthetic appeal of sub-stations infrastructural buildings. GISs are high voltage sub-stations where primary buildings are enclosed in sealed environments and insulated with Sulphur hexafluoride gas. The technology of GISs was created with the aim of creating sub-stations in smallest available spaces and in addition phase wise clearances required is far lesser when compared to airborne insulated sub-station environments. The overall space occupied by GISs amounts to less than 10% of space occupied by traditional sub-stations.

GIS are also advantageous in other aspects including their reduced vulnerability to pollutions, salts, sand, or heavy amounts of snow as the building is encased. Though, the initial costs of constructing GISs are higher than air insulated sub-stations, GISs are advantageous in their lowered operating and maintenance expenses. Since, any study on grounding needs to start with the study of soil resistivity, this work's soil resistivity measurement was taken from sub-station's accessible places. The results of the measured soil resistivity were interpreted and evaluated. Earthing fault currents generated from metallic infrastructure short circuit can get dissipated into the soil and thus jeopardizing nearby civilian facilities and pose great risks to the public in terms of safety. GISs are compact metal encapsulated switchgears with circuit breakers and disconnectors capable of handling high voltages safely within confined spaces. GISs can be installed anywhere and within limited spaces like buildings, rooftops and extensions. Offshore platforms, industrial installations, and hydro-power plants are all examples of employments of GISs. Hitachi Energy is the leader in GISs in terms of compactness, operations, switching technologies, smart controls and monitors. Hitachi Energy's GISs are extremely reliable, environmentally friendly and safe to use. They offer a variety of solutions in the range 72.5 kV to 1200 kV based on applications to cater to present and future switchgear requirements. Figure 6.1 depicts a GIS illustration.



Figure 6.1. Gas Insulated Sub-Station and Grounding Area with Gravel Surface

GIS's active components which include disconnectors, CBs, bus bars, voltage/current transducers, and other conventional HV components are situated in the midst of

aluminium alloy pipes and insulated by epoxide resins. These pipelines with earth potential are filled with insulating gas. GISs occupy only 10% area in comparison to air-insulated substations. Though GISs can be constructed indoors and outdoors, they also create a set of issues that need to be addressed. Three significant characteristics of GIS's sub-station earthing designs differ from AIS designs and are detailed below:

1. GIS for achieving compact substation designs. It subsequently reduces sub grounded station's area of spread.
2. Since, GIS phase conductors are significantly closer, electromagnetic currents develop in earthing systems when metal enclosures are used for containment of gases.
3. GIS compressed SF6 gas insulation allows narrow dielectric clearances where breakdown happens in nanoseconds or lesser times. Voltage collapses rapidly, resulting in the formation of very fast travelling wave transients that propagate throughout the GIS. When these transients are coupled with the earthing system, a TGPR (Transient Ground Potential Rise) occurs.

6.2 GIS principles of operation

GIS complete enclosures make them impermeable to their surrounding environments which is an advantage from environmental view points and specifically in the case of ocean-based oil rigs and particle or mist pollution sources. Nevertheless, as gas isolated switchgears are completely enclosed, visible disconnecting mechanisms are not possible. Grounding and disconnection switches which are mandatory to both air and gas insulated systems have view ports where GISs have smaller "footprints" than their equivalent air-insulated sub-stations (reduction of 50% space). Though such gas isolated sub-stations would initially cost more than their air insulated counterparts, they can be justified when required in areas where land is scarce like city centres. GISs can also be restructured where low profile sub-stations are required.

It is mandatory to confirm grounding and disconnect switch locations, specifically when gas isolated switchgear elements are isolated for services. Since, these switches are completely enclosed within aluminium casings, manufacturers must include view ports which helps assess the positions of disconnect and grounding switches visually. In some cases, this task can be executed even with flashlights.

GISs may or may not have protective relays installed in same locations, since SF6 gases are critical insulators and need to be maintained at required densities within GIS devices. Hence, each gas separation included an alarm and trip contacts from sensors to alert employees or separate devices when insulation integrity falls below required levels. Grounding designs were based on traditional ways of restricting power frequency enclosure potentials within safe levels and based on maximum projected fault current conditions even in the beginning of GIS.

Arcing between grounded enclosures and other components (indication of greater potentials) were commonly detected in contrast on HV testing breakdowns or during normal disconnectors operations, even in low potentials and hence extensive study was conducted to understand this particular aspect TGPR in CIS. The use of faulty current split computations helped determine earth current (current discharged by grounding systems to earth). It was found that total fault current was not discharged in the substation's grounding system under most circumstances. Faulty current that did not contribute to grounding system's average GPRs (ground potential rises), returned to remote source terminals and transformer neutrals through shield/neutral wires or grid conductors.

Table 6.1. Fault Current Split Calculation Results

	Station 1	Station 2
Remote Contribution	11.94∠-85° kA	11.45∠-85° kA
Current returning via OHGW	10.89∠-13.6° kA	10.42∠-13.6° kA
Earth Current Discharged in Grid	2.62∠-61.8° kA	2.79∠-61.8° kA

The amount of faulty current discharged directly into the soil by the grounding network is exactly proportional to GPRs and touch and step voltages connected with grounding networks. Hence, accurate measurements of faulty current returns to remote sources through overhead ground and neutral wires of transmission and distribution lines linked to the substation is critical. Table 6.1 lists values used in the grounding grid study where

earth currents discharged by grounding systems were found to be between 22-24% of the total faulty current.

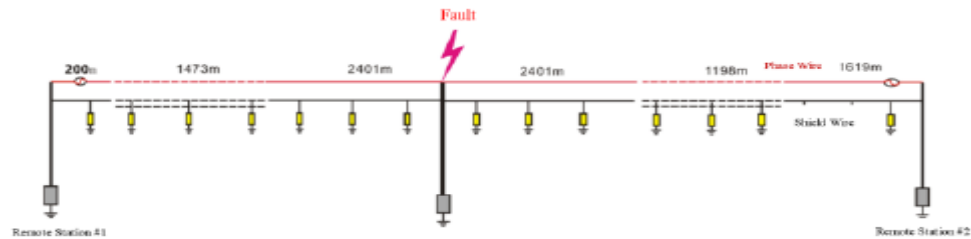


Figure 6.2. Fault Current Distribution Computation Circuit Model

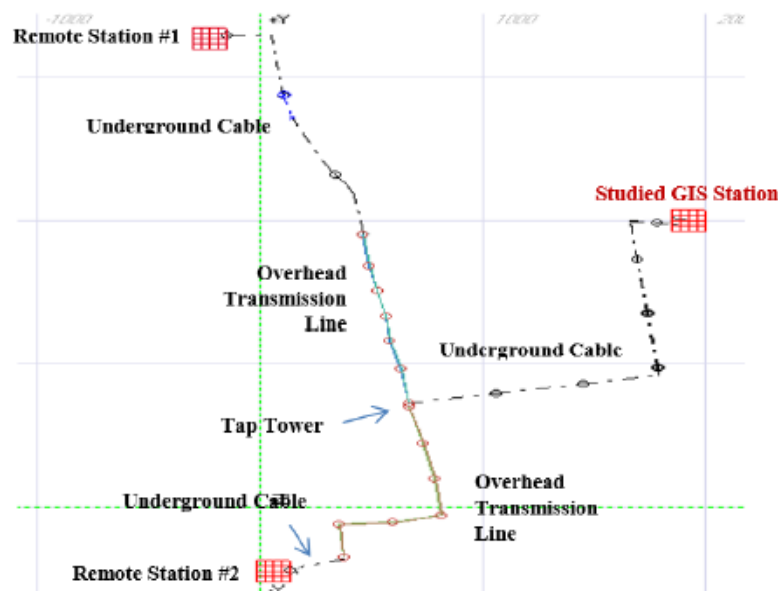


Figure 6.3. Fault Current Distribution Computation Field Approach Model

The findings of the study on a 110 kV single-line-to-ground failure at the GIS station are illustrated in Figures 6.2 and 6.3. The faulty current contributions from two distant sources are also shown in Figures 6.2 and 6.3.

Step 4: Analysis of Grid with Fault Current

The grid so designed as per Step 2 shall be energized with fault current arrived as per Step3. Touch and Step potential shall be computed by defining safety criteria and the results shall be compared with thresholds safety limits determined based on the Standard IEEE80-2000.

Step 5: Safety Criteria and Safety evaluation

When a sub-station is evaluated for safety using faulty conditions, TGPR, touch, and step voltages are significant variables that need to be studied. For grounding systems, a comprehensive network computer model was constructed in this work to account for infrastructure outside the targeted substation. Various incidents were investigated along with touch and step voltages across the substation and home water lines.

In SF6 breakdowns, over voltages with quick rise times of 5-20 ns was observed and specific coaxial bus-ducts were found good for transmission of these MHz range voltage surges, thus causing TGPRs. The technique models GIS phase conductors and enclosures accurately and efficiently as they play a key role in discharging faulty current more realistically and accurately along GIS structure's ground bonding points, which are connected to the grounding grid by steel rebar in concrete.

6.3 Analysis of Grid – 765 kV GIS Room Floor

The 765kV GIS equipments as per the given layout in the above Reference documents were modeled as “cable type” conductor in HIFREQ module of CDEGS. Each line in the layout represents phase conductors and its enclosure. The 765kV GIS enclosure and equipments were connected to Main earth grid below GIS building at 73 places by using 50x8mm Copper conductor. Flat and connected to GIS Room main earth bus. Flat and connected to Main earth grid at 28 locations in the peripheral of building. Outdoor structures supporting bus duct were also connected to Main earth grid by 50x8mm Cu. Flat at locations as shown in the reference documents. Similarly, at 400KV GIS control room, the GIS enclosure and equipment were connected to Main earth grid below GIS building with 50x8mm Cu. Flat conductor at 83 locations and connected to GIS room main earth bus. The main earth bus is modeled as 50x8mm Cu. Flat and connected to Main earth grid at 14 locations in the peripheral of building.

Fault current of 63KA has been injected in the Main earth grid near 765kV GIS room. The objective behind this study is to find out the new Touch, Step voltages and other grid parameters when Main earth grid is connected with above ground conductors that

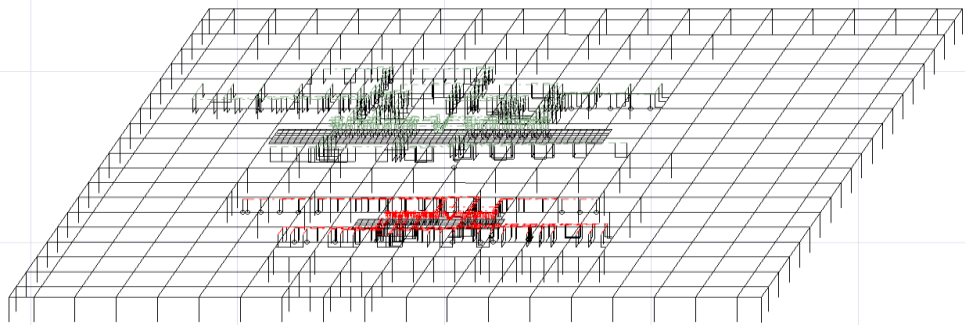


Figure 6.4. 3D View of 765kV GIS and 400kV GIS

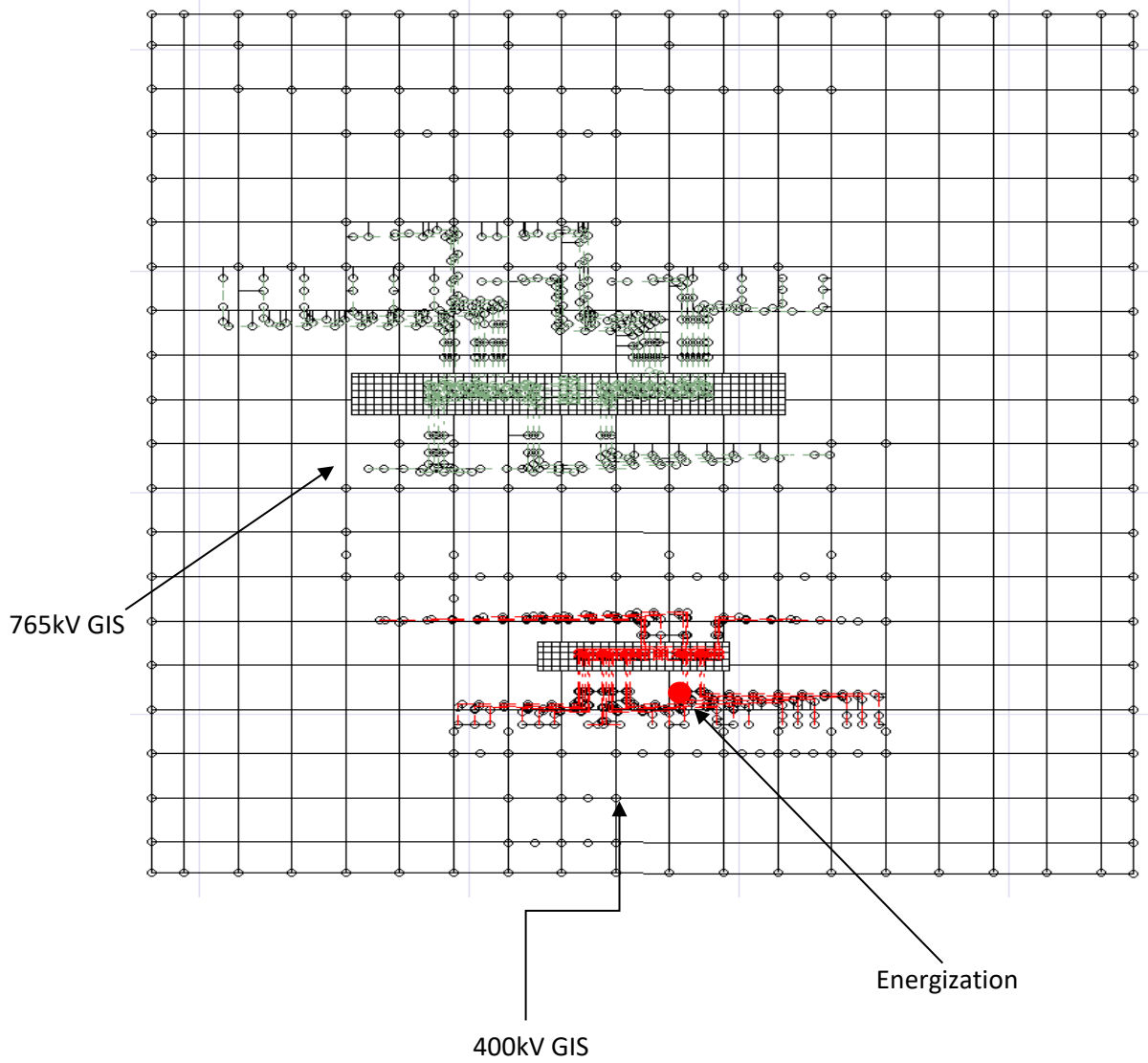


Figure 6.5. Perspective View of the System - 765 kV GIS and 400 kV GIS

is GIS equipment and bus ducts. Being the sub-station is large and that too with low resistivity soil, the above ground bus bars, conductors, bus ducts and structure should be considered for capacitive, inductive coupling between buried grid conductors. This simulation is possible by exact electromagnetic fields method of module HIFREQ. The 3D view for 765kV GIS and 400kV GIS is shown in the figure 6.4. The system under the study for 765kV GIS and 400kV GIS is shown in the figure 6.5.

1. Evaluation of safety in the Grid Area
2. Evaluation of safety in GIS room
3. Evaluation of safety outside the grid for native soil.

6.3.1 EVALUATION OF SAFETY INSIDE THE GRID AREA

The evaluation of safety inside the grid area for GIS is shown in the following figures. Fault Current of 63kA is simulated to examine the safety is discussed. Observation Profile to evaluate the safety inside the GIS Grid area is displayed in the figure 6.6.

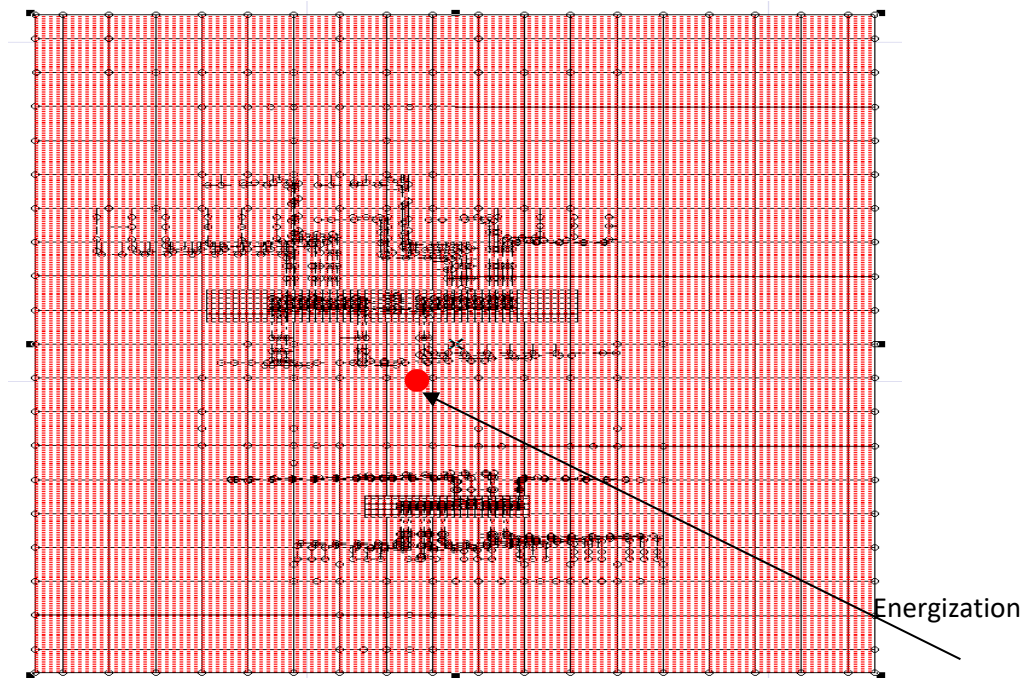


Figure 6.6. Evaluation of Safety Inside the Grid Area for GIS

Touch Voltage in grid area

The potential difference between an accessible earthed conductive component and the earth surface potential at the place where a person stands with his hands in touch with an earthed part is known as Touch Voltage. Figure 6.7 shows the touch voltage profile in the sub-station area when faults are simulated.

Attained Value: 92.45 V; Threshold Value: 128.2 V

It is observed that the touch potential in the grid area is within the tolerable limits.

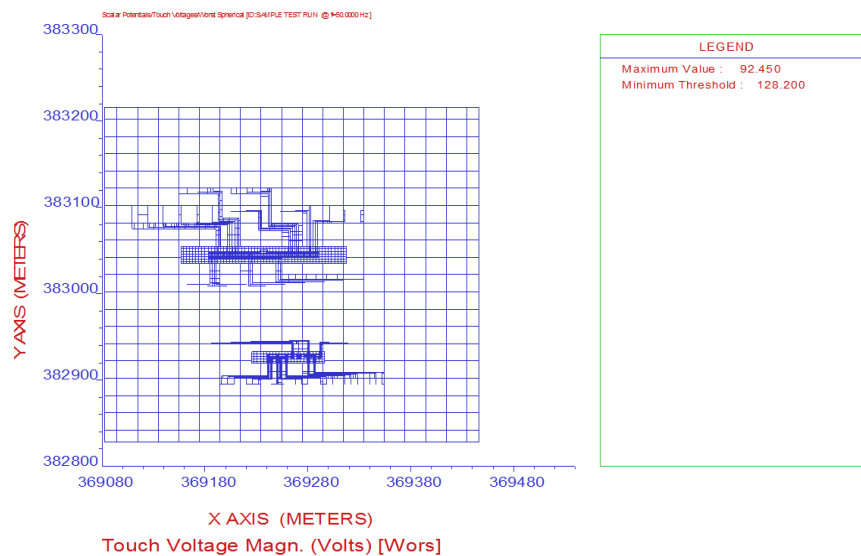


Figure 6.7. Touch Voltage Profile in the Sub-Station Area with Fault

Step Voltage in grid area

The difference in potential between two earth surface points that are 1 m apart is known as step voltage is shown in figure 6.8 and can be experienced by persons bridging a distance of 1 m (typical step size) without contacting any earthed object.

Attained Value: 15.738 V; Threshold Value: 175.5 V

It is observed that the step potential inside the grid area is within the tolerable limits. Conductor GPR inside the 1m is discussed in figure 6.9.

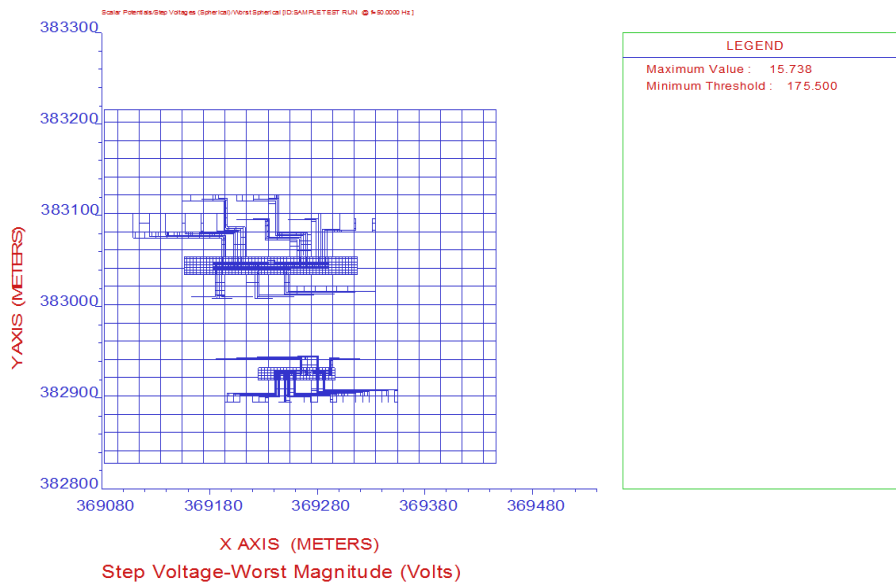


Figure 6.8. Step Voltage Profile in the Sub-Station Area with Fault

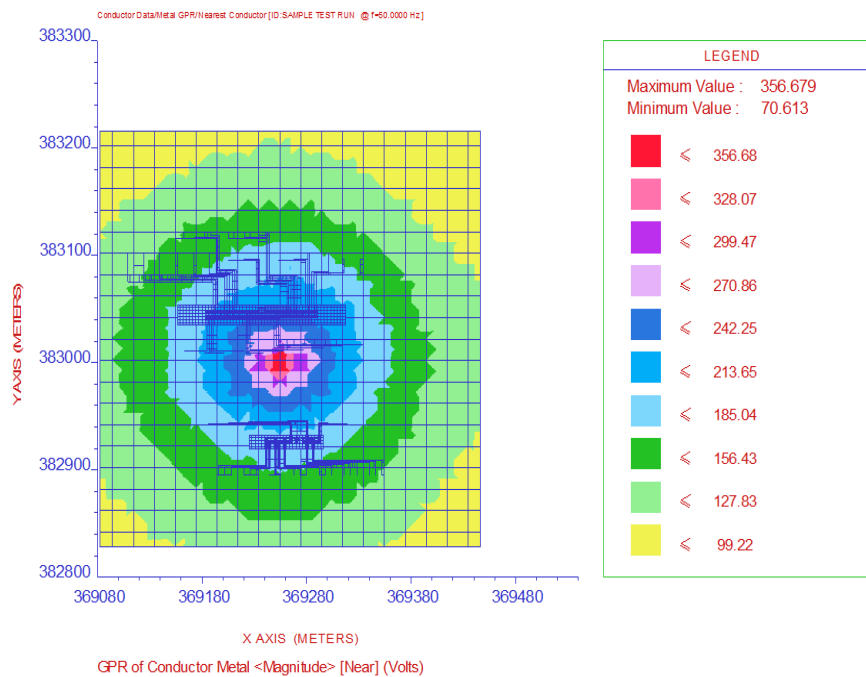


Figure 6.9. Conductor Ground Potential Rise Inside Grid

Observations:

Maximum Value: 356.679 V

Minimum Value: 70.613 V

6.3.2 EVALUATION OF SAFETY IN GIS ROOM

In this section shows the evaluation of safety for GIS room is discussed in the following section. Simulation of observation profile inside the GIS room is shown in the figure 6.10.

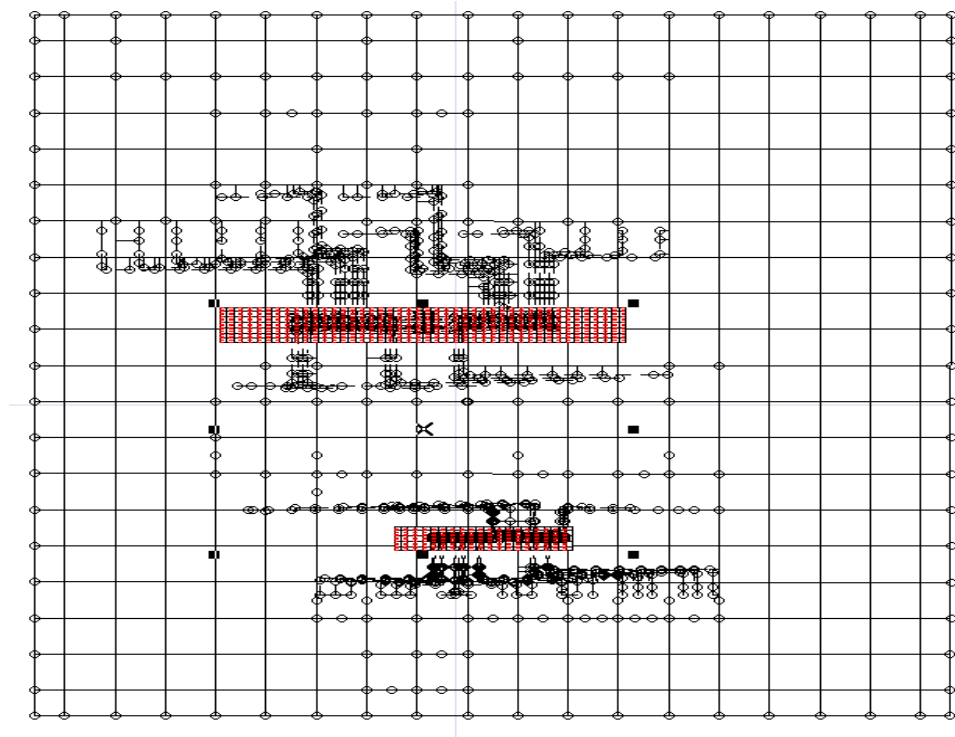


Figure 6.10. Observation Profile Inside the GIS Room

Safety Criteria with Surface layer resistivity of 100 Ω -M (concrete) for 100mm thickness: (Inside GIS room):

The following figure 6.11 shows the safety limits for Step and Touch potentials within GIS room with concrete as surface layer. (100 Ohm-m for 100mm thickness).

Touch Voltage for GIS room

The following figure 6.11 shows the safety limits for Touch potentials within GIS room with concrete as surface layer. (100 Ohm-m for 100mm thickness).

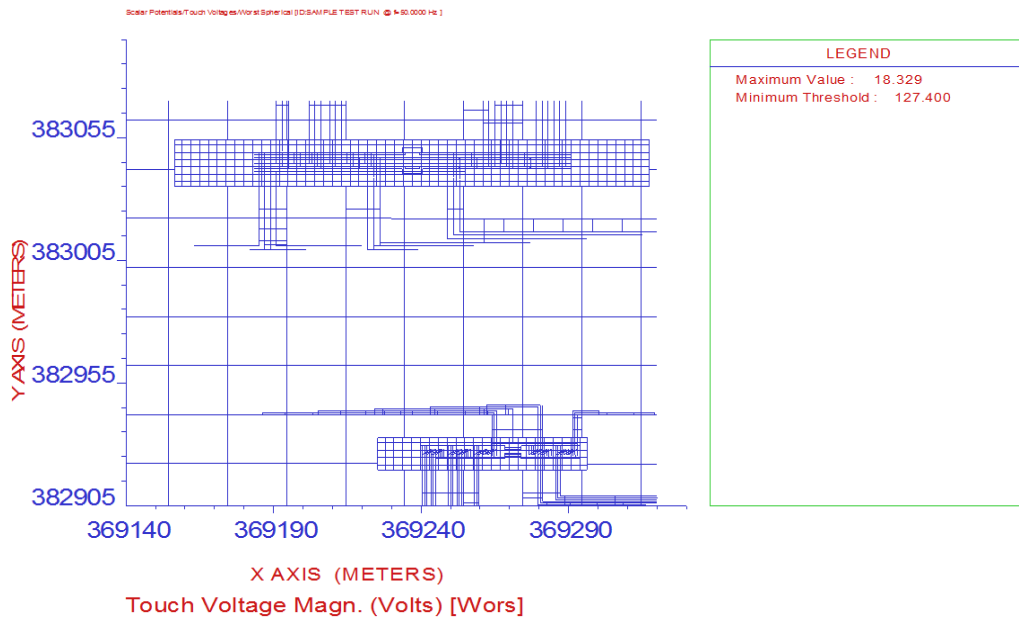


Figure 6.11. Safety Limits for Touch Voltage Within GIS Room

Attained Value: 18.329 V; Threshold Value: 127.4 V

It is observed that the touch potential in the GIS room is within the tolerable limits.

Step Voltage for GIS room

The following figure 6.12 shows the safety limits for step voltage potentials within GIS room with concrete as surface layer. (100 Ohm-m for 100mm thickness).

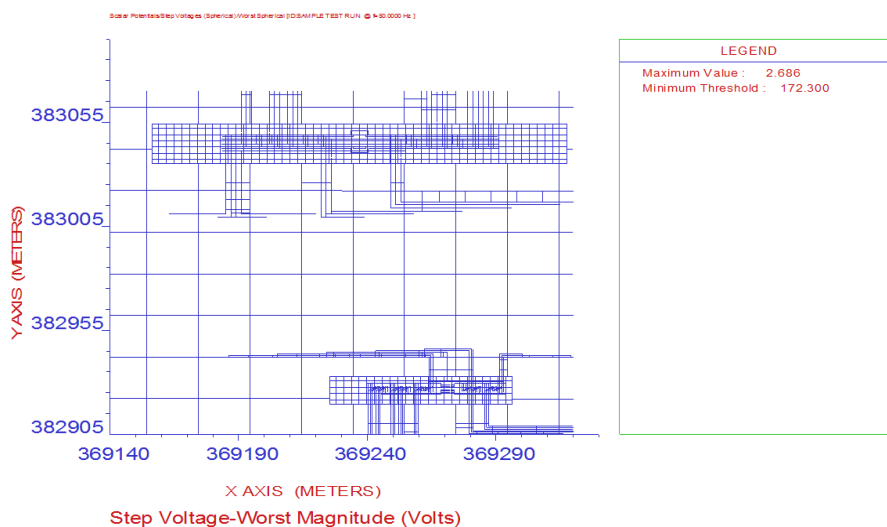


Figure 6.12. Safety Limits for Touch Voltage within GIS Room

Attained Value: 2.686 V; Threshold Value: 172.3 V

It is observed that the step potential inside the GIS room is within the tolerable limits.

6.3.3 Metal to Metal Touch Voltage (GPD on 765kV GIS Equipments inside room)

It is the potential difference between metallic items or buildings inside substations that can be bridged by direct hand-to-hand or hand-to-foot contacts only.

Tolerable $E_{mm-touch} = 116/\sqrt{T_s}$ (Where $T_s=1$) (Eq34 of IEEE80:2013)

Tolerable $E_{mm-touch} = 116V$

Ground Potential difference (GPD) is defined as the potential at a point with respect to ground potential at that point. Figure 6.13 shows the Metal to metal touch voltage (GPD on 765kv GIS equipments inside room).

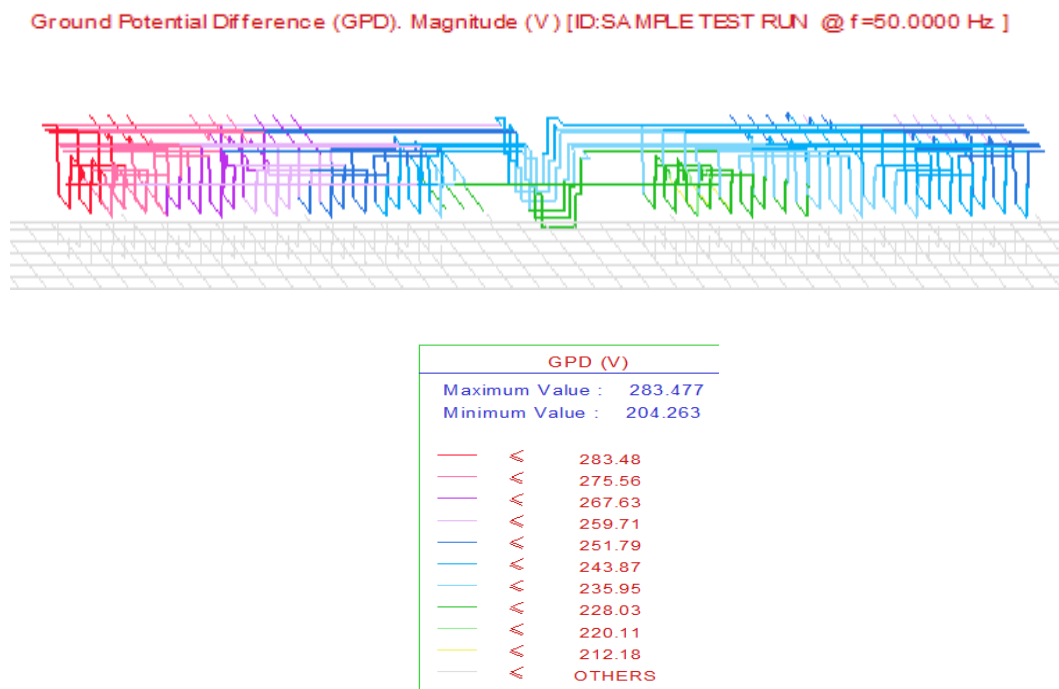


Figure 6.13. Metal to Metal Touch Voltage (GPD on 765kv GIS Equipments Inside Room)

Maximum GPD Value - 283.477; Minimum GPD Value - 204.263

Metal to Metal Touch Voltage = Maximum GPD - Minimum GPD

Metal to Metal Touch Voltage = (283.477- 204.263) = 79.214 V (<116V)

It is observed that the metal to metal touch potential inside the 765kV GIS room is within the tolerable limits.

6.3.4 Metal to Metal Touch Voltage (GPD on 400kV GIS Equipment inside room)

It is the potential difference between metallic items or buildings inside substations that can be bridged by direct hand-to-hand or hand-to-feel contacts only.

Tolerable $E_{mm-touch} = 116/\sqrt{T_s}$ (Where $T_s=1$) ; Tolerable $E_{mm-touch} = 116V$

Ground Potential difference (GPD) is defined as the potential at a point with respect to ground potential at that point. Figure 6.14 shows the Metal to metal touch voltage (GPD on 400kV GIS equipments inside room).

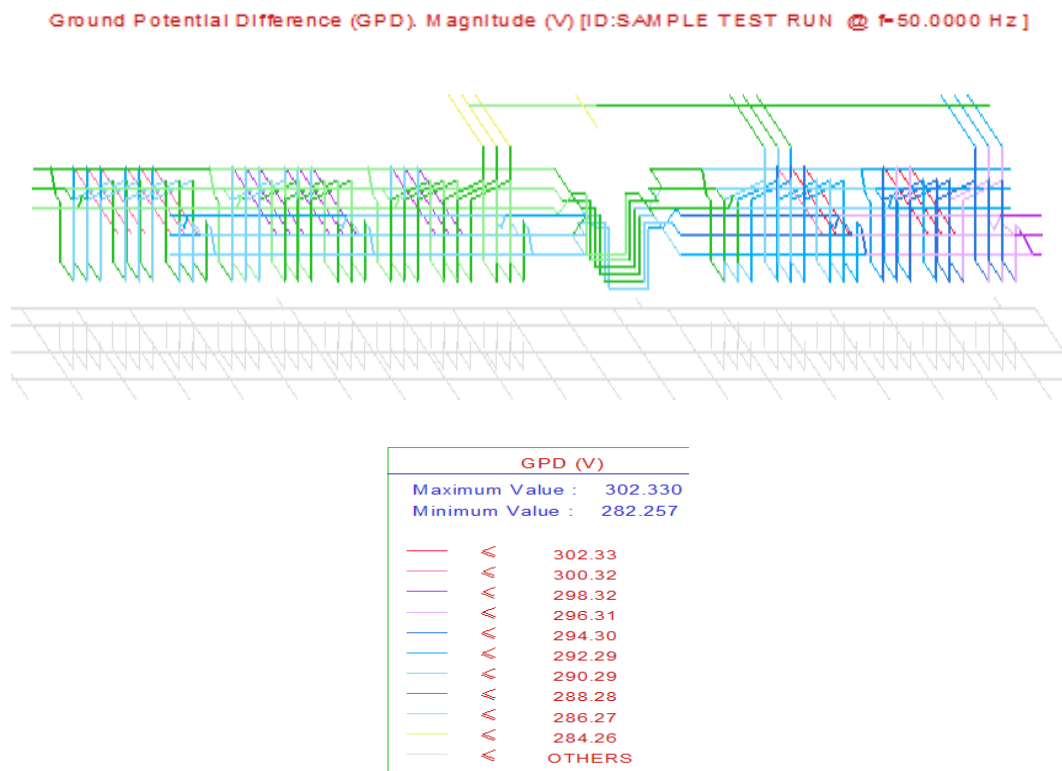


Figure 6.14 Metal to Metal Touch Voltage
(GPD on 400kv GIS Equipments Inside Room)

Maximum GPD Value - 302.33; Minimum GPD Value - 282.257

Metal to Metal Touch Voltage = Maximum GPD - Minimum GPD

Metal to Metal Touch Voltage = (302.33- 282.257) = 20.073 V

It is observed that the metal to metal touch potential inside the 400kV GIS room is within the tolerable limits.

6.3.5 Evaluation of Safety Outside Fence for Step Potential with Native Soil:

This section shows the safety outside results with native soil discussed in the following manner. The following figure 6.15 shows the simulated model for native soil. The following figure 6.16 shows the safety limits for Step voltage 1m outside grid without surface layer.

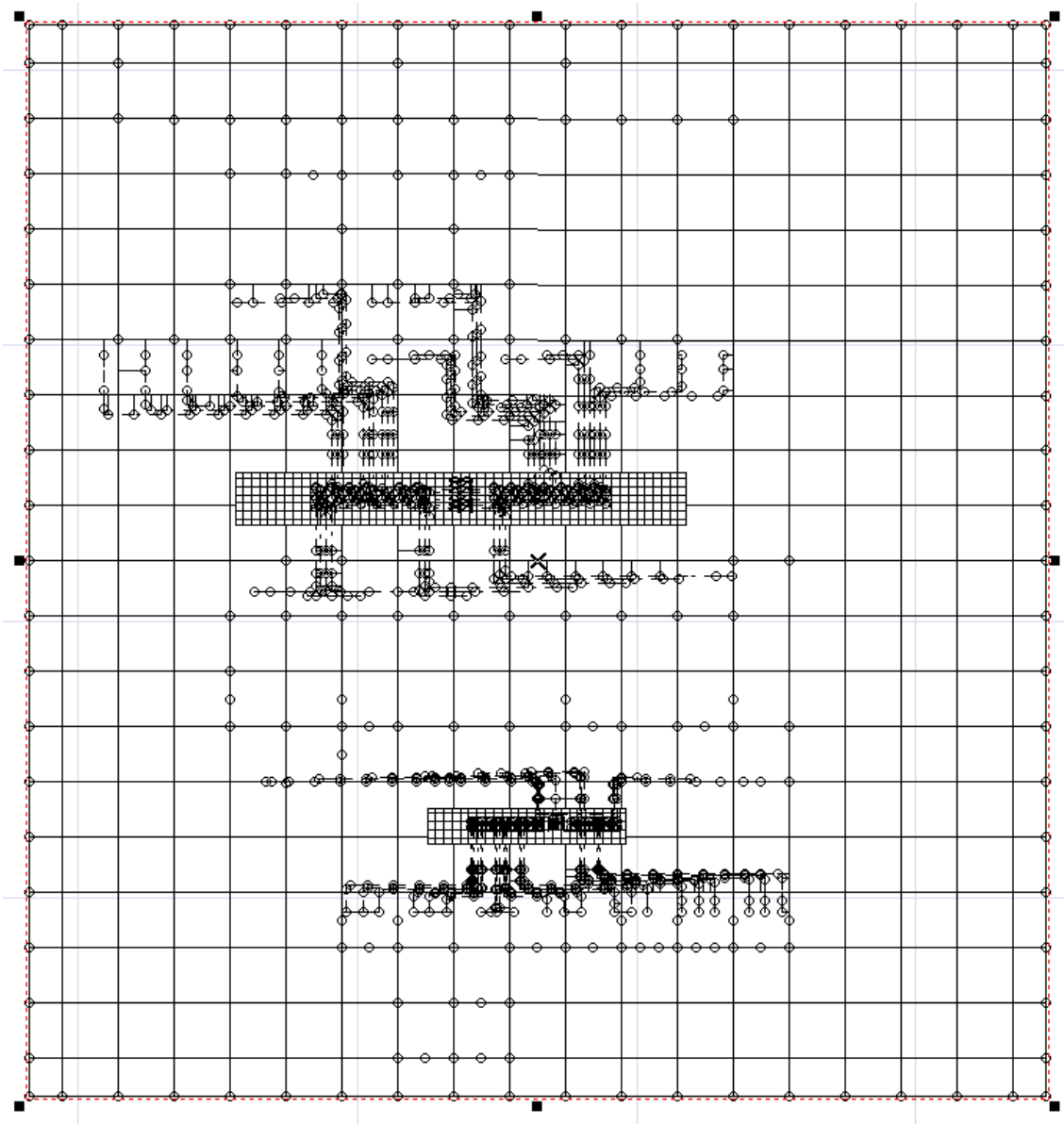


Figure 6.15. Observation Profile with Native Soil

Table 6.2. Comparison of Different Safety Criteria

Parameters		Tolerable Values	Achievable Values
Touch Voltage in Grid		128.2 V	92.45 V
Step Voltage in Grid		175.5 V	15.738 V
GPR	Maximum	-	356.679 V
	Minimum	-	70.613 V
	Differential	-	286.066 V
Touch Voltage on GIS Room		127.4 V	18.329 V
Step Voltage on GIS Room		172.3 V	2.686 V
Metal To Metal Touch Voltage On 765kv GIS Equipments (Difference Of Maximum & Minimum Of Gpd)		116 V	79.214 V
Metal To Metal Touch Voltage On 400kv GIS Equipments (Difference Of Maximum & Minimum of GPD)		116 V	20.073 V
Step Voltage 1m Outside The Grid		144.3 V	1.891 V

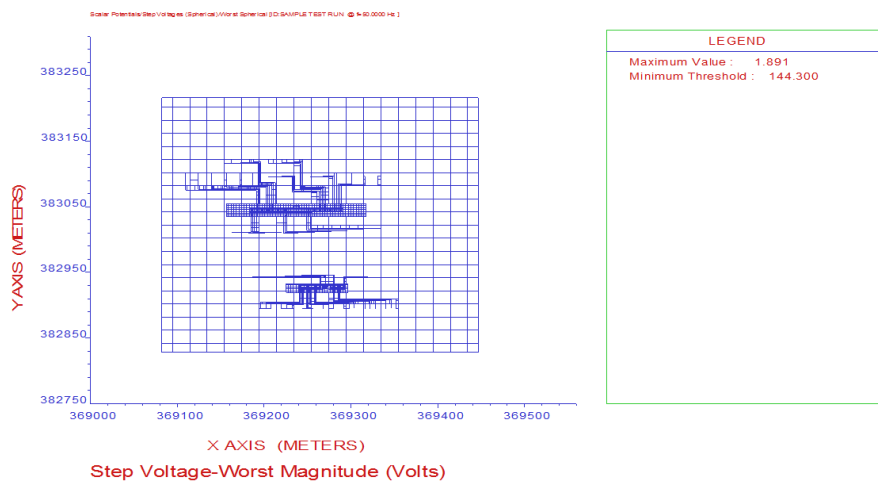


Figure 6.16 Step Voltage 1m Outside Grid for Native Soil

Attained Value: 1.891 V; Threshold Value: 144.3 V

It is observed that the step potential outside the grid area is within the tolerable limits. The results are tabulated in the table 6.2.

6.3.6 GROUND FAULT ANALYSIS AT GIS EQUIPMENTS INSIDE -765kV GIS ROOM

Ground fault analysis at GIS room is shown in the figure 6.17 and Figure 6.18 shows the fault location in the conductor segment.

Fault location:

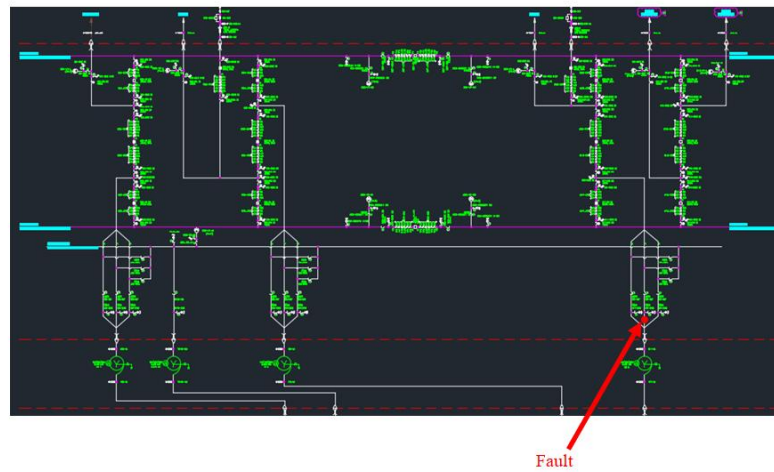


Figure 6.17. Ground Fault Analysis at GIS Room

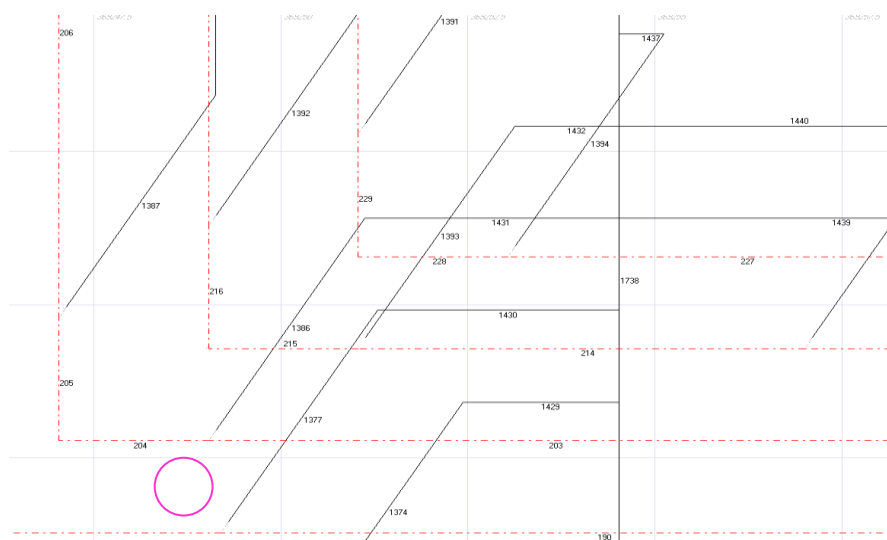


Figure 6.18. Fault Location with Conductor Segment Number

Touch Voltage on 765kV GIS room floor

Figure 6.19 shows the touch voltage on 765 kV GIS room floor.

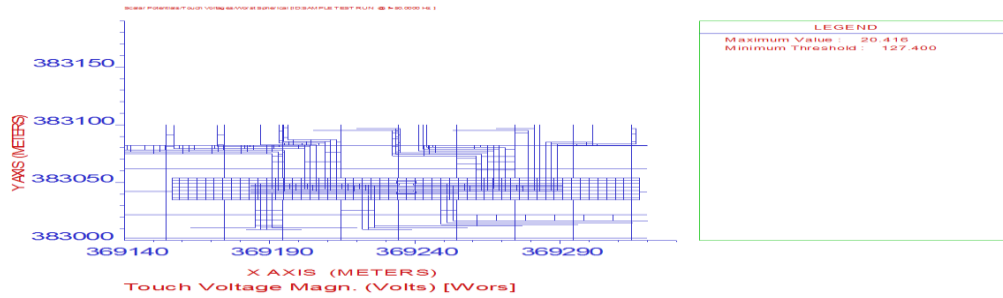


Figure 6.19. Touch Voltage Results on 765kV GIS Room Floor

Attained Value: 20.416 V

Threshold Value: 127.4 V

It is observed that the touch potential in the 765kV GIS room area is within the tolerable limits.

Step Voltage on 765kV GIS room floor

Figure 6.20 shows the step voltage on 765 kV GIS room floor .

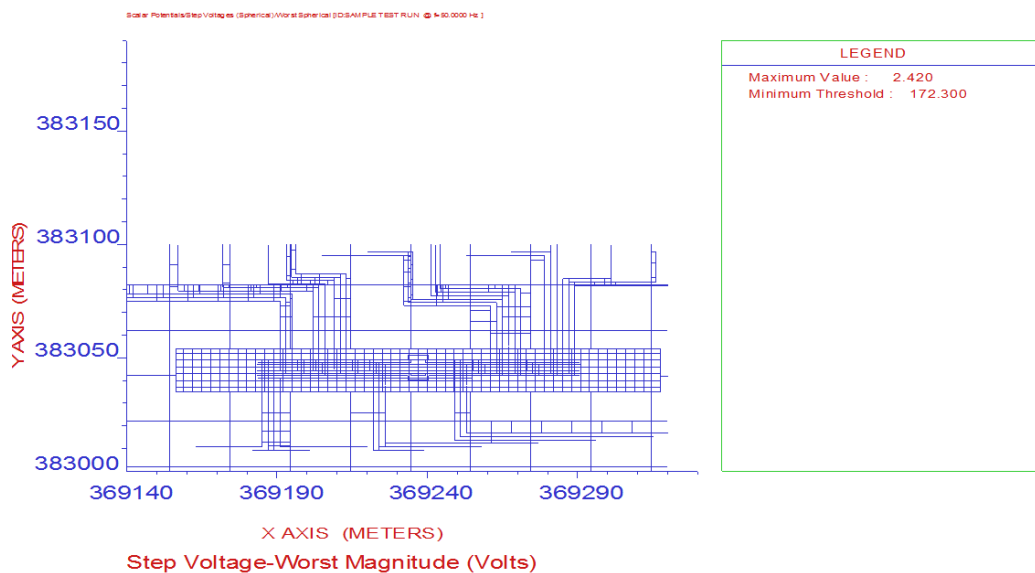


Figure 6.20. Step Voltage Results on 765kV GIS Room Floor

Attained Value: 2.42 V; Threshold Value: 172.3 V

It is observed that the step potential inside the 765kV GIS room area is within the tolerable limits.

Metal to Metal Touch Voltage (GPD on 765kV GIS Equipments inside room)

It is the potential difference between metallic items or buildings inside substations that can be bridged by direct hand-to-hand or hand-to-feel contacts only.

Tolerable $E_{mm-touch} = 116/\sqrt{T_s}$ (Where $T_s=1$) (Eq34 of IEEE80:2013)

Tolerable $E_{mm-touch} = 116V$

Ground Potential difference (GPD) is defined as the potential at a point with respect to ground potential at that point.

6.4 Ground Fault Analysis at GIS Equipments Inside 400kV GIS Room

The same AIS grid modelled as above with GIS equipments is used for the fault analysis in GIS equipments inside room. The phase to ground fault is defined by making connection between phase conductor and enclosure wall of GIS. The grid was energized with fault current of 63000 amps from the 400KV feeder to evaluate the grid performance shown in figure 6.21.

Fault location:-

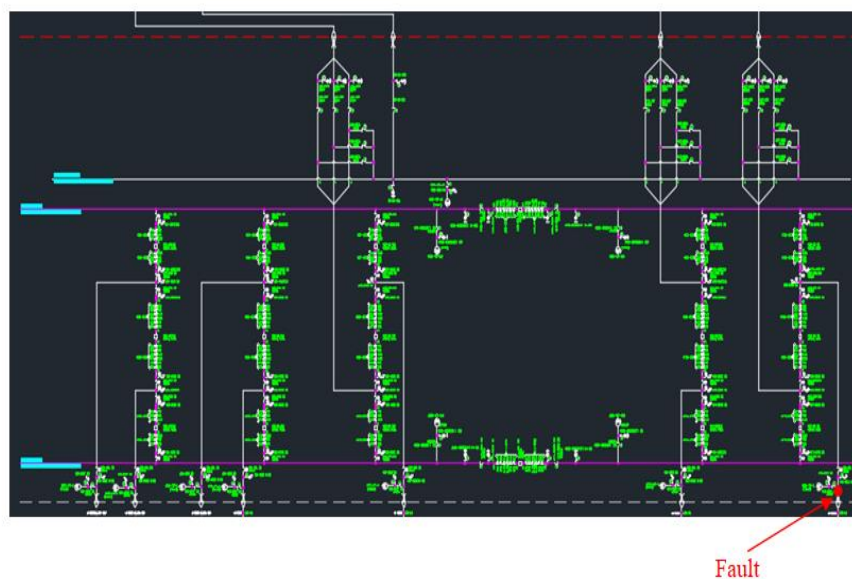


Figure 6.21. Ground Fault Analysis at 400 kV GIS Room

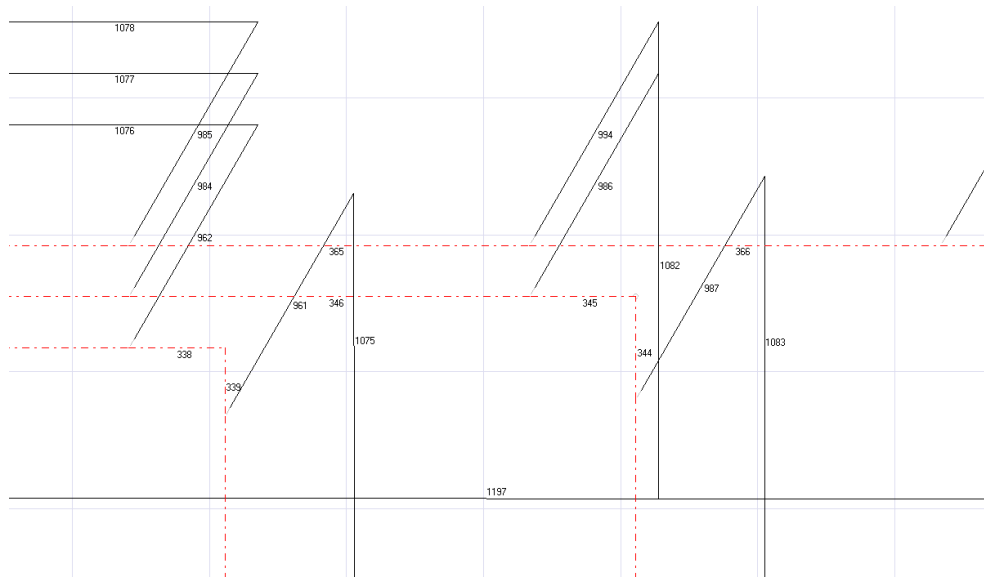


Figure 6.22. Ground Fault Location at 400 kV GIS Room

Safety Criteria with Surface layer resistivity of 100 Ω -M(concrete) for 100mm thickness (Inside 220kV GIS room)

The safety limits for Step and Touch potentials within GIS room with concrete as surface layer. (100 Ohm-m for 100mm thickness).

Touch Voltage in 400kV GIS room floor

Figure 6.23 shows the touch voltage for 400kV GIS room floor.

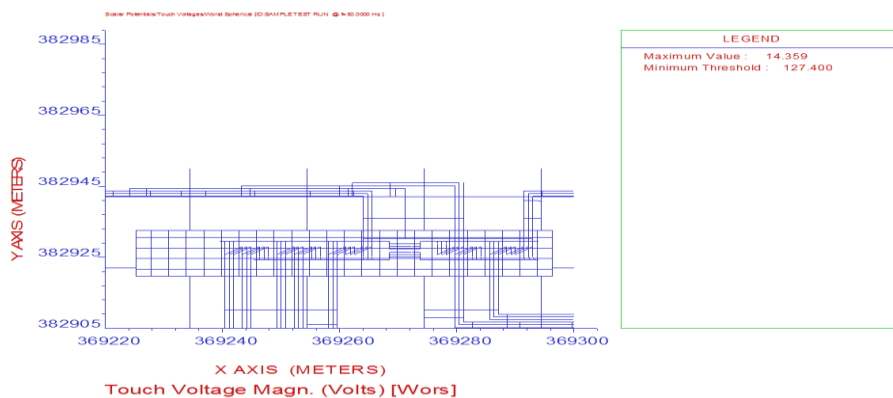


Figure 6.23. Touch Voltage (Inside 400kV GIS Room Floor)

Attained Value: 14.359 V

Threshold Value: 127.4 V

It is observed that the touch potential in the 400kV GIS room is within the tolerable limits.

Step Voltage on 400kV GIS room floor

Figure 6.24 shows the step voltage for 400kV GIS room floor.

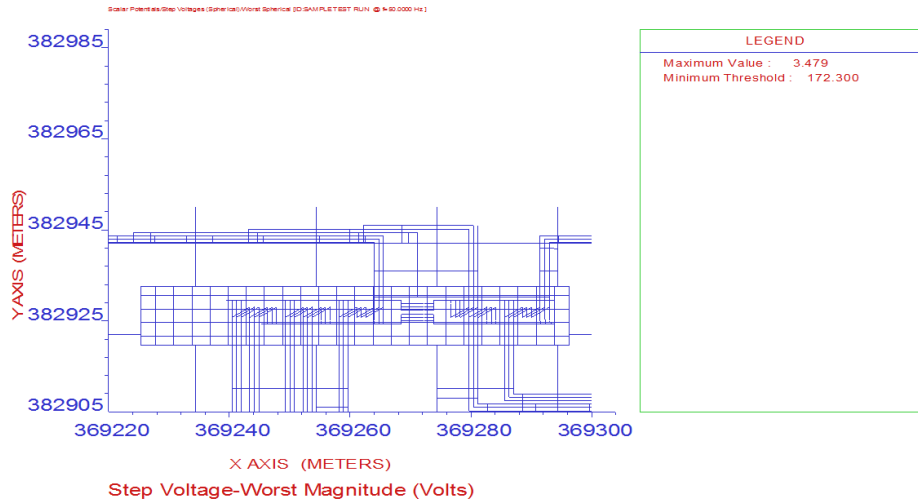


Figure 6.24. Step Voltage (Inside 400kV GIS Room Floor)

Attained Value: 3.479 V

Threshold Value: 172.3 V

It is observed that the step potential 400kV GIS room is within the tolerable limits.

Metal to Metal Touch Voltage (GPD on 400kV GIS Equipments inside room)

It is the potential difference between metallic items or buildings inside substations that can be bridged by direct hand-to-hand or hand-to-feel contacts only.

Tolerable $E_{mm-touch} = 116/\sqrt{T_s}$ (Where $T_s=1$) (Eq34 of IEEE80:2013)

Tolerable $E_{mm-touch} = 116V$

Ground Potential difference (GPD) is defined as the potential at a point with respect to ground potential at that point.

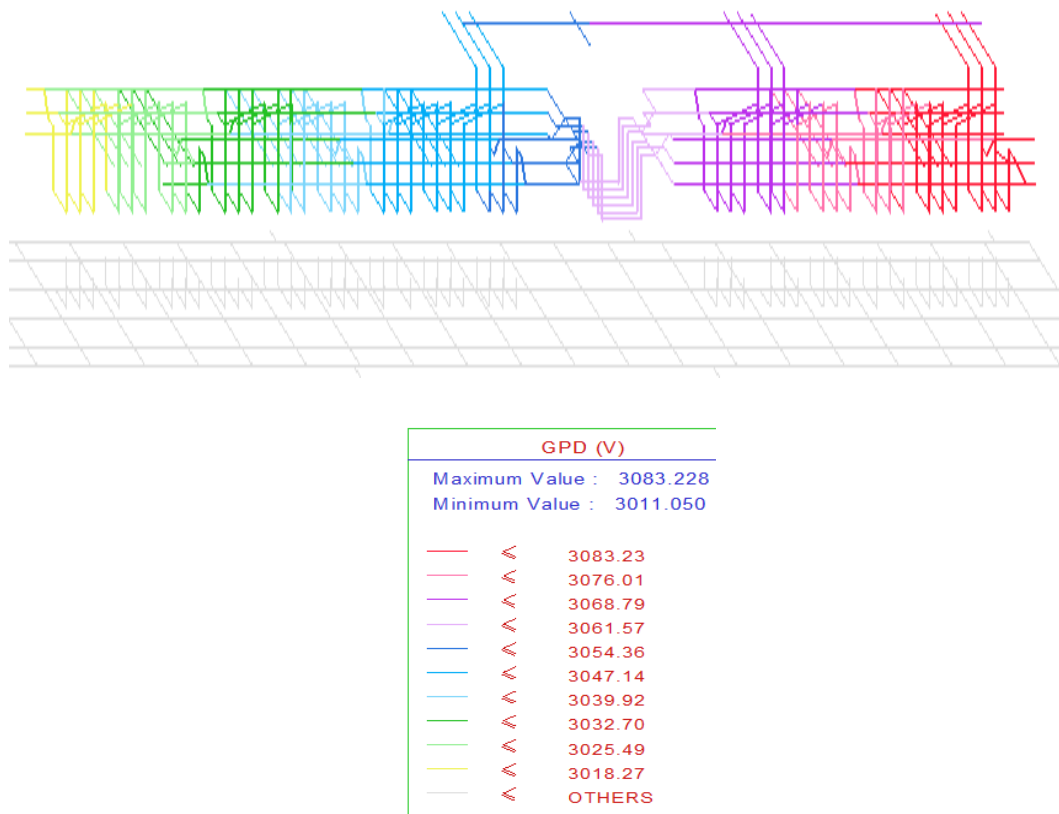


Figure 6.25. Metal to Metal Touch Voltage
(GPD On 400kV GIS Equipments Inside Room)

Figure 6.25 shows the metal to metal touch voltage of 400 KV GIS inside room.

Observations:

Maximum GPD Value - 3083.228

Minimum GPD Value - 3011.05

Metal to Metal Touch Voltage = Maximum GPD - Minimum GPD

Metal to Metal Touch Voltage = (3083.228- 3011.05) = 72.178 V

It is observed that the metal to metal touch potential inside the 400kV GIS room is within the tolerable limits. The results are summarized below in the table 6.3.

Table 6.3. Fault Analysis Comparison of Different Safety Criteria

PARAMETERS	TOLERABLE VALUES	ACHIEVABLE VALUES
		AIS GRID WITH GIS EQUIPMENTS
TOUCH VOLTAGE ON 765kV GIS ROOM FLOOR	127.4 V	20.416 V
STEP VOLTAGE ON 765kV GIS ROOM FLOOR	172.3 V	2.42 V
METAL TO METAL TOUCH VOLTAGE ON 765KV GIS EQUIPMENTS (DIFFERENCE OF MAXIMUM AND MINIMUM GPD)	116 V	87.973 V
TOUCH VOLTAGE ON 400kV GIS ROOM FLOOR	127.4 V	14.359 V
STEP VOLTAGE ON 400kV GIS ROOM FLOOR	172.3 V	3.479 V
METAL TO METAL TOUCH VOLTAGE ON 400KV GIS EQUIPMENTS (DIFFERENCE OF MAXIMUM AND MINIMUM GPD)	116 V	72.178

6.5 VERY FAST TRANSIENT OVER VOLTAGE ANALYSIS (VFTO)

When defining a lightning surge, two key factors need to be considered.

- The shape and amplitude of the surge.
- The desired time and frequency resolution.

The hoped-for increase The "Standard Surge" option allows the choice of 8/20s pulse with peak amplitude of 20kA. The signal is defined as a double exponential function, and it specifies a wave shape with a given rise time, decay time, and amplitude. The Time Duration should be chosen so that the input signal at the end of the time frame is

relatively tiny. As a result, 150 microseconds was chosen. FFTSES (Fast Fourier Transform computation based SES) analysed input signals in the time domain. The (discrete) frequency spectrum of the signal was the outcome of the study. The time resolution, or the shortest event in time that could be simulated using the software, was determined based on the number of samples utilised while discretizing data. This value, known as the Sampling Exponent, should be a power of two in FFTSES.

```

=====
SUMMARY OF INDEPENDENT FREQUENCIES RECOMMENDED
=====

FREQUENCY
INDIVIDUAL, 0
INDIVIDUAL, 6666.667
INDIVIDUAL, 13333.33
INDIVIDUAL, 20000
INDIVIDUAL, 26666.67
INDIVIDUAL, 33333.34
INDIVIDUAL, 986666.7
INDIVIDUAL, 1946667
INDIVIDUAL, 2920000
INDIVIDUAL, 3893334
INDIVIDUAL, 4866667
INDIVIDUAL, 5840001
INDIVIDUAL, 6813334
INDIVIDUAL, 7786667
INDIVIDUAL, 9733334
INDIVIDUAL, 1.168E+07
INDIVIDUAL, 1.362667E+07
INDIVIDUAL, 1.365333E+07

```

Figure 6.26 Screenshot of Summary of Independent Frequencies

Input Signal (Time Domain):

Figure 6.27 shows the input signal for time domain of the lightning surge.

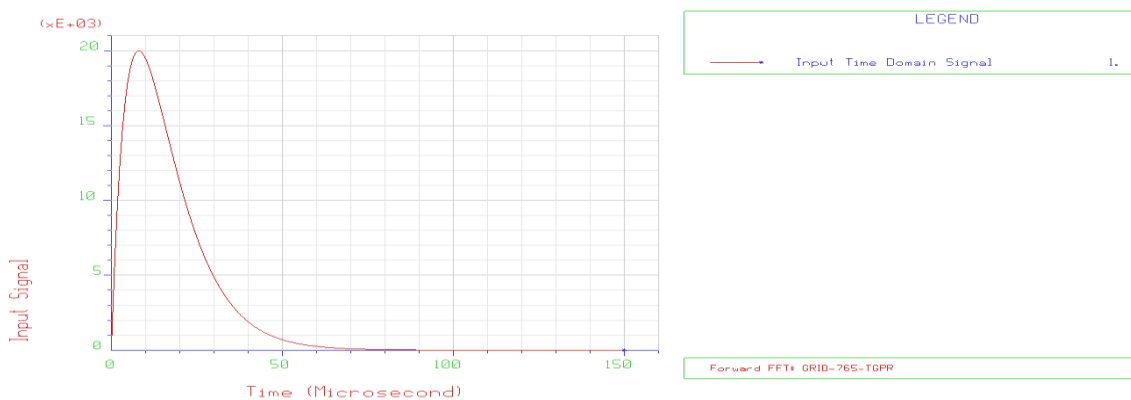


Figure 6.27. Input Signal for Lightning Surge (Time Domain)

Input Signal (Frequency Domain – Real Part)

Figure 6.28 shows the input signal for frequency domain with real part of the lightning surge.

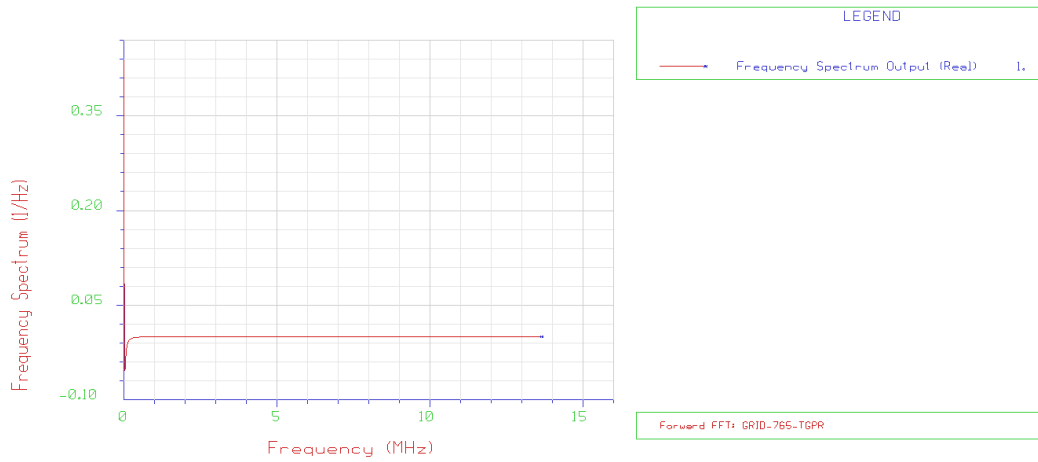


Figure 6.28. Input Signal for Lightning Surge (Frequency Domain-Real Part)

Input Signal (Frequency Domain – Imaginary Part):

Figure 6.29 shows the input signal for frequency domain with Imaginary part of the lightning surge. Figure 6.30 shows the different locations in main bus for lighting surge.

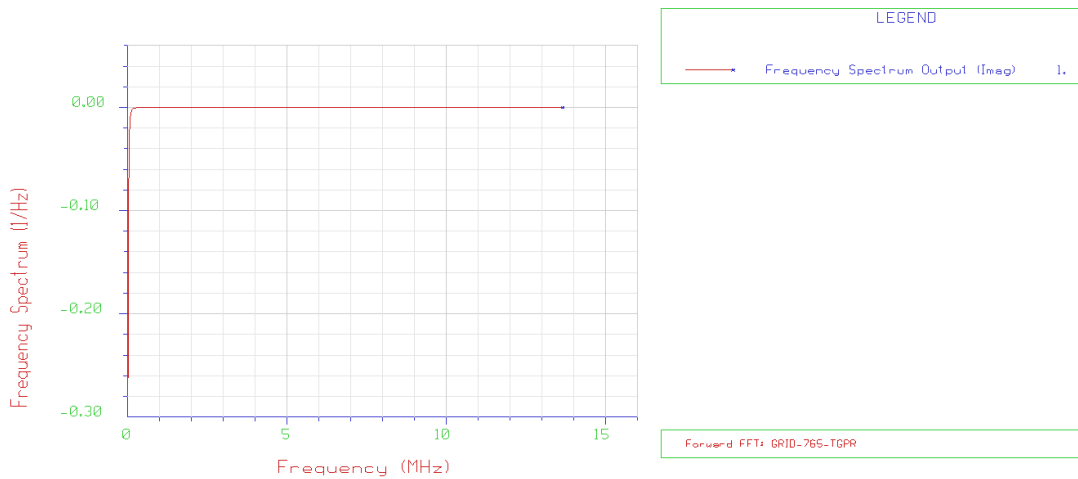


Figure 6.29. Input Signal for Lightning Surge (Frequency Domain- Imaginary Part)

TGPR at Different locations in Main Bus

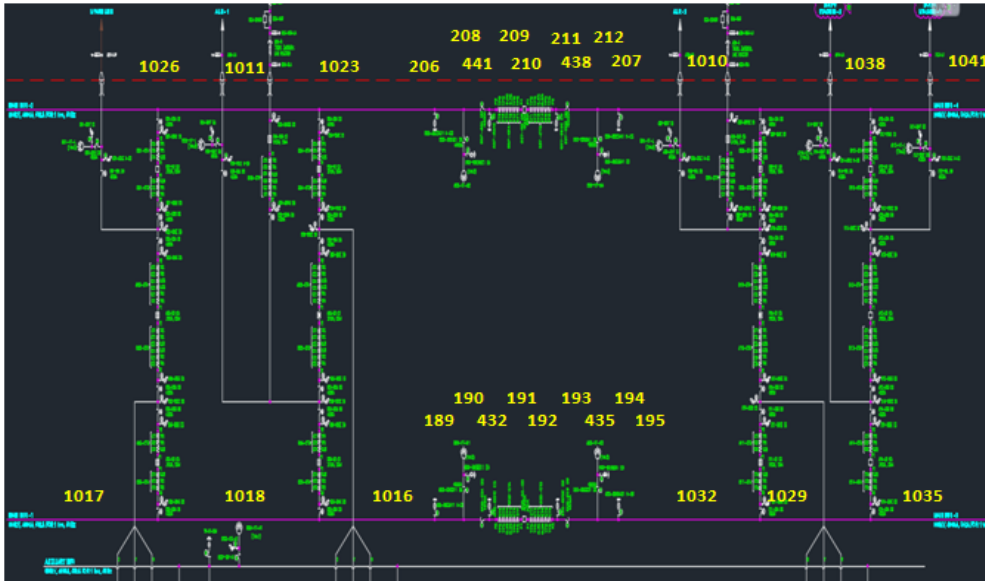


Figure 6.30. TGPR at Different Locations in Main Bus for Lightning Surge

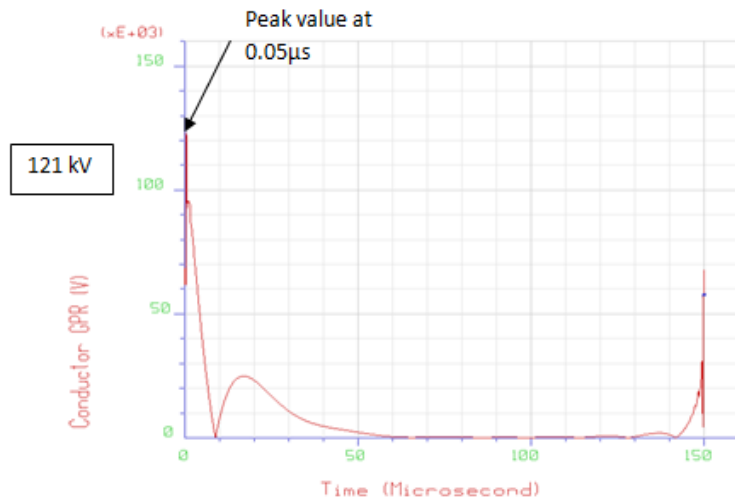


Figure 6.31. TGPR at Conductor Segment Number 1017 (Main Bus 1)

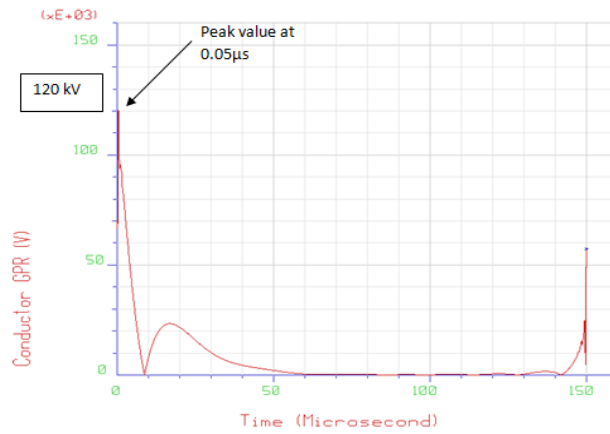


Figure 6.32. TGPR at Conductor Segment Number 1018 (Main Bus 1)

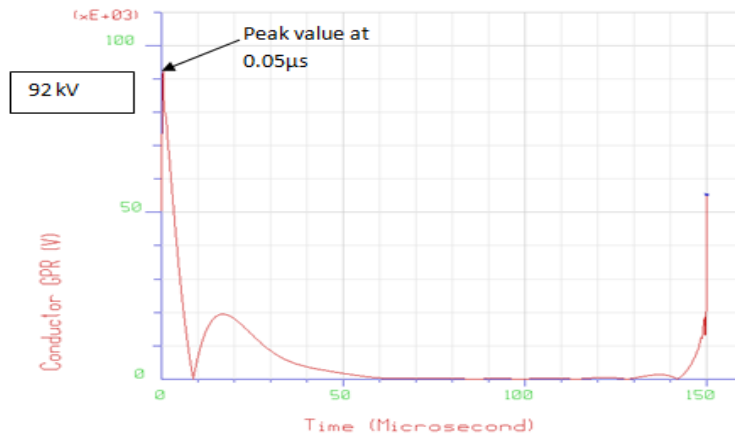


Figure 6.33. TGPR at Conductor Segment Number 1016 (Main Bus 1)

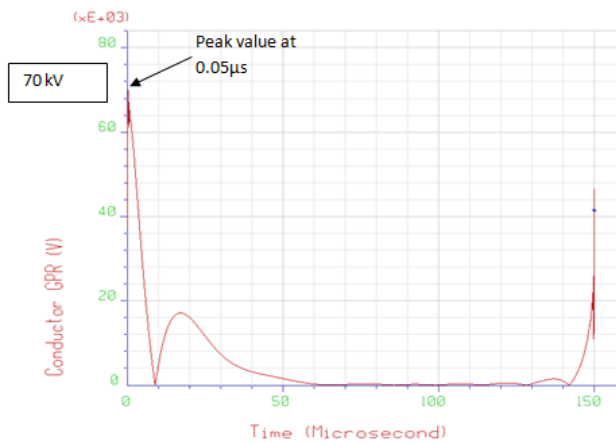


Figure 6.34. TGPR at Conductor Segment Number 189 (Main Bus 1)

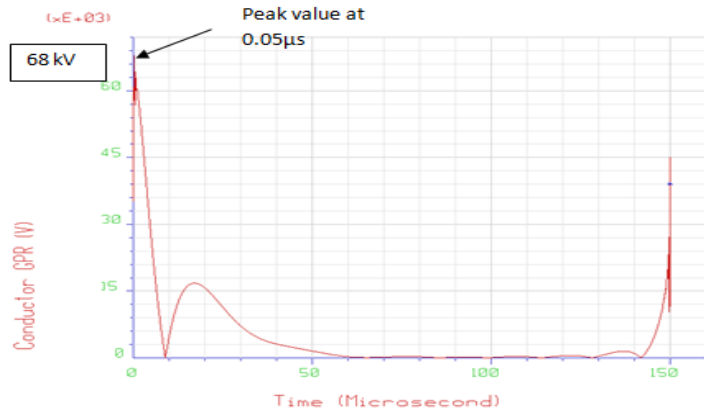


Figure 6.35. TGPR at Conductor Segment Number 190 (Main Bus 1)

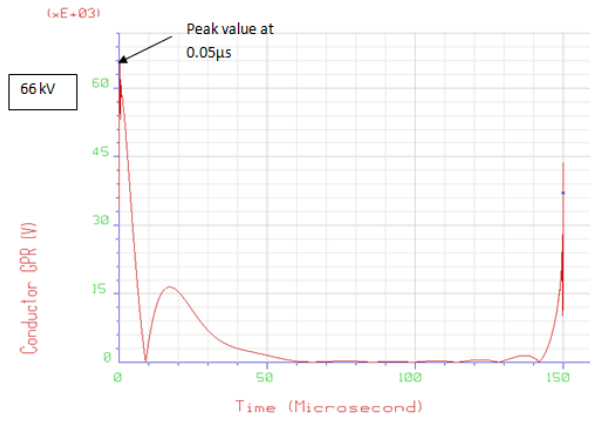


Figure 6.36. TGPR at Conductor Segment Number 432 (Main Bus 1)

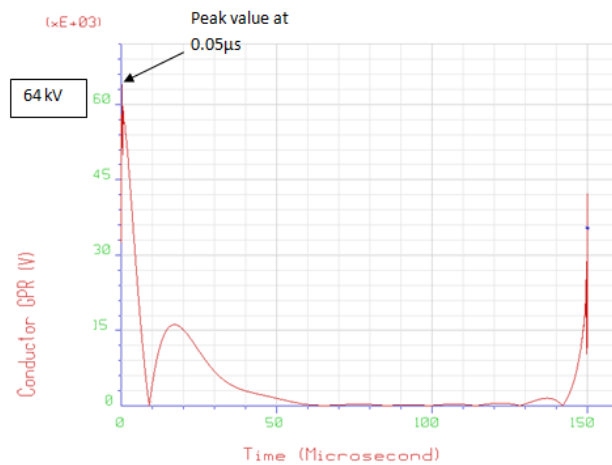


Figure 6.37. TGPR at Conductor Segment Number 191 (Main Bus 1)

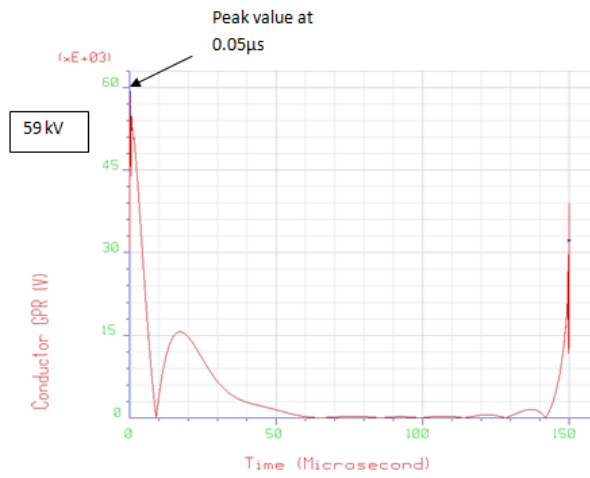


Figure 6.38. TGPR at Conductor Segment Number 192 (Main Bus 1)

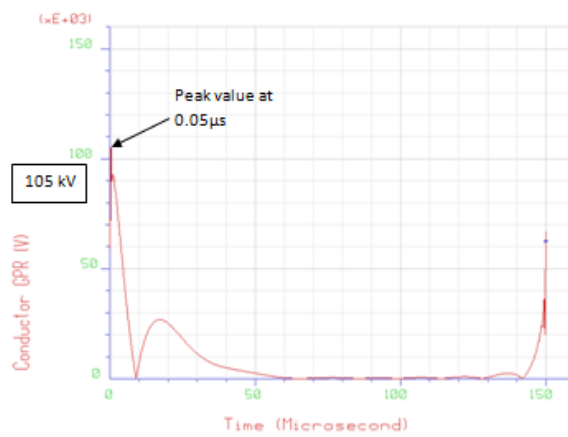


Figure 6.39. TGPR at Conductor Segment Number 1026 (Main Bus 2)

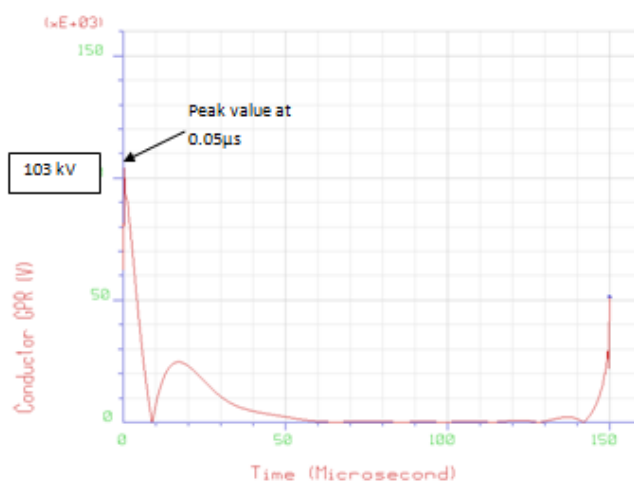


Figure 6.40. TGPR at Conductor Segment Number 1011 (Main Bus 2)

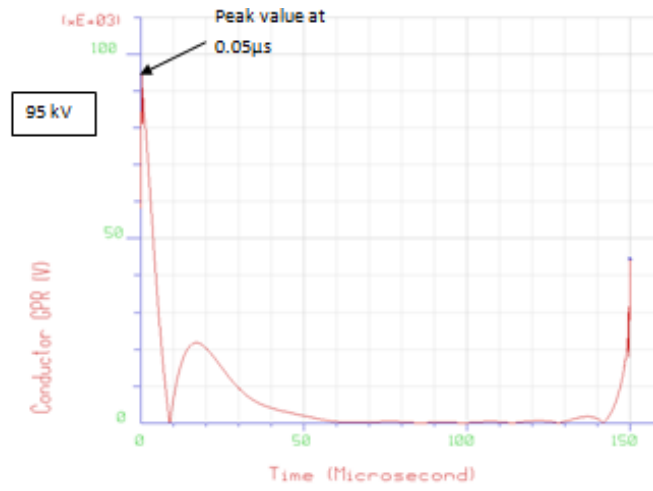


Figure 6.41. TGPR at Conductor Segment Number 1023 (Main Bus 2)

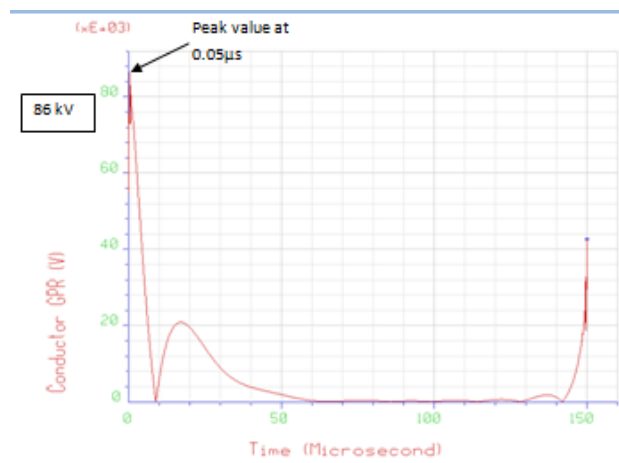


Figure 6.42. TGPR at Conductor Segment Number 206 (Main Bus 2)

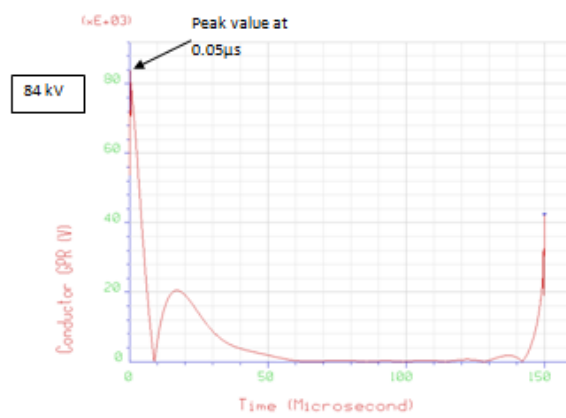


Figure 6.43. TGPR at Conductor Segment Number 208 (Main Bus 2)

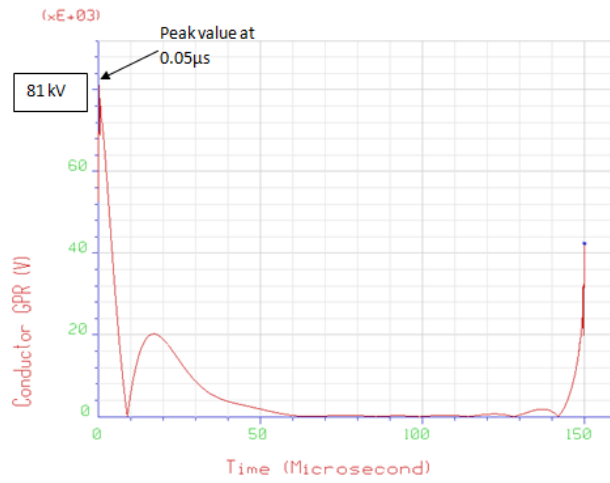


Figure 6.44. TGPR at Conductor Segment Number 441 (Main Bus 2)

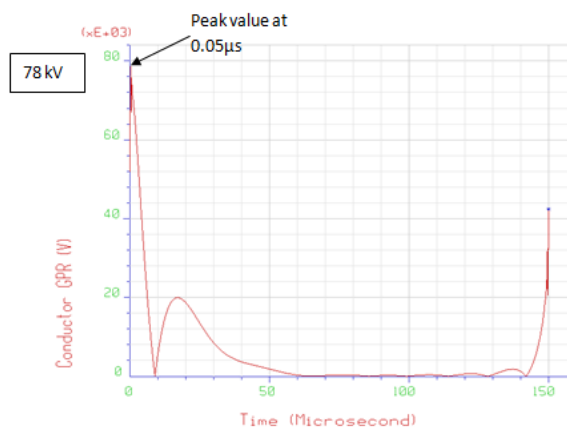


Figure 6.45. TGPR at Conductor Segment Number 209 (Main Bus 2)

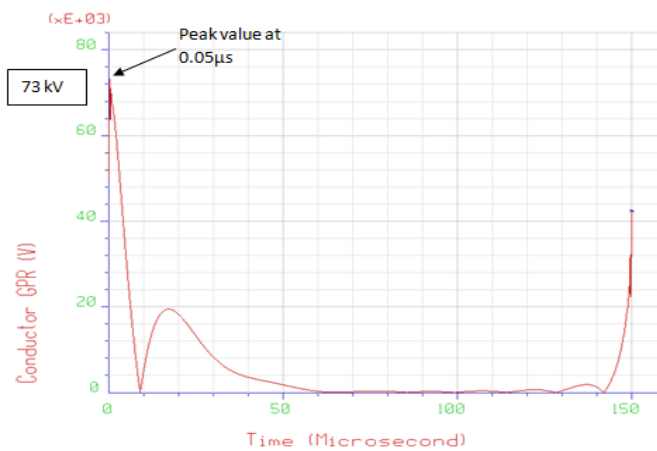


Figure 6.46. TGPR at Conductor Segment Number 210 (Main Bus 2)

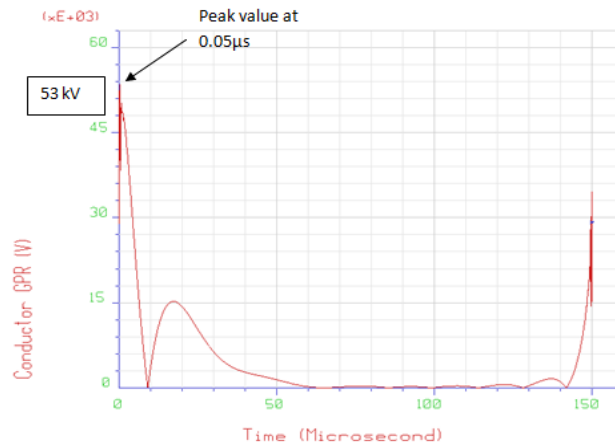


Figure 6.47. TGPR at Conductor Segment Number 193 (Main Bus 3)

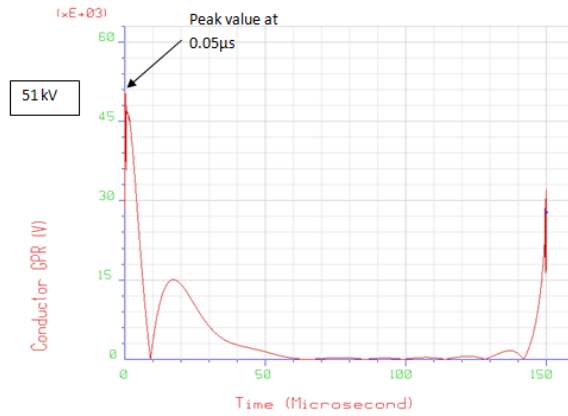


Figure 6.48. TGPR at Conductor Segment Number 435 (Main Bus 3)

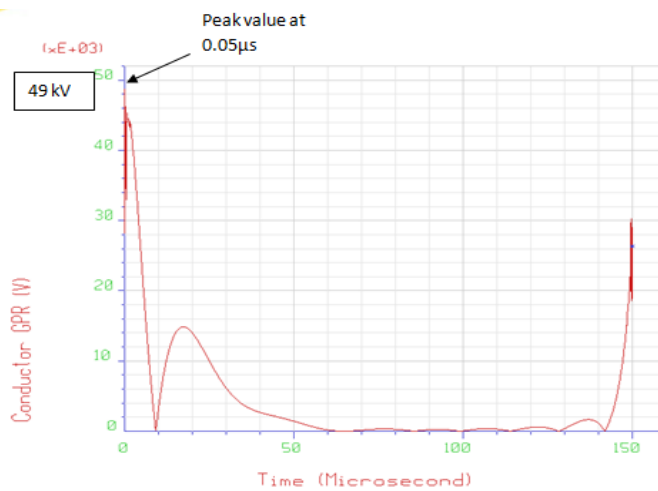


Figure 6.49. TGPR at Conductor Segment Number 194 (Main Bus 3)

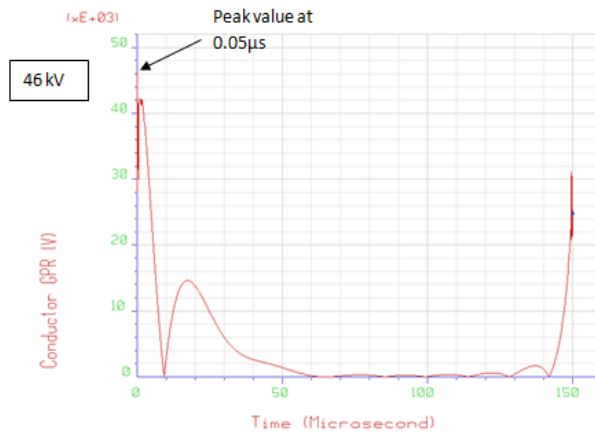


Figure 6.50. TGPR at Conductor Segment Number 195 (Main Bus 3)

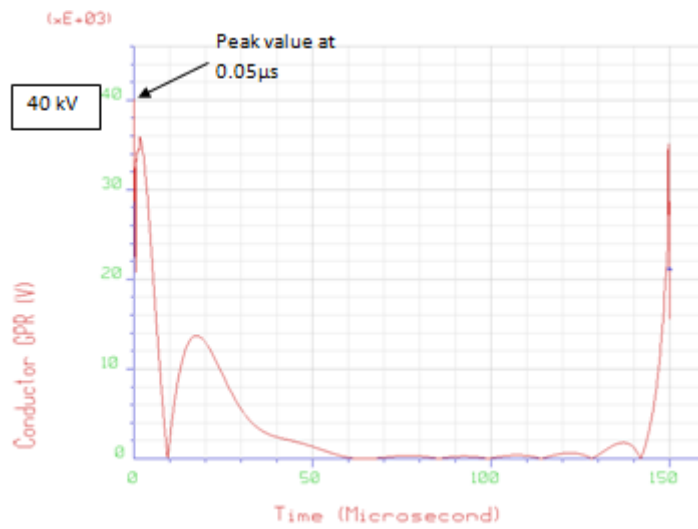


Figure 6.51. TGPR at Conductor Segment Number 1032 (Main Bus 3)

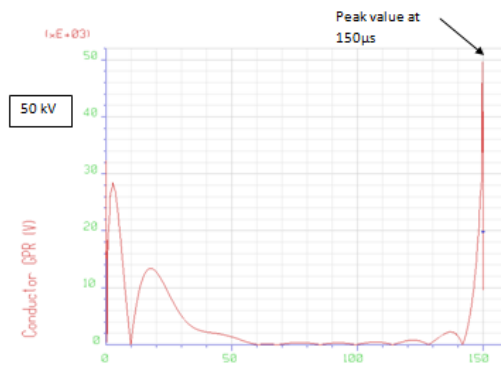


Figure 6.52. TGPR at Conductor Segment Number 1029 (Main Bus 3)

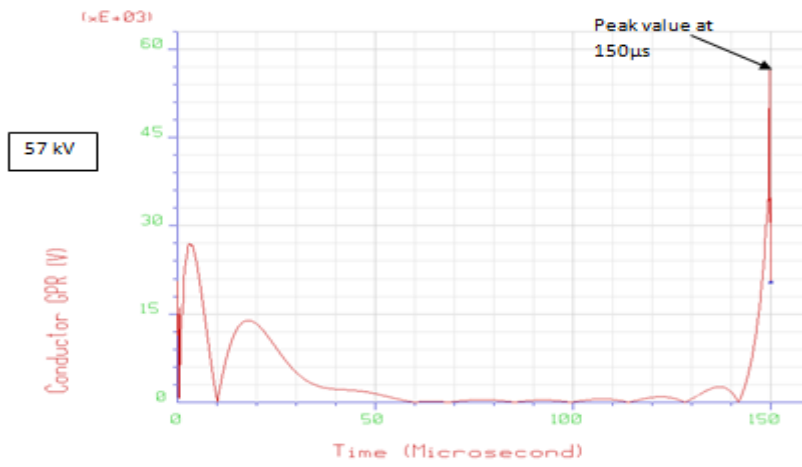


Figure 6.53. TGPR at Conductor Segment Number 1035 (Main Bus 3)

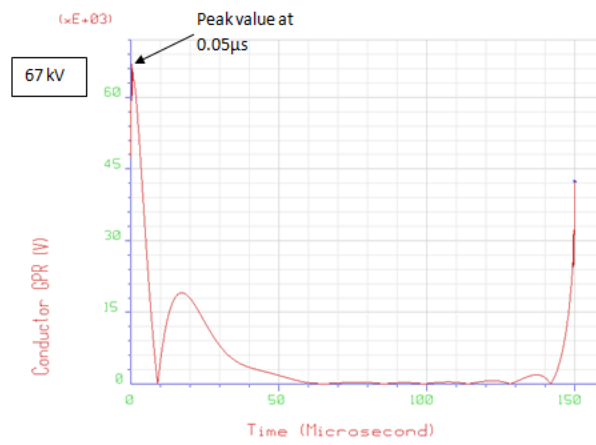


Figure 6.54. TGPR at Conductor Segment Number 211 (Main Bus 4)

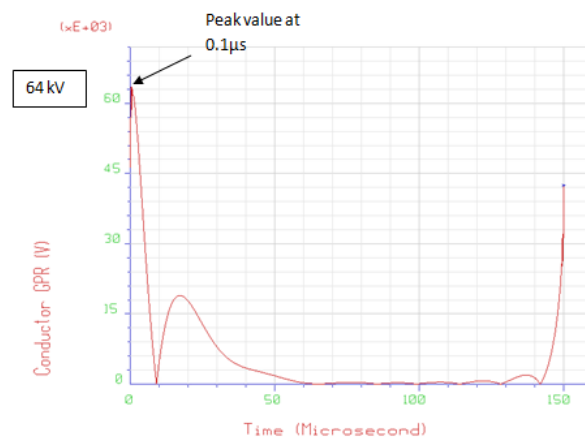


Figure 6.55. TGPR at Conductor Segment Number 438 (Main Bus 4)

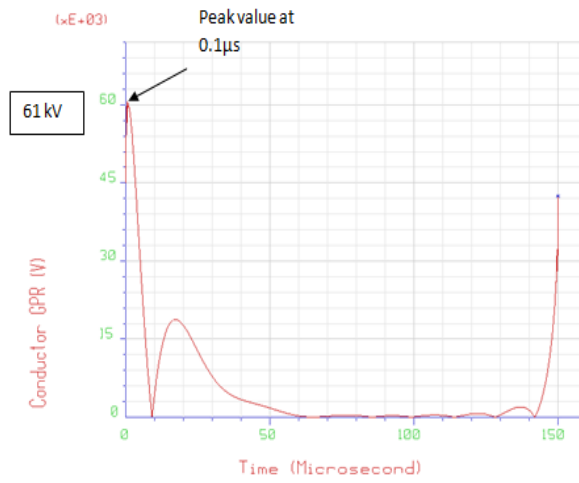


Figure 6.56. TGPR at Conductor Segment Number 212 (Main Bus 4)

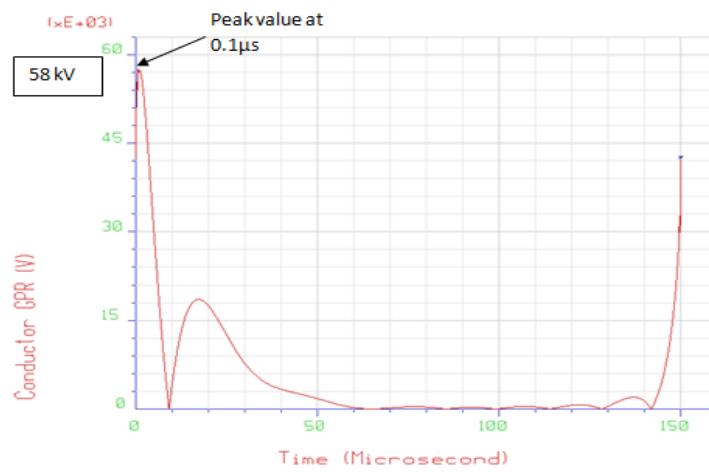


Figure 6.57. TGPR at Conductor Segment Number 207 (Main Bus 4)

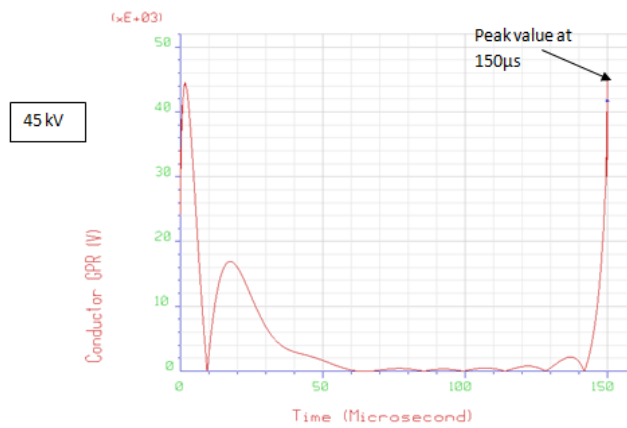


Figure 6.58. TGPR at Conductor Segment Number 1010 (Main Bus 4)

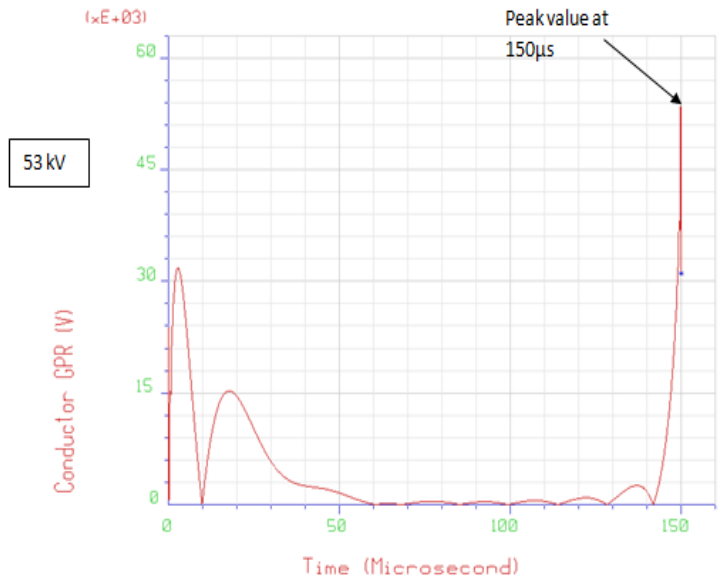


Figure 6.59. TGPR at Conductor Segment Number 1038 (Main Bus 4)

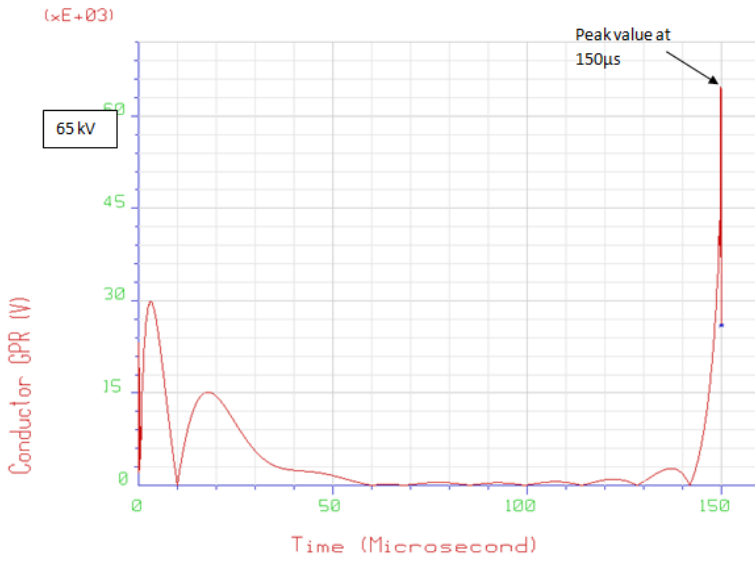


Figure 6.60. TGPR at Conductor Segment Number 1041 (Main Bus 4)

Figure 6.31 to 6.38, TGPR in the conductor at Main bus 1. Figure 6.39 to 6.46, TGPR in the conductor segment at Main bus 2. Figure 6.47 to 6.53, TGPR in the conductor segment at Main bus 3. Figure 6.54 to 6.60, TGPR in the conductor segment at Main bus 4.

Table 6.4. GIS Results of TGPR at Different Segment Numbers in Main Bus

Main Bus 1 Conductor Segment Numbers	TGPR Value	Main Bus 2 Conductor Segment Numbers	TGPR Value	Main Bus 3 Conductor Segment Numbers	TGPR Value	Main Bus 4 Conductor Segment Numbers	TGPR Value
1017	121 kV	1026	105 kV	193	53 kV	211	67 kV
1018	120 kV	1011	103 kV	435	51 kV	438	64 kV
1016	92 kV	1023	95 kV	194	49 kV	212	61 kV
189	70 kV	206	86 kV	195	46 kV	207	58 kV
190	68 kV	208	84 kV	1032	40 kV	1010	45 kV
432	66 kV	441	81 kV	1029	50 kV	1038	53 kV
191	64 kV	209	78 kV	1035	57 kV	1041	65 kV
192	59 kV	210	73 kV				

1. Maximum TGPR: 121kV at Main Bus Segment Conductor No. 1017
2. Insulation withstand capacity of 765kV GIS is 2100 kV.
3. Observed that TGPR is within the BIL limits of GIS.

6.6 SUMMARY

In this chapter, the discussed soil modelling aids in precise design of GIS substation's grounding system. IEEE80-2000 specifies formulae for designing a grounding system for a soil model, with the use of software for two or more layers. The soil structure has a significant impact on the grounding grid's performance. The consequences of probable differences in soil structure on the examined urban sub-station grounding

performance are the subject of this study. The results of GISs were evaluated using voltage levels like step and touch with respect to earth design. From the observations the following points are satisfied with each other.

CHAPTER 7

CONCLUSIONS AND FUTURE SCOPE

The statement of the problem in this research is to better quantify the behaviour of an earthing system subjected to power frequency fault and transient fault occurs in the multilayer earth structure. Importance of geological stratification is very much required to safest design of substation. Once this knowledge has been obtained it can be applied in the design of lightning protection system or an efficient earthing.

7.1 Conclusions

These are the following conclusions are drawn from the research work reported in this thesis.

- Soil investigation and optimization of soil parameters is the prerequisite to design the earth grounding grid for the substation. Steepest Descent Method is the conventional method also used to optimize the soil parameters. A study compared with existing conventional steepest method compared with Genetic Algorithm and proposed hybrid GA – PSO algorithm. The proposed GA – PSO algorithm gives better error percentage compared with the other methods.
- Three different profile of AIS substation taken for study to investigate the better designing considerations for substation. In the study three different profile of soil structure site taken for investigation. Step Voltage is safe in all the three case taken for studies, only in some cases added the surface layer thickness of 0.15 m and 5000 Ωm .
- Touch Voltage is not safe in all the cases even after added the surface layer of maximum 0.15 m as specified in the standard. Hence the grounding grid is to be redesigned by extending the size of the grid and further buried the grounding rod in the risky grounding corners to stabilize the potential.
- In the Case study 3, even after extending the size of the grid and buried grounding rod in the risky corner, touch voltage not in the tolerable limits. Thus satellite grid designed away from the substation and connected all the earthing

to the satellite grid after investigate the soil parameters. Installation of satellite grid reduced the touch and step voltage with in tolerable limits.

- In GIS, the first step in the modelling activity involves forming a grid covering the proposed equipment area with required conductor spacing so as to form 20x20 m mesh. Then the impedance of the grid was computed with a fault current of 63000 amps and with a multi-layer soil model.
- The fault current 63 kA was injected at different locations of the grid to find out a worst case scenario and confirmed that the safety parameters are within the tolerable limit
- Inside room GIS equipment along with outdoor bus ducts were modelled and defined for its dimension, material property and earthing. The outdoor Main earth grid was energized with a fault current of 63KA. The safety parameters were analysed and found within the threshold value.
- Subsequent process was to analyse Main earth grid along with GIS equipment but with a fault inside GIS equipment. A fault was created simply by making a connection between GIS core and enclosure wall. The safety parameters were analysed with a fault current of 63KA and found within the threshold limit.

7.2 Future Scope

These are the possible scope in future to improve the safety earthing system, which are left in this research studies.

- Better electrode corrosion study and mitigation methods to improve the better life and healthy earthing system.
- Extends the methods developed to grids of arbitrary shapes.
- Supply to the GIS substations through cables rather than Overhead lines helps the division of current between the system, computational and experimental investigations have to be done for the same.

REFERENCES

- [1] A.P.Meliopoulos, A.D.Papalaxopoulos, R.P. Webb, and C.Blartner [1984], “Estimation of Soil Parameters from Driven Rod Measurements”, *proceedings of the IEEE Power Engineering Society*, IEEE/PES 1984 Winter Meeting, Texas, January 29 – February 3, 1984.
- [2] A.P.Meliopoulos and A.D.Papalexopoulos, “Interpretation of Soil Resistivity Measurements: Experience with the MODEL SOMIP”, *IEEE Trans. Power Del.*, Vol. PWRD – 1, no.4, pp. 142 – 150, Oct. 1986.
- [3] Bo Zhang, Xiang Cui, and Jinliang He, “Parameter Estimation of Horizontal Multilayer Earth by Complex Image Method”, *IEEE Trans. Power Del.*, vol.20, no.2, pp.1394 – 1401, Apr. 2005.
- [4] B.R.Gupta and B.Thapar, “Impulse Impedance of Grounding Grids”, *IEEE Trans. Power App. Syst.*, vol.PAS – 99, no. 6, pp.2357 – 2362 , Nov/Dec. 1980.
- [5] C.J.Blattner, “Analysis of Soil Resistivity Test Methods in Two Layer Method”, *IEEE Trans. Power App. and Syst.*, vol.Pas – 104, no.12, pp.3603 – 3608, Dec.1985.
- [6] F.Dawalibi and C.J.Blattner, “Earth Resistivity Measurement Interpretation Techniques”, *IEEE Trans. Power App. And Syst.*, vol.PAS – 103, no.2, pp.374 – 380, Feb.1984.
- [7] F.E.Asimakoupoulo, I.F.Gonos and I.A. Stathopoulos, “Estimation of Uncertainty Regarding Soil Breakdown Parameters”, *IET Science, Measurement and Tech.*, vol.5, Iss.1, pp.14 – 20, July 2010.

[8] Guide for Measuring Earth Resistivity, Ground Impedance and Earth Surface Potentials of a Ground System, *IEEE Standard 81 – 1983*, 1983.

[9] I.F. Gonos and I.A.Stathopoulos, “Estimation of Multilayer Soil Parameters Using Genetic Algorithms”, *IEEE Trans. Power Del.*, vol.20, no.1, pp.100 – 106, Jan.2005.

[10] Jingli Li, Tao Yuan, Qing Yang, and Markus Zahn, “Numerical and Experimental Investigation of Grounding Electrode Impulse Current Dispersal Regularity Considering the Transient Ionization Phenomenon”, *IEEE Trans. Power Del.*, vol. 26, no. 4, pp.2647 – 2658, Oct. 2011.

[11] Jinliang He, Boaping Zhang, and Bo Zhang, “Lightning Impulse Breakdown Characteristics of Frozen Soil”, *IEEE Trans. Power Del.*, vol. 23, no. 4, pp. 2216 – 2223, Oct. 2008.

[12] Jinliang He, Boaping Zhang, Rong Zeng, and Bo Zhang, “Experimental Studies of Impulse Breakdown Delay Characteristics of Soil”, *IEEE Trans. Power Del.*, vol. 26, no. 3, pp.1600 – 1607, July 2011.

[13] Jinliang He, Xi Wang, Rong Zeng, and Xiangyang Peng, “Influence of Impulse Breakdown Delay of Soil on Lightning Protection Characteristics of Transmission Line”, *Electric Power System Research* (85), pp.44 – 49, 2012.

[14] Jinliang He, Rong Zeng, Bo Zhang, “Methodology and Technology for Power System Grounding”, *Wiley Publication*, 2013.

- [15] J.L.del Alamo, “A Comparison Among Eight Different Techniques to Achieve an Optimum Estimation of Electrical Grounding Parameters in Two Layered Earth”, *IEEE Trans. Power Del.*, vol.8, no.4, pp.1890 – 1899, Oct. 1993.
- [16] J.L.del Alamo, “A Second Order Gradient Technique for an Improved Estimation of Soil Parameters in a Two Layer Earth”, *IEEE Trans. Power Del.*, vol.6, no.3, pp.1166 – 1170, July 1991.
- [17] M.Mittolo, “Grounding the Neutral of Electrical Systems Through Low – Resistance Grounding Resistors: An Application case”, *IEEE Trans. Ind. Appl.*, vol.44, no.5, Sep./Oct. 2008.
- [18] M.Mokhatri, Z.Abdul Malek, and Z.Asalam, “An Improved Circuit Based Model of a Grounding Electrode by Considering the Current Rate of Rise and Soil Ionization Factors”, *IEEE Trans. Power Del.*, vol.30, no.1, pp.211 – 219, Feb. 2015.
- [19] Rooney R.A. Coelha, A.E. Pereira and L.M.Neto, “A High Performance Multilayer Earth Parameter Estimation rooted in Chebyshev Polynomial”, *IEEE Trans. Power Del.*, pp.1 – 8, 2017.
- [20] R.Verma and D. Mukhedkar, “Fundamental Considerations and Impulse Impedance of Grounding Grids”, *IEEE Trans. Power App. and Syst.*, vol.PAS – 100, no.3, pp. 1023 – 1030, Mar. 1981.
- [21] Sherif Ghoneim, “Optimal Grounding Grid Design to Suit Safety Conditions”, *Int. Jour. Of Electrical, Electronics and Telecommunication Engineering*, vol.44, issue.2, pp.1143 – 1149, July 2013.

[22] S.Visacro, “A Comprehensive Approach to the Grounding Response to Lightning Currents”, *IEEE Trans. Power Del.*, vol.22, no.1, Jan.2007.

[23] S.Visacro, “Response of Grounding Electrodes to Impulsive Currents: An Experimental Evaluation”, *IEEE Trans. Elect. Compat.*, vol.51, no.1, Feb. 2009.

[24] S.Visacro, “Frequency Dependence of Soil Parameters: Experimental Results, Predicting Formula and Influence on the Lightning Response of a Grounding Electrodes”, *IEEE Trans. Power Del.*, vol.27, no.2, pp.927 – 935, Apr. 2012.

[25] S.Visacro, R.Alipio, M.H.M.Vale, and C.Pereira, “The Response of Grounding Electrodes to Lightning Currents: The Effect of Frequency – Dependent Soil Resistivity and Permittivity”, *IEEE Trans. Elect. Compat.*, vol.53, no.2, May 2011.

[26] S.Visacro, “Experimental Impulse Response of Grounding Grids”, *Electric Power Systems Research* (94), pp.92 – 98, 2013.

[27] T.Islam, “Estimation of Soil Electrical Properties in a Multilayer Earth Model with Boundary Element Formulation”, *Mathematical Problems in Engineering (Hindawi)*, pp.1 – 13, 2012.

[28] T.Takahashi and T.Kawase, “Analysis of Apparent Resistivity in a Multi Layer Earth Structure”, *IEEE Trans. Power Del.*, vol.5, no.2, pp.604 – 612, Apr.1990.

- [29] T.Takahashi and T.Kawase, "Calculation of Earth Resistance for a Deep Driven Rod in a Multi Layer Earth Structure", *IEEE Trans. Power Del.*, vol.6, no.2, pp.608 – 614, Apr.1991.
- [30] W.P.Calixto, L.M.Neto, and Emerson da Paz Moreira, "Parameter Estimation of a Horizontal Multilayer Soil Using Genetic Algorithm", *IEEE Trans. Power Del.*, vol.25, no.3, pp.1250 – 1257, July 2010.
- [31] W.P.Calixto and Marcel Wu,"Horizontal Stratification of the Soil in Multilayer using non linear Optimization", *Revista Clencias Exatas e Naturais*, vol.11, no.1, pp.68 – 89, Jan/Jun 2009.

PUBLICATIONS BASED ON THESIS

Refereed Journals:

1. R. T. Senthilkumar, and Selvakumar, "Investigation of GPR in Multilayered Soil Structure," *Journal of Advanced Research in Dynamical and Control Systems, (JARDCS)*, vol. 11, no.3, pp. 1084 -1092, May 2019. (Scopus)

Conference Proceedings:

1. R.T.Senthilkumar, Selvakumar, and K.Nagarajan, "Optimization of Multilayer Earth Structure by using Steepest Descent Method and Estimation of Transient Ground Potential Rise in Substation", in *Proc. IEEE International conference on Asia Pacific Power and Energy Conference (APPEEC 2018)*, Kota Kinabalu, Malaysia, Oct. 2018, pp. 123-127. (Scopus)
2. 3. R.T.Senthilkumar, "Optimization of Soil Parameters in Multiple Layers of Ground Structure", in *Proc. IEEE International conference on Asia Pacific Power and Energy Conference (APPEEC 2017)* , Bangalore, India on Nov. 2017, pp. 1-5. (Scopus)

CURRICULUM VITAE



Name: R. T. Senthilkumar

Date of birth: December 16, 1983

E-mail: senthilpowersystems@gmail.com

Mobile: +91-8072818842

ADDRESS

S/o: R. Thayalan

B2 – 102, Provident Green Park Apartment,

Muthusamy Colony Extension,

Selvapuram, Coimbatore – 641026, Tamilnadu.

EDUCATION

- Master of Engineering (M.E.) in Power Systems Engineering
(July 2010 – May 2012)
Institute: K S Rangasamy College of Technology (Autonomous Institution
Affiliated to Anna University, Chennai), Tamil Nadu.
CGPA: 8.4/10 (Class Obtained: First Class)

- Bachelor of Engineering (B.E.) in Electrical and Electronics Engineering
(July 2003 – May 2006)
Institute: Mahendra Engineering College (Autonomous Institution
Affiliated to Anna University, Chennai), Tamil Nadu
Percentage: 64 (Class Obtained: First Class)

TEACHING EXPERIENCE

- Assistant Professor, Department of Electrical and Electronics Engineering, Sengunthar Engineering college, Duration: June 2012 – December 2013 (1 year)